Walter A. Rosenblith New Investigator Award
RESEARCH REPORT

HEALTH EFFECTS INSTITUTE

Number 182
November 2014

Synergistic Effects of Particulate Matter and Substrate Stiffness on Epithelial-to-Mesenchymal Transition

Thomas H. Barker, Marilyn M. Dysart, Ashley C. Brown, Alison M. Douglas, Vincent F. Fiore, and Armistead G. Russell

Synergistic Effects of Particulate Matter and Substrate Stiffness on Epithelial-to-Mesenchymal Transition

Thomas H. Barker, Marilyn M. Dysart, Ashley C. Brown,
Alison M. Douglas, Vincent F. Fiore, and Armistead G. Russell

with a Critique by the HEI Health Review Committee

Research Report 182
Health Effects Institute
Boston, Massachusetts

Trusted Science • Cleaner Air • Better Health

Publishing history: This document was posted at *www.healtheffects.org* in November 2014.

Citation for document:

Barker TH, Dysart MM, Brown AC, Douglas AM, Fiore VF, Russell AG. 2014. Synergistic Effects of Particulate Matter and Substrate Stiffness on Epithelial-to-Mesenchymal Transition. Research Report 182. Boston, MA:Health Effects Institute.

 Cameographics, Belfast, Me., Compositor. Printed by Recycled Paper Printing, Boston, Mass. Library of Congress Catalog Number for the HEI Report Series: WA 754 R432.

Cover paper: made with at least 55% recycled content, of which at least 30% is post-consumer waste; free of acid and elemental chlorine. Text paper: made with 100% post-consumer waste recycled content; acid free; no chlorine used in processing. The book is printed with soy-based inks and is of permanent archival quality.

CONTENTS

ABOUT HEI

The Health Effects Institute is a nonprofit corporation chartered in 1980 as an independent research organization to provide high-quality, impartial, and relevant science on the effects of air pollution on health. To accomplish its mission, the institute

- Identifies the highest-priority areas for health effects research;
- Competitively funds and oversees research projects;
- Provides intensive independent review of HEI-supported studies and related research;
- Integrates HEI's research results with those of other institutions into broader evaluations; and
- Communicates the results of HEI's research and analyses to public and private decision makers.

HEI typically receives half of its core funds from the U.S. Environmental Protection Agency and half from the worldwide motor vehicle industry. Frequently, other public and private organizations in the United States and around the world also support major projects or research programs. HEI has funded more than 330 research projects in North America, Europe, Asia, and Latin America, the results of which have informed decisions regarding carbon monoxide, air toxics, nitrogen oxides, diesel exhaust, ozone, particulate matter, and other pollutants. These results have appeared in more than 260 comprehensive reports published by HEI, as well as in more than 1000 articles in the peer-reviewed literature.

HEI's independent Board of Directors consists of leaders in science and policy who are committed to fostering the public–private partnership that is central to the organization. The Health Research Committee solicits input from HEI sponsors and other stakeholders and works with scientific staff to develop a Five-Year Strategic Plan, select research projects for funding, and oversee their conduct. The Health Review Committee, which has no role in selecting or overseeing studies, works with staff to evaluate and interpret the results of funded studies and related research.

All project results and accompanying comments by the Health Review Committee are widely disseminated through HEI's Web site (*www.healtheffects.org*), printed reports, newsletters and other publications, annual conferences, and presentations to legislative bodies and public agencies.

ABOUT THIS REPORT

Research Report 182, *Synergistic Effects of Particulate Matter and Substrate Stiffness on Epithelial-to-Mesenchymal Transition,* presents a research project funded by the Health Effects Institute and conducted by Dr. Thomas H. Barker of the Wallace H. Coulter Department of Biomedical Engineering, Georgia Institute of Technology and Emory University, Atlanta, Georgia, and his colleagues. This research was funded under HEI's Walter A. Rosenblith New Investigator Award Program, which provides support to promising scientists in the early stages of their careers. The report contains three main sections.

The HEI Statement, prepared by staff at HEI, is a brief, nontechnical summary of the study and its findings; it also briefly describes the Health Review Committee's comments on the study.

The Investigators' Report, prepared by Barker and colleagues, describes the scientific background, aims, methods, results, and conclusions of the study.

The Critique is prepared by members of the Health Review Committee with the assistance of HEI staff; it places the study in a broader scientific context, points out its strengths and limitations, and discusses remaining uncertainties and implications of the study's findings for public health and future research.

This report has gone through HEI's rigorous review process. When an HEI-funded study is completed, the investigators submit a draft final report presenting the background and results of the study. This draft report is first examined by outside technical reviewers and a biostatistician. The report and the reviewers' comments are then evaluated by members of the Health Review Committee, an independent panel of distinguished scientists who have no involvement in selecting or overseeing HEI studies. During the review process, the investigators have an opportunity to exchange comments with the Review Committee and, as necessary, to revise their report. The Critique reflects the information provided in the final version of the report.

HEI STATEMENT

Synopsis of Research Report 182

Synergistic Effects of Particulate Matter and Substrate Stiffness on Epithelial-to-Mesenchymal Transition

BACKGROUND

Exposure to particulate matter (PM) from combustion sources has been associated with lung inflammation and injury, which trigger repair responses to restore normal tissue function. Dysregulation of these responses can result, over time, in fibrotic changes characterized by increased numbers of fibroblasts and myofibroblasts and abnormal deposition of collagen and fibronectin in the extracellular matrix, with consequent increases in matrix stiffness and impairment of gas exchange. One theory proposes that the fibroblasts are derived from alveolar epithelial cells that differentiate into mesenchymal cells. This process is referred to as epithelial-to-mesenchymal transition (EMT). Fibrosis in the lung can be progressive and fatal, as in idiopathic fibrosis, and is also a feature of chronic pulmonary diseases such as asthma, and it is thus important to understand profibrotic processes.

In the current study Dr. Thomas H. Barker, who was a recipient of HEI's Walter A. Rosenblith New Investigator Award, and his colleagues tested the hypotheses that alveolar epithelial cells grown on fibronectin substrates of increasing stiffness would undergo EMT and that the addition of fine PM (PM $\leq$ 2.5 µm in aerodynamic diameter [$PM_{2.5}$]) would enhance these effects.

APPROACH

These hypotheses were tested in cells grown in vitro using a combination of mechanical and biologic approaches. The investigators addressed the following specific aims: (1) determine the effects of substrate stiffnesses that ranged from values seen in healthy tissue to those seen in fibrotic tissue on lung-epithelial-cell contractility, induction of EMT, and activation of transforming growth factor beta (TGF-β), a key factor in the development of fibrosis, and (2) determine whether exposure to $PM_{2.5}$ exacerbates the effects of substrate stiffness on EMT and cell contractility.

The substrates on which the cells were grown consisted of polyacrylamide–bisacrylamide gels cross-linked to fibronectin. Various concentrations of bisacrylamide were used to achieve increasing degrees of stiffness. After allowing the cells to grow

What This Study Adds

- Barker and colleagues developed a useful and novel in vitro cell model to study the interaction between extracellular matrix stiffness and the transition of lung epithelial cells to mesenchymal cells — a process that could lead to fibrosis — and the potential effects of PM on this process.
- The results showed that ATII epithelial cells transitioned to mesenchymal cells on substrates of greater stiffness, as documented by loss of cell circularity, changes in the expression of E-cadherin and α-SMA, and increased activation of TGF-β and that the addition of ambient PM enhanced the effect of substrate stiffness on EMT and TGF-β activation, as compared with non-exposed cells.
- This study highlights the potential importance of cell–matrix interactions when evaluating the effects of environmental triggers, but more work will be needed to understand how PM might affect such interactions and to determine whether the mechanisms are relevant to in vivo processes.

This Statement, prepared by the Health Effects Institute, summarizes a research project funded by HEI and conducted by Dr. Thomas H. Barker at the Georgia Institute of Technology and Emory University, Atlanta, Georgia, and colleagues. Research Report 182 contains both the detailed Investigators' Report and a Critique of the study prepared by the Institute's Health Review Committee.

on the substrates for five days, Barker and colleagues assessed EMT through changes in cell shape, cell contractility (measured as stiffness), and expression of the cellular protein E-cadherin, a marker of epithelial cells, and alpha smooth muscle actin (α-SMA), a marker of mesenchymal cells. They also measured activation of TGF-β. To study the effects of ambient PM on EMT, the investigators grew the cells in the presence of resuspended $PM_{2.5}$ previously collected on filters in areas near roads in Atlanta.

RESULTS AND INTERPRETATION

Cultured alveolar type II (ATII) rat epithelial cells transitioned to mesenchymal cells on substrates of increased stiffness, as documented by loss of cell circularity, decreased expression of E-cadherin, and increased expression of α-SMA. Increased substrate stiffness was associated with increased cell stiffness and increased activation of TGF-β. The role of TGF-β was further demonstrated in an experiment in which ATII cells were grown on a soft substrate in media containing various concentrations of active TGF-β for two or five days. Exposure to TGF-β for five days was associated with decreased cell circularity, changes in surface markers, and increased cell stiffness.

Addition of ambient $PM_{2.5}$ at the highest concentration (corresponding to 10 μg/cm^2) increased EMT as measured by reduced cell circularity, decreased expression of E-cadherin, and increased expression of α-SMA, as compared with the responses in non-exposed cells at the same substrate stiffness. Cell stiffness also increased after exposure to $PM_{2.5}$, as compared with the non-exposed cells. In addition, ATII cells showed greater TGF-β activation with increasing substrate stiffness when exposed to $PM_{2.5}$ compared with the non-exposed cells.

In its independent review of the study, the HEI Health Review Committee noted that this was a carefully performed study with interesting mechanistic observations. The in vitro model of cell cultures grown on substrates of various degrees of stiffness was seen as novel and potentially useful for understanding the role of matrix stiffness in EMT. The methods used were thought to be appropriate and to reflect the state of the art. The combination of biologic and mechanical techniques for assessing interactions between airway epithelial cells and the underlying matrix and for characterizing EMT was a strength of the work.

Although the Committee had some concerns about the statistical analyses, it agreed with the investigators' overall conclusions that the results supported the hypothesis that the stiffness of the extracellular matrix drives EMT and increases cell contractility and that activation of TGF-β played a key role in EMT in the investigators' cell culture system. The results also supported the investigators' hypothesis that exposure to PM would enhance the effect of substrate stiffness on EMT and TGF-β activation.

CONCLUSIONS

Overall, the study by Barker and colleagues highlighted the potential importance of cell–matrix interactions when evaluating the effects of environmental triggers and provides a basis for future research. Considerable work will be needed to confirm these initial observations, understand the mechanisms, and determine whether they are relevant to in vivo processes and the development of fibrosis.

INVESTIGATORS' REPORT

Synergistic Effects of Particulate Matter and Substrate Stiffness on Epithelial-to-Mesenchymal Transition

Thomas H. Barker, Marilyn M. Dysart, Ashley C. Brown, Alison M. Douglas, Vincent F. Fiore, and Armistead G. Russell

Wallace H. Coulter Department of Biomedical Engineering, Georgia Institute of Technology and Emory University, Atlanta, Georgia (T.H.B., M.M.D., A.C.B., A.M.D., V.F.F.); and School of Civil and Environmental Engineering, Georgia Institute of Technology, Atlanta, Georgia (A.G.R.)

ABSTRACT

Dysfunctional pulmonary homeostasis and repair, including diseases such as pulmonary fibrosis, chronic obstructive pulmonary disease (COPD*), and tumorigenesis, have been increasing steadily over the past decade, a fact that heavily implicates environmental influences. Several investigations have suggested that the lung "precursor cell" — the alveolar type II (ATII) epithelial cell — is central in the initiation and progression of pulmonary fibrosis. Specifically, ATII cells have been shown (Iwano et al. 2002) to be capable of undergoing an epithelial-to-mesenchymal transition (EMT). EMT, the de-differentiation of an epithelial cell into a mesenchymal cell, has been theorized to increase the number of extracellular matrix (ECM)-secreting mesenchymal cells, perpetuating fibrotic conditions and resulting in increased lung tissue stiffness. In addition, increased exposure to pollution and inhalation of particulate matter (PM) have been shown to be highly correlated with an increased incidence of pulmonary fibrosis. Although both of these events are involved in the progression of pulmonary fibrosis, the relationship between tissue stiffness, exposure to PM, and the initiation and course of EMT remains unclear.

The hypothesis of this study was twofold:

1. That alveolar epithelial cells cultured on increasingly stiff substrates become increasingly contractile, leading to enhanced transforming growth factor beta (TGF-β) activation and EMT; and
2. That exposure of alveolar epithelial cells to PM with an aerodynamic diameter $\leq$ 2.5 μm ($PM_{2.5}$; also known as fine PM) results in enhanced cell contractility and EMT.

Our study focused on the relationship between the micromechanical environment and external environmental stimuli on the phenotype of alveolar epithelial cells.

This relationship was explored by first determining how increased tissue stiffness affects the regulation of fibronectin (Fn)-mediated EMT in ATII cells in vitro. We cultured ATII cells on substrates of increasing stiffness and evaluated changes in cell contractility and EMT. We found that stiff, but not soft, Fn substrates were able to induce EMT and that this event depended on a contractile phenotype of the cell and the subsequent activation of TGF-β. In addition, we were able to show that activation or suppression of cell contractility by way of exogenous factors was sufficient to overcome the effect of substrate stiffness. Pulse–chase experiments indicated that the effect on cell contractility is dose- and time-dependent. In response to low levels of TGF-β on soft surfaces, either added exogenously or produced through contraction induced by the stiffness agonist thrombin, cells initiate EMT; on removal of the TGF-β, they revert to an epithelial phenotype. Overall, the results from this first part of our study identified matrix stiffness or cell contractility as critical targets for the control of EMT in fibrotic diseases.

This Investigators' Report is one part of Health Effects Institute Research Report 182, which also includes a Critique by the Health Review Committee and an HEI Statement about the research project. Correspondence concerning the Investigators' Report may be addressed to Dr. Thomas H. Barker, the Wallace H. Coulter Department of Biomedical Engineering at Georgia Institute of Technology and Emory University, 313 Ferst Drive, Suite 2108, Atlanta, GA 30332-0535; e-mail: *thomas.barker@bme.gatech.edu*.

Although this document was produced with partial funding by the United States Environmental Protection Agency under Assistance Award CR-83467701 to the Health Effects Institute, it has not been subjected to the Agency's peer and administrative review and therefore may not necessarily reflect the views of the Agency, and no official endorsement by it should be inferred. The contents of this document also have not been reviewed by private party institutions, including those that support the Health Effects Institute; therefore, it may not reflect the views or policies of these parties, and no endorsement by them should be inferred.

* A list of abbreviations and other terms appears at the end of the Investigators' Report.

For the second part of our study, we wanted to investigate whether exposure to $PM_{2.5}$, which might have higher toxicity than coarser PM because of its small size and large surface-to-mass ratio, altered the observed stiffness-mediated EMT. Again, we cultured ATII cells on increasingly stiff substrates with or without the addition of three concentrations of $PM_{2.5}$. We found that exposure to $PM_{2.5}$ was involved in increased stiffness-mediated EMT, as shown by increases in mesenchymal markers, cell contractility, and TGF-β activation. Most notably, on substrates with an elastic modulus (*E*) of 8 kilopascals (kPa), a physiologically relevant range for pulmonary fibrosis, the addition of $PM_{2.5}$ resulted in increased mesenchymal cells and EMT; these were not seen in the absence of the $PM_{2.5}$.

Overall, this study showed that there is a delicate balance between substrate stiffness, TGF-β, and EMT. Furthermore, we showed that exposure to $PM_{2.5}$ is able to further mediate this interaction. The higher levels of EMT seen with exposure to $PM_{2.5}$ might have been a result of a positive feedback loop, in which enhanced exposure to $PM_{2.5}$ through the loss of cell–cell junctions during the initial stages of EMT led to the cells being more susceptible to the effects of surrounding immune cells and inflammatory signals that can further activate TGF-β and drive additional EMT progression. Overall, our work — showing increased cell contractility, TGF-β activation, and EMT in response to substrate stiffness and $PM_{2.5}$ exposure — highlights the importance of both the micromechanical and biochemical environments in lung disease. These findings suggest that already-fibrotic tissue might be more susceptible to further damage than healthy tissue when exposed to $PM_{2.5}$.

INTRODUCTION

Dysfunctional pulmonary homeostasis and repair, including diseases such as pulmonary fibrosis, COPD, and tumorigenesis, have been steadily increasing over the past decade. Mounting evidence suggests that the ATII epithelial cell is a key player in the initiation and progression of these diseases. Although the exact mechanisms have yet to be elucidated, it is generally accepted that ATII epithelial cells can undergo EMT, leading to secretory fibroblasts (Selman and Pardo 2006; Thannickal and Horowitz 2006; Thiery et al. 2009).

In addition, pollution and PM have been linked to adverse pulmonary health effects and increased mortality. Environmental PM is capable of depositing in the airways, penetrating into the alveoli, increasing respiratory distress, and exacerbating pre-existing pulmonary conditions. Previous studies have highlighted the potential role of PM exposure in predisposing patients to asthma and pulmonary fibrosis (Thevenot et al. 2013). In addition, PM has been shown to have secondary effects that can induce cellular damage that stimulates fibrotic remodeling. To date, the link between PM exposure and a predisposition to pulmonary conditions has remained unclear. In addition, the interplay between the presence of lung disease, such as pulmonary fibrosis, and subsequent PM interactions has yet to be studied.

Furthermore, recent evidence indicates (1) that the mechanical properties of the ECM, specifically its stiffness, play a critical role in directing the cell phenotype and (2) that the mechanical properties of lung tissue change during fibrotic progression. The mechanical properties of the ECM can exert both biophysical and biochemical (molecular) effects on resident cells. First, cells actively engage their contractile machinery in order to "match" their internal stiffness with their extracellular environment. Second, many ECM proteins, such as Fn, show force-mediated unfolding, resulting in the exposure of cryptic, or hidden, sequences that then influence the cell phenotype. These facts imply a role for lung ECM stiffness, associated with pulmonary fibrosis, in regulating lung cell behaviors, such as PM-induced EMT. In this study, we explored the contribution of ECM mechanics to pulmonary homeostasis and pathologic progression by examining the relationship between increases in lung ECM stiffness, exposure to $PM_{2.5}$, and ATII epithelial cell EMT.

BACKGROUND

ATII CELLS IN PULMONARY HOMEOSTASIS AND REPAIR

The ATII epithelial cell is the primary cell type associated with the proper maintenance of pulmonary tissue (i.e., alveolar homeostasis and repair). Adult pulmonary tissue consists of more than 40 cell types and 300 million alveoli, the primary functional structure of the lung. Two primary epithelial cells populate the alveolus, alveolar type I (ATI) and ATII epithelial cells. ATI cells, separated from capillaries by only a thin basement membrane, are the primary gas-exchange cells and make up 90% of the alveolar surface but only 10% of epithelial cells by number (Fehrenbach 2001; Mason 2006). ATII cells are pseudocuboidal, multifunctional cells that are considered the "protector of the alveolus" because of their central role in defense and repair. ATII cells act as the primary surfactant-secreting cell, as precursors to ATI cells, and in many instances as nonprofessional antigen-presenting cells (Mason 2006). They also contribute significantly to the

fluid balance across the epithelial barrier through sodium-transport functions (Jain et al. 2001). These various functions underscore the vital importance of these cells in maintaining pulmonary function. During normal repair, ATII cells are thought to proliferate, migrate onto a provisional matrix, and differentiate into ATI cells. Despite these cells' obvious beneficial effects, recent evidence suggests that repeated injury of ATII cells might be a primary cause of pulmonary fibrotic disorders (Fehrenbach 2001; Selman and Pardo 2006; Thannickal and Horowitz 2006; Uhal et al. 1998). Lung biopsies of patients with pulmonary fibrosis show fragmented DNA (indicative of apoptosis) in alveolar epithelium (Kuwano et al. 1996), and apoptotic alveolar epithelial cells have been observed adjacent to myofibroblast foci (Batlle et al. 2000; Guaita et al. 2002; Uhal et al. 1998). One emerging, albeit controversial, hypothesis is that ATII cells undergo a process of EMT, resulting in an increase in the number of ECM-secreting mesenchymal cells and subsequent increases in tissue stiffness.

EPITHELIAL-TO-MESENCHYMAL TRANSITION IN LUNG FIBROSIS

Fibrotic pathologies are characterized by excessive ECM production, formation of interstitial scar tissue, and an increase in tissue stiffness. During the course of idiopathic pulmonary fibrosis, functional lung tissue of the alveoli is replaced with collagen-rich ECM, leading to rapid and severe decreases in lung compliance and irreversible loss of lung function (Maher et al. 2007; Meltzer and Noble 2008). Idiopathic pulmonary fibrosis is a currently untreatable and ultimately fatal condition with three- and five-year mortality rates of 50% and 80%, respectively (Spruit et al. 2009). In addition to the formation of scar tissue, another hallmark of idiopathic pulmonary fibrosis and other fibrotic conditions is the influx of extremely contractile myofibroblasts. This influx further exacerbates the disease through persistent matrix production and contraction, contributing to increased cytokine activation. Lack of effective treatment options for the disease, and for many other fibrotic diseases, is largely caused by lack of understanding of the exact mechanisms that initiate fibrosis. However, recent studies implicate alveolar EMT in the onset and progression of fibrosis (Degryse et al. 2011; Kasai et al. 2005; Kim et al. 2006; Willis et al. 2005; Wynn 2008; Xu et al. 2009). EMT has been theorized to increase the number of ECM-secreting mesenchymal cells, and cell tracking studies have demonstrated that a considerable number of myofibroblasts arise from EMT (Degryse et al. 2011; Iwano et al. 2002; Kim et al. 2006; Wynn 2008; Xu et al. 2009).

EMT is the de-differentiation of an epithelial cell into a mesenchymal cell and is defined through the loss of apical–basolateral polarity, loss of tight cell junctions, and a marked down-regulation of E-cadherin. These changes are accompanied by a concomitant up-regulation of alpha smooth muscle actin (α-SMA), increased stress-fiber formation and alignment, increased migration through filopodia and lamellopodia formation, and increased synthesis of ECM. EMT is important during normal cellular processes in wound healing, embryogenesis, and development, contributing to wound closure, blastocyst implantation, gastrulation, generation of the neural crest, and palate closure (Duband and Thiery 1982; Hay 1995; Vicovac and Aplin 1996). Though EMT is an important cellular transition, it can, if not tightly regulated, lead to aberrant wound healing and scar tissue formation in mature tissues, contributing to pathologic conditions such as pulmonary fibrosis.

EMT has been shown to occur in response to several factors, including growth factors such as TGF-β, tumor necrosis factor alpha (TNF-α), and epidermal growth factor; reactive oxygen species; and ECM proteins such as Fn (Arnoux et al. 2008; Camara and Jarai 2010; Felton et al. 2009; Gharaee-Kermani et al. 2009; Willis and Borok 2007). The role of TGF-β is the most well defined of these factors and is known to be a potent inducer of EMT. TGF-β signaling is quite complex and can activate a number of different pathways, including SMAD-dependent and -independent pathways (Derynck and Zhang 2003; Rahimi and Leof 2007; Shi and Massague 2003). SMAD-dependent signaling can lead to Snail1 activation, which plays a role in EMT by down-regulating E-cadherin expression and up-regulating a number of mesenchymal genes, including α-SMA (Batlle et al. 2000; Boutet et al. 2006; Guaita et al. 2002). Though many advances have been made in understanding the factors contributing to EMT, the exact events leading to its initiation are still unclear. In this study, we explored how both increases in tissue stiffness and exposure to $PM_{2.5}$ affect the induction and progression of EMT.

MECHANICS IN TISSUE HOMEOSTASIS AND REPAIR

The composition of the ECM surrounding a cell has great consequences for the fate of the cell. However, evidence is mounting that cells also sense and respond to the ECM's mechanical properties, particularly the stiffness of the matrix. This cellular sensing of and responding to the ECM's mechanical properties has been termed mechanotransduction. Matrix stiffness has been shown to influence many aspects of cellular behavior, including stem cell, myoblast, and breast epithelial cell differentiation; cellular motility; contractility; and focal adhesion formation. It has

also been shown to contribute to or prevent a malignant phenotype (Choquet et al. 1997; Engler et al. 2004, 2006; Georges and Janmey 2005; Paszek et al. 2005; Pelham and Wang 1997, 1998; Vogel and Sheetz 2006; Wozniak et al. 2003). Previous work has shown that stem cell differentiation can be guided by underlying matrix mechanics, with mesenchymal stem cells on stiff substrates differentiating down an osteoblastic lineage and, on soft substrates, differentiating down a neuronal lineage, which suggests a potential mechanism through which stem cells "match" their differentiation based on the surrounding tissue (Engler et al. 2006). Interestingly, as previously described (Abe et al. 1994), changes in tissue stiffness, specifically an increase in rigidity and hardening of tissue, are associated with the pathologic progression of fibrotic responses. Recent atomic force microscopy (AFM) analyses of fibrotic tissue from mice with bleomycin-induced pulmonary fibrosis showed a nine-fold increase in the stiffness of fibrotic tissue, as compared with that of normal tissue (Liu et al. 2010).

It has also recently been shown that mesenchymal cells respond to substrate stiffness by engaging their actin–myosin contractile machinery in a manner that facilitates cell–ECM compliance matching. This has been demonstrated by AFM analysis of single-cell stiffness, which showed that fibroblasts become increasingly contractile (i.e., stiff) on increasingly stiff substrates, indicating that a cell might adjust its internal stress through contraction to "match" its external environment (Georges and Janmey 2005). As a consequence of this mechano-homeostasis between the cell and its ECM, cells in increasingly stiff environments show increased activation of contractile signals such as Rho and Rho-associated kinase (ROCK), resulting in multiple and diverse secondary effects. An elegant example of this was shown by Wipff and colleagues, who demonstrated that fibroblast activation of TGF-β increases on increasingly stiff substrates, leading to greater myofibroblast differentiation on stiff, but not soft, substrates (Wipff and Hinz 2008; Wipff et al. 2007). Because fibrotic diseases are characterized by increased tissue stiffness, and because of TGF-β's prominent role in the onset of EMT, we hypothesized that a similar mechanism of increased TGF-β activation with increasing tissue stiffness would contribute to EMT.

Although the exact mechanism of cell stiffness sensing remains unknown, it likely involves the transduction of stiffness-mediated signaling via the ECM. Our study explored the role of mechanotransduction events in the onset and progression of EMT by studying the role of substrate stiffness in Fn-mediated EMT.

FIBROTIC RESPONSES TO PM EXPOSURE

A complex set of reactions must occur for the formation and accumulation of fibrous tissue seen in pulmonary fibrosis. The pathogenesis of pulmonary fibrosis is thought to begin as an inflammatory response to injury when immune cells are excessively or improperly activated. These immune cells release toxic mediators that compromise epithelial integrity and promote further tissue injury (Bonner 2007; Maher et al. 2007; Meltzer and Noble 2008; Spruit et al. 2009; Wynn 2008). The repair process involves recruitment of mesenchymal cells, which lay down ECM; re-epithelialization; and restoration of normal lung structure. However, aberrant tissue remodeling can occur, which results in excessive matrix deposition leading to pulmonary fibrosis. Although yet to be studied, inhalation of PM might under some conditions cause a sustained inflammatory response that can lead to aberrant tissue remodeling. This remodeling might be involved in the initiation and progression of pulmonary diseases such as pulmonary fibrosis (Holgate et al. 2000).

PM generated from a variety of sources has the ability to cause or exacerbate lung diseases, including asthma, bronchitis, and COPD (Anderson et al. 2008; Becker et al. 1996; Bonner 2007). Fibrotic responses are seen in each of these diseases and involve increases in the deposition of ECM by pulmonary fibroblasts. The fibrogenic potential of PM has been shown to be caused by several factors, including particle size, surface area, and composition; smaller inhaled PM in the range of 1 to 10 μm can reach the distal lung and have a greater potential to cause injury because of its high surface-to-mass ratio (Abbey et al. 1999; Bonner 2007; Oberdörster et al. 2005; Riva et al. 2011). In addition, PM composition is likely an important determinant of the effect of the PM on the progression of fibrotic diseases. Both organic and inorganic agents, such as transition metals, hydrocarbons, and endotoxins, can contribute to the composition of PM (Diaz-Sanchez et al. 2000; Dreher et al. 1997; Oberdörster et al. 2005). Previous studies have found that many of the components of PM are able to activate the inflammatory response, leading to widespread secondary effects. For example, several air pollution sources have been shown to stimulate the release of TNF-α. Although TNF-α does not directly promote fibroblast growth or the deposition of ECM proteins, it stimulates the production of TGF-β, a major stimulant for EMT that leads to the presence of myofibroblasts and the subsequent ECM deposition commonly seen in pulmonary fibrosis (Mazzoli-Rocha et al. 2010; Riva et al. 2011; Veljkovic et al. 2011; Zhou et al. 2009).

SPECIFIC AIMS

The central hypothesis of this study was that increased stiffness of Fn ECM, which is commonly associated with pulmonary fibrosis, induces cell contractility, TGF-β activation, and subsequent EMT — and that the addition of an environmental stimulus ($PM_{2.5}$) enhances these effects. The hypothesis was tested through the completion of the following specific aims:

SPECIFIC AIM 1

Our first specific aim was to determine the effects of physiologically relevant healthy and fibrotic matrix stiffnesses on cell contractility and the induction of EMT. Nanoindentation testing of the interstitial spaces of healthy and fibrotic lung tissues was performed to evaluate differences in tissue stiffness in vivo. Alveolar epithelial cells were then cultured on increasing substrate stiffnesses corresponding to the range of stiffnesses found in healthy and fibrotic lung tissues, and cell contraction, TGF-β activity, and EMT events were evaluated.

SPECIFIC AIM 2

Our second specific aim was to determine whether exposure to $PM_{2.5}$ exacerbates the induction of stiffness-mediated EMT. Alveolar epithelial cells were cultured on increasingly stiff substrates with or without the addition of various concentrations of $PM_{2.5}$-treated media. Cell contractility, TGF-β activity, and EMT events were analyzed and compared with the results from Aim 1 to determine whether exposure to the $PM_{2.5}$ exacerbated the effects of the stiffness-mediated EMT.

METHODS

ANIMALS AND BLEOMYCIN-INDUCED FIBROSIS

Eight-to-10-week-old C57BL/6 mice were purchased from Charles River Laboratories (Wilmington, MA) and housed in an animal facility approved by the National Institutes of Health (NIH) and the Institutional Animal Care and Use Committee (IACUC) of the Georgia Institute of Technology. The mice were housed in laminar-flow cages under controlled temperature and humidity conditions and a 12-hour light–dark cycle. Food and water were provided ad libitum. The mice were intubated, and 3.2 U/kg bleomycin (EMD Chemicals, Gibbstown, NJ) was instilled intratracheally. The mice were killed after 14 days for lung tissue harvesting. All experiments were performed in accordance with guidelines set forth by the NIH and the IACUC-approved protocols of the Georgia Institute of Technology.

LUNG TISSUE PREPARATION

The lungs were inflated using 2% ultralow-melting-point agarose (SeaPrep; Lonza, Allendale, NJ), warmed to 37°C, and subsequently allowed to solidify on ice. The left lobe was dissected, and 100-μm-thick slices were generated using a vibratome (VT100S; Leica Microsystems, Buffalo Grove, IL). The slices were stained with fluorescein-labeled lectin from the crybaby tree (*Erythrina crysta-galli*) (ECL; Vector Laboratories, Burlingame, CA), red-fluorescent dye (LysoTracker Red; Invitrogen, Carlsbad, CA), and nucleic-acid stain (Hoechst 33258; Invitrogen) to visualize ATII, ATI, and nuclei, respectively.

NANOINDENTATION ANALYSIS

The lung slices were mounted on a 0.17-mm-thick glass-bottom Petri dish (World Precision Instruments, Sarasota, FL) using surgical-grade cyanoacrylate for AFM analysis. The analysis took place in fully supplemented media within four to six hours after harvesting the lungs to ensure tissue and host cell viability. Using an AFM instrument with an inverted optical platform (MFP-3D-BIO; Asylum Research, Goleta, CA), 20-by-20-μm regions of tissue were measured by force spectroscopy using the contact mode at a scan rate of 1.2 Hz. Thirty-two measurements were taken per 20-μm line, yielding 1024 data points per scan field. The silicon nitride AFM tip (Veeco, Plainview, NY) was customized with a 4.74-μm-diameter polystyrene bead to allow for imaging at appropriate resolution scales and for elastic-modulus determination using the Hertz contact model. The single cantilever's unique spring constants were determined using the thermal resonance frequency method, with values typically ranging from 0.1 to 0.3 N/m. To determine the Young elastic modulus (E) of each contact point, the Hertz contact model for determining the elastic forces between two spheres was used:

$$\frac{E}{1-\nu^2} = \frac{3}{4}\frac{kx_c}{\sqrt{R}\left(x_s - x_c - cp\right)^{3/2}}. \quad (1)$$

Using known values from the AFM measurements (x_s is the scanner displacement, x_c is the cantilever displacement, and cp is the contact point) and predetermined values for the cantilever spring constant (k) and beaded-tip radius (R), the equation can be solved for E (bead force, F_b, is equal to kx_c). The assumption of an isotropic material (i.e., that the Poisson ratio [ν] is equal to 0.5) is valid for the small indentation depths under consideration.

POLYACRYLAMIDE GEL PRODUCTION

Polyacrylamide (PA) gels of varying bisacrylamide concentrations were created on amino-silanated coverslips, as previously described (Tse and Engler 2010). PA gel solutions were produced by combining acrylamide and bisacrylamide to final concentrations of 8% acrylamide (Biorad, Hercules, CA) and 0.048%, 0.117%, 0.208%, 0.260%, or 0.391% bisacrylamide (Biorad) to obtain gels with final elastic moduli of 2, 8, 16, 24, or 32 kPa, respectively. Fifty μL of each solution was polymerized by the addition of ammonium persulfate (VWR, West Chester, PA) and N,N,N′,N′-tetramethylethylenediamine (Biorad) (at 1% and 0.1% final concentrations, respectively). The gels were allowed to polymerize for approximately 30 minutes, then washed three times with phosphate-buffered saline. Fn was covalently attached to the surface using the heterobifunctional cross-linker sulfosuccinimidyl 6-(4′-azido-2′-nitrophenylamino) hexanoate (sulfo-SANPAH; Pierce Chemical, Rockford, IL). Following an overnight incubation with the Fn, the gels were washed three times with phosphate-buffered saline.

CELL ISOLATION AND MAINTENANCE

RLE-6TN Cell Line

Rat lung epithelial-T-antigen negative (RLE-6TN) cells (an immortalized cell line derived from ATII cells) (American Type Culture Collection, Manassas, VA) were maintained in Dulbecco's Modified Eagle's Medium with Ham's F-12 Nutrient Mixture (DMEM/F12), 10% fetal bovine serum (FBS), and 1% penicillin–streptomycin at 37°C and 5% CO_2. The medium was refreshed every two to three days, and the cells were split upon reaching 95% confluency.

Isolation and Culture of Primary ATII Cells

Primary pulmonary ATII cells were isolated from Sprague Dawley male rats, as previously described (Annes et al. 2004). Briefly, after pentobarbital–heparin anesthesia, the rat renal artery was ligated, the trachea was cannulated with a 14-gauge trachea tube, and the chest was opened. The lungs were perfused with a balanced salt solution, lavaged with a balanced salt solution containing ethylene glycol tetraacetic acid, digested with elastase, and selected through immunoglobulin panning. The cells were then plated immediately in DMEM/F12 medium with 10% Fn-depleted FBS and incubated at 37°C and 5% CO_2. After 24 hours, the medium was changed to a serum-free minimally defined medium containing DMEM/F12 with 10 mM HEPES buffering agent, 2mM glutamine, 1% penicillin–streptomycin, 1% bovine serum albumin, and 0.1 mM nonessential amino acids.

CELL CULTURE STUDIES OF SUBSTRATE STIFFNESS

To determine the effects of substrate stiffness on EMT in ATII cells, primary alveolar epithelial cells or RLE-6TN cells were plated on PA gels with Fn cross-linked on the surface for various stiffnesses ranging from 2 to 32 kPa or on glass coverslips coated with 2 μM Fn or laminin (Ln) as positive and negative controls, respectively. The primary ATII cells were isolated from Sprague Dawley male rats and plated immediately on the PA gels or glass controls in DMEM/F12 medium with 10% FBS and incubated at 37°C and 5% CO_2. The RLE-6TN cells were grown in DMEM/F12 medium supplemented with 10% FBS and 1% penicillin–streptomycin. The cells were plated at a density of 100,000 cells/cm^2 in growth media in the absence or presence of 10 μM ROCK inhibitor Y-27632 (EMD Millipore, Billerica, MA). To determine the roles of contractility or TGF-β in stiffness-mediated EMT, the cells were cultured on soft substrates (2 kPa) in the presence of 0.5–4.0 U/mL thrombin (MP Biomedicals, Santa Ana, CA), 0.01–5 ng/mL active TGF-β (R&D Systems, Minneapolis, MN), or 5 ng/mL TGF-β and 10 μg/mL TGF-β-neutralizing antibody (9016, R&D Systems). Cells were also cultured on stiff substrates (32 kPa) in the presence of 10 μg/mL TGF-β-neutralizing antibody or 10 μg/mL integrin-αvβ6-inhibiting antibody (10D5, EMD Millipore, Billerica, MA). The media were changed every 48 hours. EMT events were analyzed after five days in culture, because RLE-6TN cells are known to undergo EMT in response to EMT-inducing stimuli in this time frame (Felton et al. 2009). In dose–response and time-course experiments determining the role of the TGF-β and thrombin in EMT induction on soft substrates, the EMT was also characterized after two days.

$PM_{2.5}$ ISOLATION AND CELL CULTURE EXPERIMENTS

$PM_{2.5}$ samples were collected on Teflon filters in DeKalb County, in the Atlanta, Georgia, area, as part of the Assessment of Spatial Aerosol Composition in Atlanta (ASACA) study conducted by the Georgia Tech School of Civil and Environmental Engineering. The sampling site was in South DeKalb near two busy interstate highways (I-20 and I-285) with elevated concentrations of PM generated by mobile sources.

The samples were collected daily, using three-channel particle composition monitors (PCMs). In each channel of the PCMs, the air first passed through a cyclone to remove particles greater than 10 μm in diameter. In the first channel, the air next passed through a Well Impactor Ninety-Six (WINS) impactor to remove particles greater than 2.5 μm in diameter, and the remaining particles (i.e., the $PM_{2.5}$ fraction) were collected on a Teflon filter. In the second channel, after passing though the cyclone, the air

passed through an annular denuder to remove acidic and alkaline gases. It then passed through a WINS impactor, and the remaining particles were captured on a nylon filter for analysis of ionic species. In the third channel, after passing through the cyclone, the air passed through a denuder in order to remove organic gases, followed by a WINS impactor, and the particles were collected on a quartz filter for analysis of organic and elemental carbon. After collection, the filters were stored at −20°C for later chemical analysis; the Teflon filters were stored for exploratory studies (such as the work presented in the current study). The PCM setup is shown in Figure 1.

In order to prepare the $PM_{2.5}$ fraction for our cell culture experiments, five different $PM_{2.5}$-containing Teflon filters were weighed to determine the total particulate mass on each filter. The five samples were pooled together to minimize variation based on the day of collection. First, they were placed in a sterile 50-mL centrifuge tube fully covered with 5 mL deionized water, and sonicated for 10 minutes five times to release the particles captured on the filters. The solution containing the samples were passed through a filter with a 5-µm-diameter pore size to remove any larger particle debris and resuspended in DMEM/F12 medium to a final concentration of 100 µg/mL. Serial dilutions were then performed to prepare our final experimental dilutions of 1:100, 1:1000, and 1:10,000, which correspond to concentrations of approximately 10, 1.0, and 0.1 µg/cm^2, respectively. RLE-6TN cells were maintained and passaged in DMEM/F12 medium supplemented with 10% FBS and 1% penicillin–streptomycin. The particulate-containing media were made fresh for each experiment, keeping the total $PM_{2.5}$ mass from the pooled filters consistent for each preparation. The fresh media were then added directly to cell culture wells of varying substrate stiffnesses. Each cell culture well corresponded to a single experimental condition. Each condition was repeated in triplicate within each whole experiment, and the whole experiment was repeated three times.

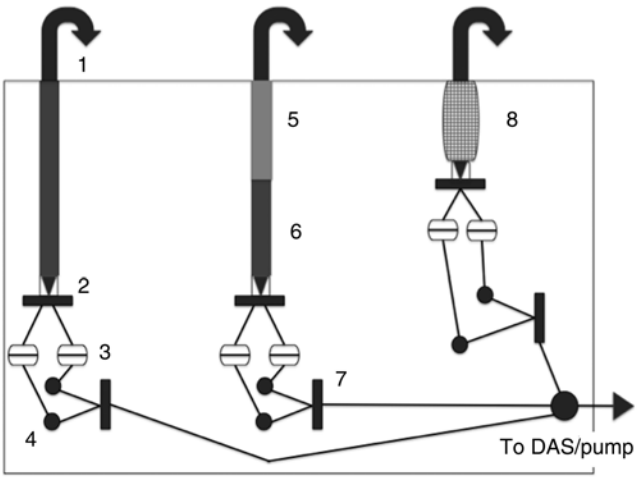

Figure 1. Schematic of particle composition monitor. 1 = 10-mm cyclone inlet. 2 = WINS impactor. 3 = filter pack with Teflon filter for quantification of metal species. 4 = solenoid valves. 5 = annular denuder coated with sodium carbonate. 6 = annular denuder coated with citric acid. 7 = mass flow controller. 8 = parallel-plate charcoal-impregnated cellulose fiber filter denuder. (Adapted from Butler et al. 2003.)

IMMUNOFLUORESCENCE STAINING FOR EMT MARKERS AND CELL SHAPE ANALYSIS

After culturing for five days, the cells were washed with phosphate-buffered saline, fixed with 4% formaldehyde, permeabilized with 0.2% Triton-X 100, and blocked with 10% goat serum. Primary anti-α-SMA (1A4, Sigma-Aldrich, St. Louis, MO) or anti-E-cadherin (36/E-cadherin, BD Biosciences, San Jose, CA) antibodies were incubated overnight and then washed thoroughly with phosphate-buffered saline and 1.5% goat serum. Alexa Fluor 488–conjugated goat anti-mouse antibody (Invitrogen) was used as the secondary antibody. To characterize cell shape, actin was stained with Texas Red phalloidin (Invitrogen), and nuclei were stained with Hoechst stain (Invitrogen). Images were acquired with an inverted fluorescence microscope (Eclipse Ti-E; Nikon, Melville, NY) at 20× magnification (PlanFluor 20×, 0.5 NA objective; Nikon) with a monochrome CCD camera (CoolSNAP HQ2; Photometrics; Tucson, AZ). Experiments were performed in triplicate, and the images shown are representative from five to 10 random fields for each independent experiment. To characterize circularity, the area and perimeter of individual cells stained for actin were determined for each condition using image-processing software (ImageJ freeware; NIH, Bethesda, MD), and an equation was then applied in which circularity = 4π (area/perimeter^2). Three independent images were analyzed for each condition, and at least 10 cells were analyzed per image. Data were pooled from all three images analyzed per condition.

IMMUNOBLOT FOR EMT MARKER PROTEIN LEVELS

RLE-6TN cells were cultured for five days as described above, washed with phosphate-buffered saline, and lysed directly in Laemmli buffer containing protease inhibitors (Roche Applied Sciences, Indianapolis, IN). Total protein concentrations were determined using a protein assay kit (BCA; Pierce Chemical). Forty mg of total protein were separated by electrophoresis on a 4–15% gel, transferred to a nitrocellulose membrane using a semi-dry transfer system, blocked with 5% nonfat dry milk in tris buffered

saline, and incubated with anti-E-cadherin (36/E-cadherin; BD Transduction Laboratories), anti-pan cytokeratin (5D3 + LP34; Abcam, Cambridge, MA), anti-α-SMA (1A4; Sigma-Aldrich), anti-prolyl 4-hydroxylase (1D3; Santa Cruz Biotechnology, Dallas, TX), or glyceraldehyde 3-phosphate dehydrogenase (GAPDH) (14C10; Cell Signaling Technologies, Danvers, MA) antibodies overnight at 4°C. After washing with tris buffered saline and 0.1% polysorbate 20 (Tween 20; Sigma-Aldrich), membranes were incubated for two hours with secondary antibody conjugated with infrared dye (LI-COR, Lincoln, NE), washed, and imaged using an infrared imaging system (Odyssey; LI-COR). Western blots were quantified with the image-processing software, using GAPDH as the endogenous control.

TGF-β ACTIVATION ASSAY

RLE-6TN cells were cultured on Fn-coated PA gels, Fn-coated glass, or Ln-coated glass, as described above. TGF-β activation was determined by the mink lung epithelial cell (MLEC) co-culture assay, as previously described. MLECs stably transfected with an expression construct containing a truncated Pai-1 promoter fused to the firefly luciferase reporter gene respond in a dose-dependent manner to active TGF-β but are incapable of activating TGF-β. After five days of RLE-6TN culture on the various substrates, MLECs were added at a density of 50,000 cells/cm^2 on top of the RLE-6TN cells in serum-free DMEM/F12 medium with 1% bovine serum albumin. The cells were co-cultured for 16 hours and lysed, and luciferase activity was determined using a luciferase assay (ONE-Glo; Promega, Madison, WI). To determine total levels of TGF-β, samples were heated to 85°C for 10 minutes before plating the MLECs. Luminescence was measured with a multi-mode plate reader (Synergy H4; BioTek, Winooski, VT). Luminescence values were normalized to MLECs cultured in the absence of TGF-β. Levels of active or total TGF-β were then calculated through interpolation using a standard curve. Results presented here are from three independent experiments, each conducted in triplicate.

STUDY DESIGN

Given that one of the hallmarks of fibrotic diseases is an increase in tissue stiffness, we first characterized the mechanical environment of the alveolus in normal and pathologic conditions in order to determine a physiologically relevant range of stiffnesses that ATII cells encounter in vivo. Mice were treated intratracheally with 3.2 U/kg bleomycin and killed after 14 days, and lung tissue was harvested. Tissue sections of lung were examined by AFM to measure the range of stiffnesses encountered. These measurements were then used for our in vitro model of fibrosis by creating PA gels that matched the range of physiologic healthy and fibrotic stiffnesses.

EXPERIMENTAL PROTOCOL 1

Our preliminary work proposed looking at how tissue mechanics affect particle uptake by cells.

To explore this relationship, ATII cells were seeded on PA gels of increasing stiffness or on tissue culture plastic (TCP) coated with Fn or Ln as positive and negative controls, respectively. The cells were allowed to attach and spread for 16 hours before being treated with 2-μm fluorescent polystyrene particles. The cells were then washed, and particle uptake was quantified by flow cytometry.

We next wanted to explore whether different conformations of Fn would affect particle uptake. Fn, a molecularly flexible molecule, has been hypothesized to display different conformational states in response to cell contractile forces that direct integrin-specific responses. For this purpose, Fn fragments with different degrees of unfolding were used that allowed for differential integrin engagement. Much as described above, ATII cells were seeded on various Fn-fragment substrates and allowed to attach and spread for 16 hours, polystyrene beads were added, the cells were washed, and particle uptake was quantified by flow cytometry.

Finally, in order to determine how cell contractility affected particle endocytosis, ATII cells were seeded on the various Fn-fragment substrates and allowed to attach and spread for 16 hours before Y-27632 (which inhibits contractility) was added. The polystyrene beads were then added, the cells were washed, and particle endocytosis was quantified by flow cytometry.

Overall, the results were not conclusive but gave direction to our future work. They are summarized in Appendix A (available on the HEI Web site).

EXPERIMENTAL PROTOCOL 2

We used PA gels of varying stiffnesses ranging from 2 to 32 kPa. ATII cells were cultured for five days on a single gel per cell culture well for each experimental condition, on Fn surfaces as positive controls or on Ln surfaces as negative controls, and then analyzed for EMT events by immunofluorescence staining of actin and epithelial and mesenchymal markers and by western blotting for epithelial and mesenchymal markers. Cell circularity was calculated in order to quantify the observed differences in cell shape in each of the different stiffness conditions. Decreased cell circularity was interpreted as an indicator of mesenchymal

cells. Finally, levels of active TGF-β or total TGF-β were determined by the MLEC assay. In order to look downstream of TGF-β, levels of Pai-1, a TGF-β-responsive gene, mRNA were determined in response to increasing gel stiffness.

To look more mechanistically at how increased substrate stiffness affects EMT, we sought to correlate TGF-β activation with increased cell stiffness, an indicator of cell contractility. Contractility was measured as stiffness. Here, the average elastic modulus of individual cells cultured on the substrates of various stiffnesses was determined by AFM. To determine the role of cell contractility in cellular stiffness matching, we measured the elasticity of cells with the addition of the ROCK inhibitor and again characterized the EMT events described above. To show more specifically that stiffness-mediated EMT is associated with increased cell contractility and subsequent TGF-β activation, EMT was characterized for ATII cells cultured on soft substrates (2 kPa) in the presence of active TGF-β, thrombin, or a combination of thrombin and TGF-β-neutralizing antibodies. For each of these conditions, the MLEC assay was repeated to characterize the role of TGF-β activation.

Finally, to determine the relative time course of events, a pulse–chase experiment was performed with cells cultured on soft gels. ATII cells were pulsed with active TGF-β or thrombin for 48 hours and chased with standard media for three days, recapitulating the total time of the earlier five-day experiments. EMT events were then analyzed. To further elucidate the roles of TGF-β and sustained contraction in the induction of EMT, EMT was characterized in response to various levels of TGF-β and thrombin after two or five days in culture.

EXPERIMENTAL PROTOCOL 3

$PM_{2.5}$ from the Atlanta area was collected on Teflon filters and analyzed for water-soluble sulfate, nitrate, and ammonium as well as for elemental and organic carbon. The measurements were used to conduct a chemical-mass-balance source apportionment. After analyzing the particles, total $PM_{2.5}$ was isolated from the filters by sonication and resuspended in cell culture media at 1:100, 1:1000, and 1:10,000 dilutions. These dilutions were used for each of the following experiments.

Again, PA gels cross-linked with Fn were used in a range of stiffnesses that corresponded with those used in protocol 2. ATII cells were cultured for five days on the various gels, with or without the addition of each concentration of $PM_{2.5}$. For each experiment, each cell culture well corresponded to a single experimental condition, containing a single gel of a specific stiffness with or without the addition of a specific concentration of $PM_{2.5}$. Each experimental condition was performed in triplicate. This resulted in experiments involving 72 separate cell culture wells. After five days, the cells were analyzed for EMT events, including cell circularity as well as expression of various epithelial and mesenchymal markers by immunofluorescent staining and western blot. Each experiment was then repeated in triplicate (on different days).

As described previously, epithelial cell stiffness was measured by AFM to determine if the addition of $PM_{2.5}$ resulted in increased cell stiffness with increased substrate stiffness.

Finally, we used the MLEC assay to correlate increases in TGF-β activation with the induction of EMT events. Again, cells were cultured on PA gels of various stiffnesses for five days with or without the addition of the various concentrations of $PM_{2.5}$ and analyzed using the MLEC assay. Cells with no PM added were used as a control.

STATISTICAL METHODS AND DATA ANALYSIS

In Aim 1 of this study, all the described experiments were performed as three independent triplicate experiments (i.e., triplicates of each experimental condition, each repeated three times on different days in order to show repeatability despite any minor changes in experimental conditions caused by day [e.g., temperature or humidity]). To confirm the repeatability of our experiments on different days, two-way analysis of variance (ANOVA) using graphing and statistics software (Prism; GraphPad Software, La Jolla, CA) was undertaken to make sure there were no interactions based on day. After this, all statistical analysis was performed by one-way ANOVA using this software. Statistical significance between groups was determined by the Tukey post hoc analysis. All data are presented as the mean ± standard deviation, and statistical significance is shown for $P < 0.05$ (*), $P < 0.01$ (**) or $P < 0.001$ (***).

In Aim 2 of this study, similar analyses were performed, again repeating each experiment three times to take into account any innate variations in experimental conditions caused by the day on which they were performed, specifically any differences in $PM_{2.5}$ collection. The statistical analysis was first performed by three-way ANOVA using statistical analysis software (SPSS Statistics; IBM, Armonk, NY), for which the three independent variables were the batch of $PM_{2.5}$, the concentration of $PM_{2.5}$ added, and the stiffness of the gel. This analysis allowed us to determine if there were interactions caused by the pooling of $PM_{2.5}$ from different filters on different days. Five different filters were pooled for each batch of $PM_{2.5}$ treatment to minimize differences between collection days. In addition, each $PM_{2.5}$ stock solution was made to a consistent

100 μg/mL. Because we took these factors into consideration in the preparation of our samples, we did not expect to see any significant differences in our results caused by the batches of $PM_{2.5}$. All reported analyses were performed by two-way ANOVA using the statistical analysis software. Statistical significance between groups was determined for each experiment by again performing the Tukey post hoc analysis. Results were statistically significant ($P < 0.05$) and are shown for each experimental group, as compared with controls of the same substrate stiffness without the added $PM_{2.5}$.

RESULTS

AIM 1: THE ROLE OF SUBSTRATE STIFFNESS IN EMT

EMT is a fundamental hallmark of fibrotic pathologies, in which enhanced fibroblastic cellularity within scarring regions can arise from epithelial origin (Coward et al. 2010; Iwano et al. 2002). EMT has been theorized to increase the number of ECM-secreting mesenchymal cells perpetuating the fibrotic conditions and resulting in increased tissue stiffness. However, recent reports indicate that an increase in tissue stiffness might actually precede fibrotic responses (Georges et al. 2007). It remains unclear precisely how tissue stiffness contributes to EMT in fibrosis. Understanding the relationship between and the course sequence of tissue stiffness and EMT during fibrotic progression has major implications in how we approach these diseases therapeutically. EMT has previously been shown to occur in response to stiff (i.e., glass or TCP) Fn surfaces through contraction-dependent TGF-β activation mechanisms (Kim et al. 2006, 2009). In the first part of the current study, we aimed to expand on these findings and to determine the role of stiffness in Fn-mediated EMT. We hypothesized that as alveolar epithelial cells engage increasingly stiff Fn substrates, they become increasingly contractile, leading to enhanced TGF-β activation and EMT.

Alveolar Epithelial Cells Experience Significantly Greater Stiffness in Fibrotic Versus Normal Lung

Given that one of the hallmarks of fibrotic diseases is an increase in tissue stiffness, we characterized the mechanical environment of the alveolus in normal and pathologic conditions to determine the range of stiffnesses encountered by ATII cells in vivo. Intratracheal instillation of bleomycin was used to model pulmonary fibrosis in C57BL/6 mice. Fixed lung sections isolated from fibrotic lung showed increased cellularity and alveolar-wall thickening compared with lung from saline-treated mice, as observed through hematoxylin and eosin staining (Figure 2).

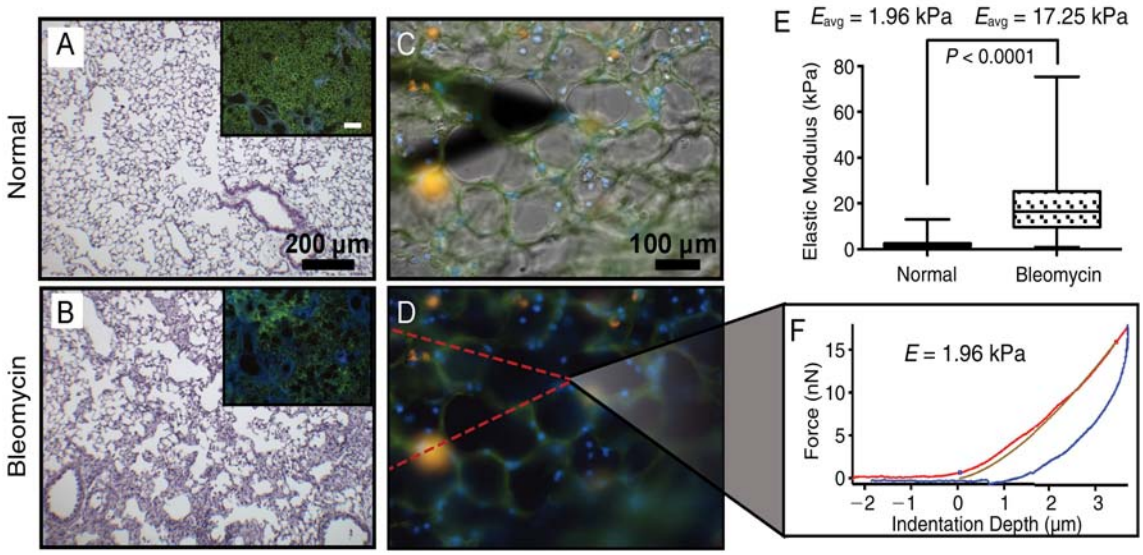

Figure 2. Lung slices from mice exposed to bleomycin show higher elastic moduli than those from healthy mice. Hematoxylin and eosin staining was performed on (**A**) normal and (**B**) bleomycin-treated lung sections, and living lung slices were imaged using vital stains for (**A** and **B insets**) ATI and ATII cells. The average elastic modulus of the lung tissue was measured using AFM. Representative (**C**) ATI (AlexaFluor 488-*e. cristagalli* lectin) and ATII epithelial cell (LysoTracker Red) vital stain fluorescence overlay and (**D**) vital stain fluorescence-only images were used to guide the position of the AFM tip. (**E**) Mean and standard deviation (95th percentile) values of the elastic modulus versus bleomycin-treated lungs are shown. (**F**) A force-indentation profile for the depicted region is shown.

In addition, isolated lung slices from these mice were used for AFM nanoindentation testing of tissue elasticity. The lung tissue was tested within six hours of harvesting to ensure tissue integrity and resident cell viability (although lung slices were found to remain viable for up to 24 hours) (Figure 3). Lung architecture observed in fixed tissues was recapitulated in thick (~100-µm) living lung slices as observed by fluorescence microscopy of vital stains for ATI and ATII cells (Figure 2A and 2B inserts). Mean and standard deviations are shown for all samples (5 mice per condition, n = 180 measurements/mouse; Figure 2E); values for the elastic moduli of samples obtained from individual mice are shown in Figure 3. The average elastic moduli of normal lung tissue and of lung tissue from the bleomycin-treated mice were 1.96 kPa (±1.21) and 17.25 kPa (±11.06), respectively. This was in agreement with previously published work exploring the micro-scale tissue mechanics of lung (Liu et al. 2010). The range of stiffnesses seen in healthy and fibrotic tissues in vivo was used to create an in vitro cell culture system using as substrates PA gels in the same stiffness range (2 to 32 kPa). The following experiments used this system to explore how microenvironmental stiffness affects alveolar epithelial cell phenotype and morphogenesis.

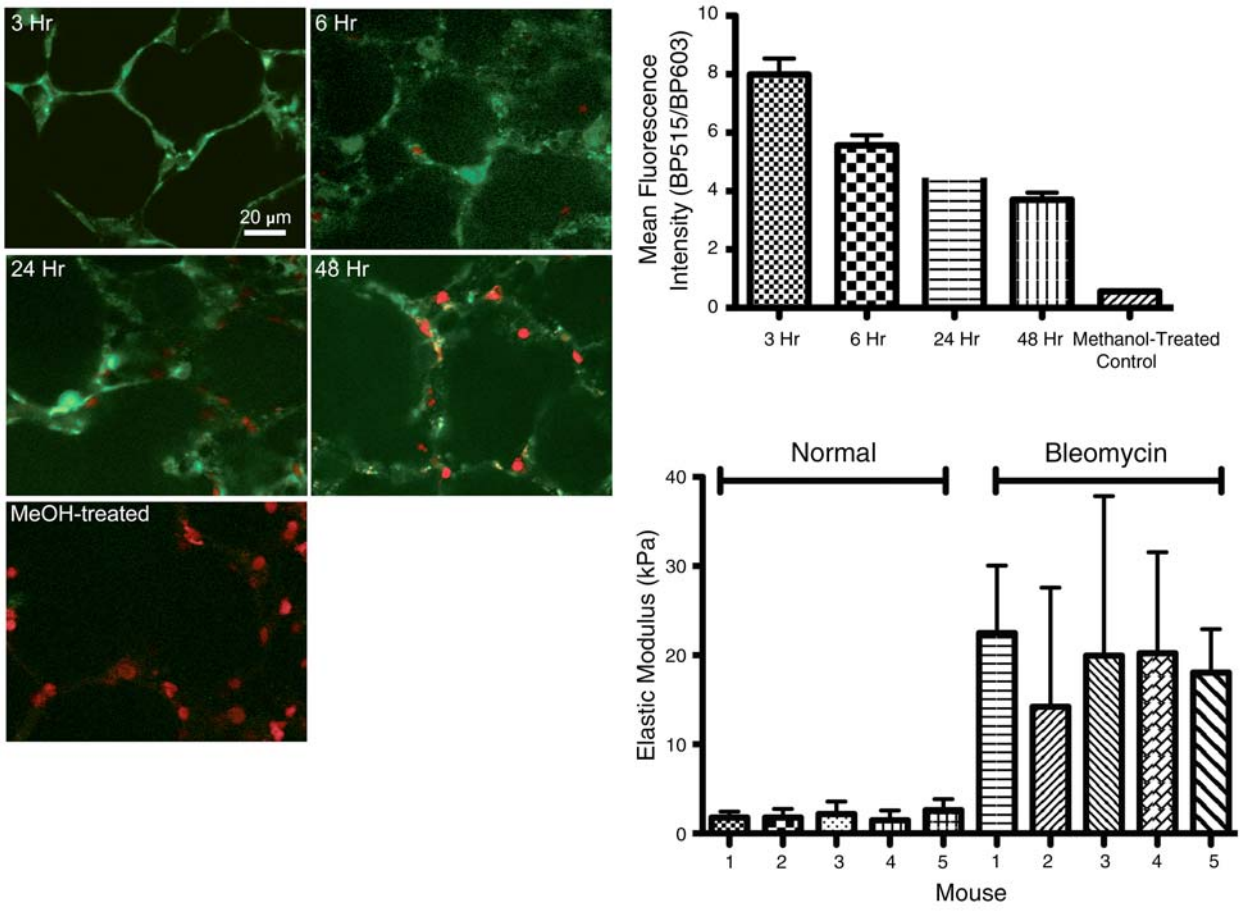

Figure 3. Living lung slices remain viable for up to 24 hours. The time course of cell viability in tissue slices used for AFM analysis was assayed using calcein acetomethoxy dye and ethidium homodimer-1 stain. (**Left** and **top right**) Cells were viable for more than 24 hours after harvesting; some cell death was observed at 48 hours. (**Bottom right**) The average elastic modulus of lung tissue was characterized through AFM analysis. Samples were obtained from individual mice. Mean and standard deviation (95th percentile) values are shown.

ATII Cells Undergo EMT on Increased Substrate Stiffnesses

EMT has previously been observed in vivo in fibrotic lung regions of both human idiopathic pulmonary fibrosis patients and bleomycin-treated mice (Kim et al. 2006). Because we observed a range of stiffness in vivo in fibrotic mouse lung regions, we sought to determine if increases in stiffness alone would be sufficient to induce EMT in vitro. Using PA gels with surface-immobilized Fn and various stiffnesses from 2 to 32 kPa, primary ATII cells were cultured for five days on PA gels or Fn- or Ln-coated glass and then analyzed for EMT by immunofluorescence staining of actin and epithelial and mesenchymal markers. Primary ATII cells cultured on substrates of the lower stiffnesses (E = 2 or 8 kPa) showed typical rounded epithelial morphology and diffuse cortical staining for actin, clear cell–cell borders observed through actin staining, and minimal staining for α-SMA-containing stress fibers. In contrast, cells cultured on substrates of the higher stiffnesses (E = 16, 24, or 32 kPa on Fn-coated glass) became elongated and showed increasingly aligned, thick actin filaments characteristic of stress fibers, minimal staining for E-cadherin, and positive staining for α-SMA-containing stress fibers (Figure 4 A–U). E-cadherin staining was observed on 2-kPa surfaces at cell–cell contacts; however, staining at these contacts was less apparent on 8-kPa surfaces, and E-cadherin was predominantly localized intracellularly. ATII cells have previously been shown to undergo EMT on Fn-coated glass surfaces (~30 kPa) but to retain epithelial phenotypes on Ln-coated glass (Kim et al. 2006). Using these conditions as control experiments, we observed identical results. Cell circularity was calculated in order to quantify observed differences in cell shape (Figure 4V) and decreased significantly with increasing substrate stiffness ($P < 0.001$). Freshly harvested alveolar epithelial cells from rats expressed high levels of surfactant protein C, an ATII cell marker, and low levels of α-SMA (Figure 4W), indicating low levels of fibroblast contamination in an isolated cell population (however, even low levels of fibroblast contamination can confound EMT analysis). RLE-6TN cells, an ATII cell line that is widely used for studying ATII EMT events (Aoyagi-Ikeda et al. 2011; Felton et al. 2009; Jain et al. 2007; Willis et al. 2005; Xu et al. 2007; Zhou et al. 2009), were therefore used for all remaining analyses. Like primary ATII cells, the RLE-6TN cells underwent EMT on increasingly stiff Fn surfaces but retained an epithelial phenotype on Ln surfaces (Figure 5). Representative western blots for epithelial and mesenchymal protein levels are shown in Appendix B (available on the HEI Web site).

Stiffness-Mediated EMT Is Driven by Increased Contraction and Integrin-Mediated TGF-β

To characterize TGF-β activation, the MLEC assay was performed (Figure 6A). RLE-6TN cells were found to activate TGF-β increasingly in response to increasing substrate stiffness; total levels of TGF-β were similar on all PA gels (Figure 7A). As expected, control groups cultured on Fn-coated glass activated TGF-β to a significantly greater degree than those cultured on Ln-coated glass ($P < 0.01$). We also observed an increase in levels of expression of the TGF-β-responsive gene Pai-1 as determined in the experiment described below (Figure 8).

RLE-6TN cells were cultured for five days on substrates of various stiffnesses in the absence (Figure 8A) or presence of 10 μM Y-27632 (Figure 8B). Levels of expression of the TGF-β-responsive gene Pai-1 were determined by quantitative polymerase chain reaction (qPCR). Fold changes in gene expression were determined by the comparative method of analyzing qPCR data, using β-actin and GAPDH as endogenous controls and comparing expression with that of cells cultured on 2-kPa substrates in the absence or presence of Y-27632, respectively. Controls included cells cultured on Fn- or Ln-coated glass coverslips in the absence or presence of Y-27632 and on Fn-coated coverslips incubated with a combination of both Y-27632 and active TGF-β (Figure 8C). In addition, TGF-β mRNA expression was determined in the absence (Figure 8D) or presence of 10 μM Y-27632 (Figure 8E). Levels of expression of TGF-β mRNA were determined by qPCR in the same manner as described for Pai-1. Finally, Pai-1 mRNA expression was characterized in cells cultured on 32-kPa substrates in the presence of 10 μg/mL TGF-β-neutralizing antibodies, 10 μM HA-1077, 50 μM blebbistatin, 100 nM cytochalasin D, or media only (Figure 8F). Pai-1 expression was significantly lower in the presence of all contractility inhibitors analyzed, as compared with that of cells cultured on 32-kPa substrates in media alone ($P < 0.01$). These results further demonstrate a stiffness-dependent increase in active TGF-β.

We then sought to correlate increased TGF-β activation with increased ATII cell stiffness, an indicator of cell contractility. Using AFM nanoindentation testing, the average elastic modulus of individual cells was measured (Figure 6B); average cell stiffness increased with increasing substrate stiffness, reaching a maximum at approximately 6 kPa. Interestingly, cells on Ln-coated glass showed values similar to those of cells on soft Fn substrates, with average elastic moduli of approximately 1 kPa, suggesting that cellular stiffness matching is dependent on the ECM composition.

To determine the role of cell contractility in cellular stiffness matching, we measured the stiffness of cells on

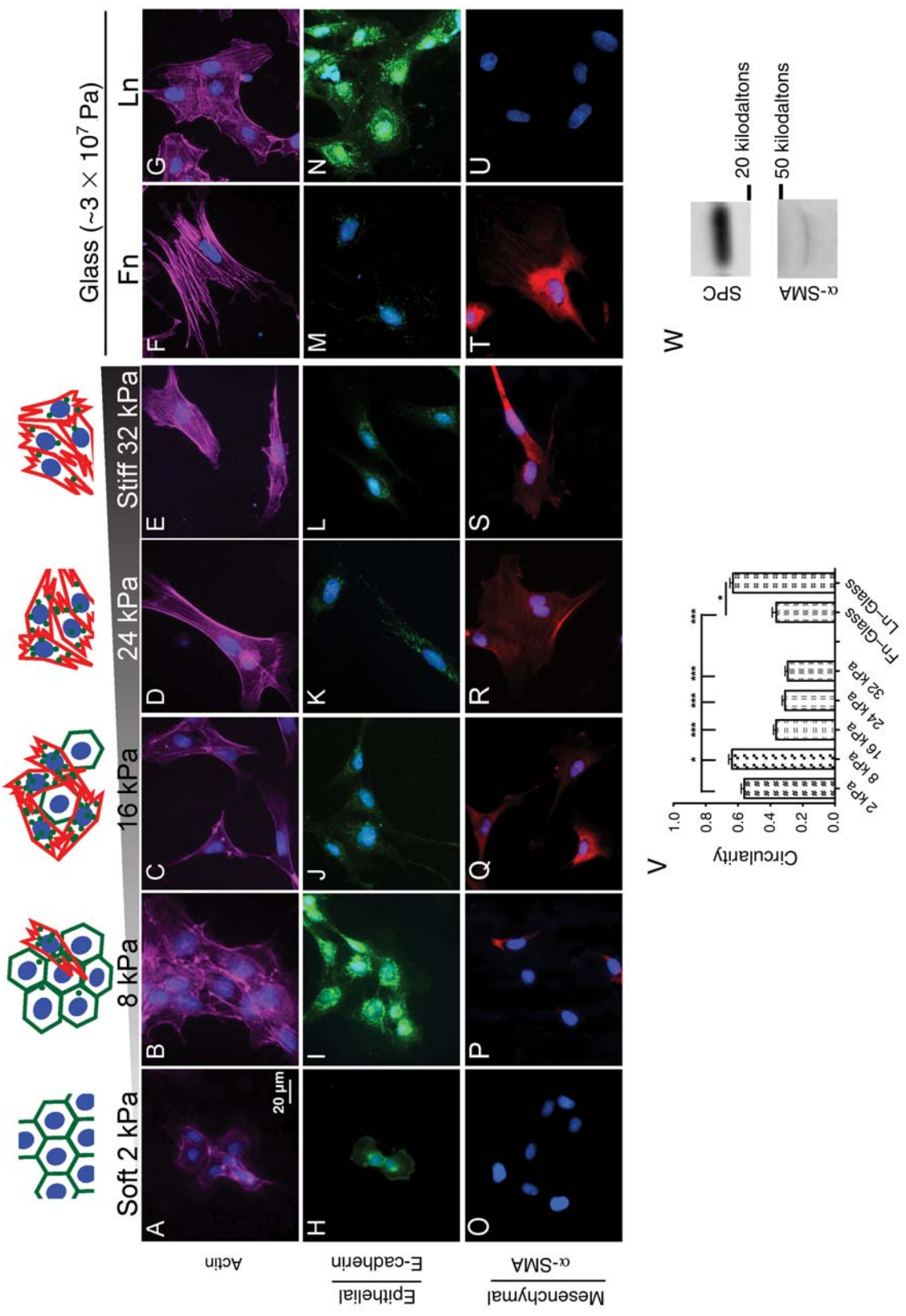

Figure 4. Analysis of EMT in primary ATII cells cultured on Fn substrates of increasing stiffness. Primary ATII cells were isolated and cultured on Fn PA gels or on Fn- or Ln-coated glass for five days, and EMT responses were analyzed through (**A–G**) changes in actin cytoskeleton alignment and (**V**) cell circularity and through immunofluorescence staining for (**H–N**) E-cadherin and (**O–U**) α-SMA. (**W**) To demonstrate the purity of isolated ATII cells, levels of surfactant protein C (SPC) and α-SMA in freshly isolated cells were determined through western blotting. Experiments were performed in triplicate; representative images are shown. In **V**, *** and * denote $P < 0.001$ and $P < 0.05$, respectively.

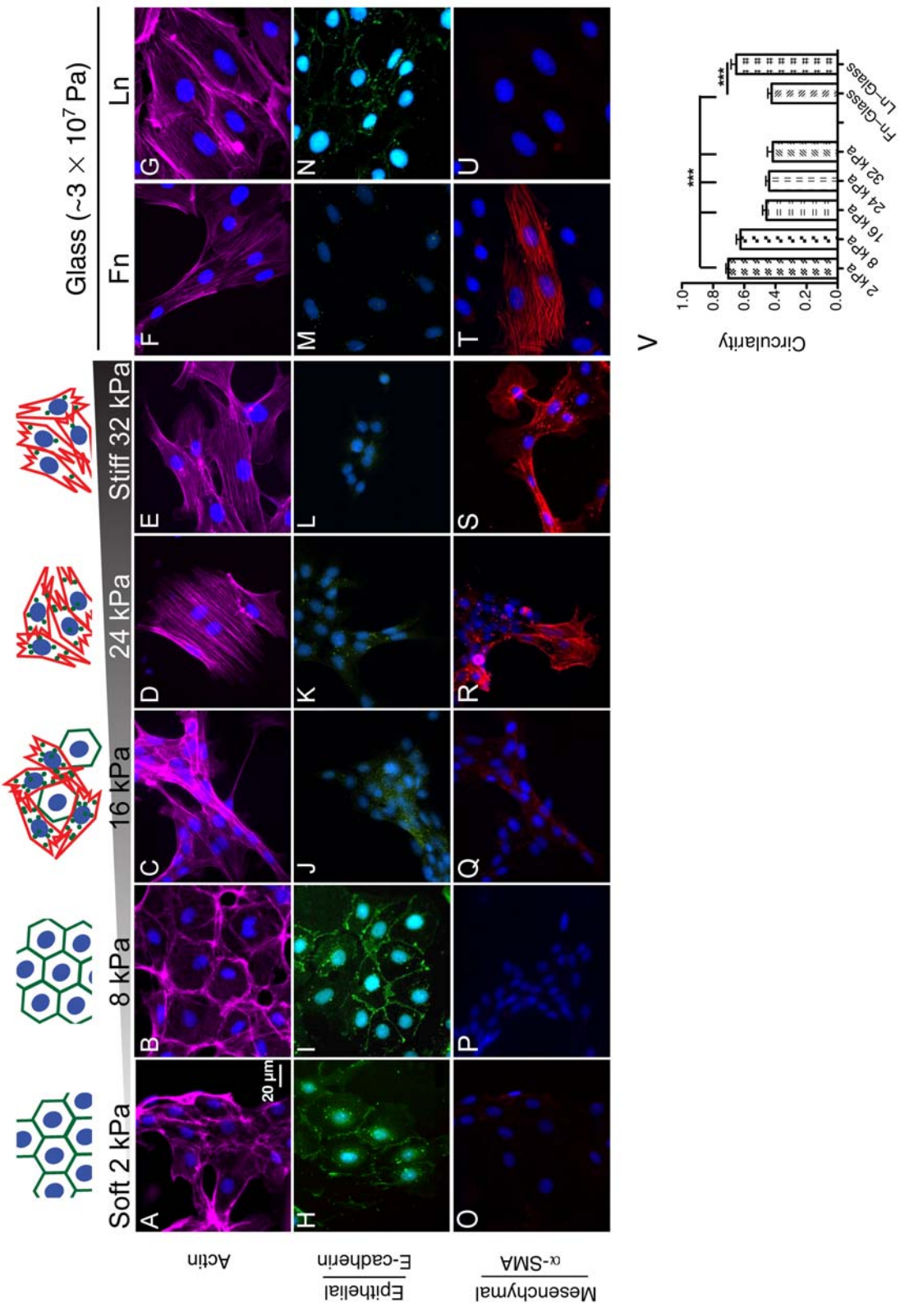

Figure 5. Analysis of EMT in RLE-6TN cells cultured on Fn substrates of increasing stiffness. RLE-6TN cells were cultured for five days on Fn PA gels, Fn-coated glass (Fn-Glass), or Ln-coated glass (Ln-Glass), and EMT responses were analyzed through (**A–G**) changes in actin cytoskeleton alignment and (**V**) cell circularity and through changes in epithelial and mesenchymal protein expression through immunofluorescence staining for (**H–N**) E-cadherin and (**O–U**) α-SMA. Experiments were performed in triplicate; representative images are shown. In **V**, *** denotes $P < 0.001$.

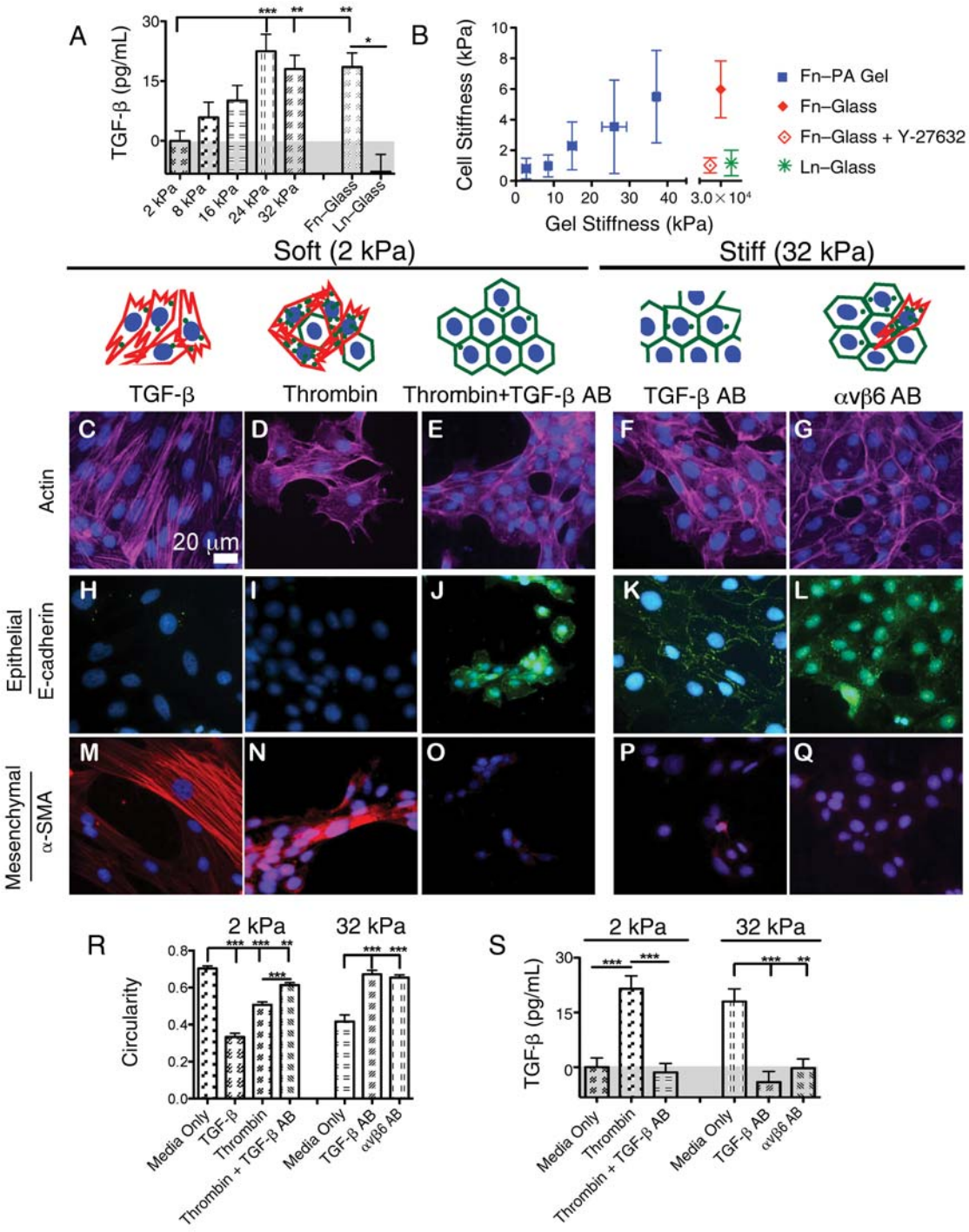

Figure 6. Stiffness-mediated EMT is driven by increased contraction and integrin-mediated TGF-β activation. RLE-6TN cells were cultured for five days on substrates of increasing stiffness, and (**A**) levels of TGF-β activation were determined using the MLEC assay. (**B**) Single-cell elasticity was measured using AFM nanoindentation to characterize cell stiffening in response to substrate stiffness and/or ECM ligand. Averages of cell stiffness and stiffness of each gel mixture are shown. RLE-6TN cells were also cultured for five days on either soft (2-kPa) substrates in the presence of (**C, H, M**) active TGF-β, of (**D, I, N**) the contractility agonist thrombin, or of (**E, J, O**) thrombin and TGF-β-neutralizing antibodies (TGF-β AB) or on stiff (32-kPa) substrates in the presence of (**F, K, P**) TGF-β or of (**G, L, Q**) integrin-αvβ6-neutralizing antibodies (αvβ6 AB). EMT events were analyzed through (**C–G**) changes in actin cytoskeleton alignment and (**R**) cell circularity and changes in epithelial and mesenchymal protein expression through immunofluorescence staining for (**H–L**) E-cadherin and (**M–Q**) α-SMA. (**S**) TGF-β activation was determined for these conditions through the MLEC assay. A minimum of three independent experiments were performed; representative images are shown. In **A**, **R**, and **S**, ** and *** denote $P < 0.01$ and $P < 0.001$, respectively.

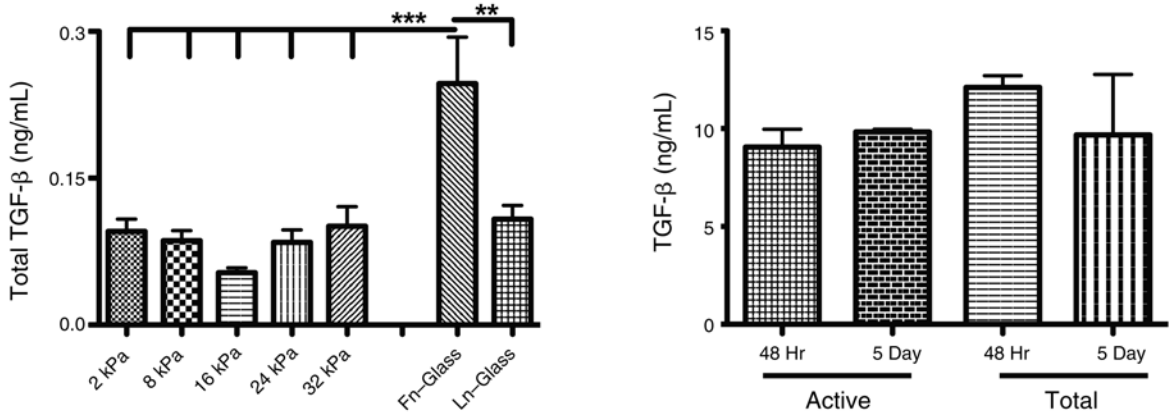

Figure 7. Levels of total TGF-β on substrates of various degrees of stiffness and active and total TGF-β on soft substrates in the presence of 5 ng/mL TGF-β. (**Left**) RLE-6TN cells were cultured for five days on substrates of increasing stiffness, and total levels of TGF-β activation were determined using the MLEC assay. It was found that cells cultured on Fn-coated glass (Fn–Glass) expressed significantly more TGF-β than cells cultured on PA gels ($P < 0.01$) or Ln-coated glass (Ln–Glass) ($P < 0.01$). No statistical differences in total TGF-β levels were observed between cells cultured on PA gels and Ln-coated glass. ** and *** denote $P < 0.01$ and $P < 0.001$, respectively. (**Right**) RLE-6TN cells were also cultured for 48 hours or five days on soft (2-kPa) substrates in the presence of 5 ng/mL active TGF-β. Levels of both active and total TGF-β were determined through the MLEC assay. Results shown were pooled from three independent triplicate experiments.

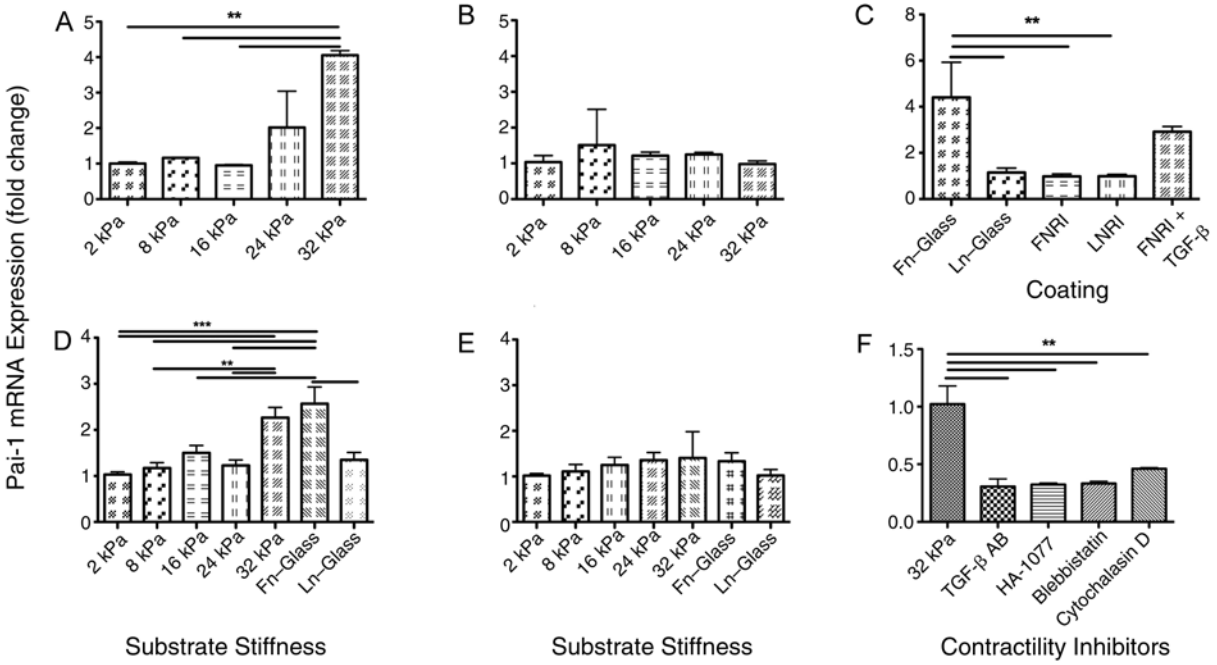

Figure 8. Pai-1 mRNA expression increases in ATII cells cultured on increasingly stiff substrates. RLE-6TN cells were cultured for five days on substrates of various degrees of stiffness in (**A**) the absence or (**B**) the presence of 10 μM ROCK inhibitor Y-27632. Levels of expression of the TGF-β-responsive gene Pai-1 were determined by qPCR. Fold changes in gene expression were determined by the comparative method of analyzing qPCR data, using β-actin and GAPDH as endogenous controls and comparing expression with that of cells cultured on 2-kPa substrates in the absence or presence of Y-27632, respectively. (**C**) Controls included cells cultured on Fn-coated (Fn–Glass) or Ln-coated (Ln–Glass) glass coverslips in the absence or presence of Y-27632 (FNRI or LNRI) and on Fn-coated coverslips incubated with a combination of both Y-27632 and active TGF-β (FNRI + TGF-β). Levels of TGF-β mRNA expression in (**D**) the absence or (**E**) the presence of 10 μM Y-27632 were determined by qPCR. Fold changes in gene expression were determined by the comparative method of analyzing qPCR data, using β-actin and GAPDH as endogenous controls and comparing expression with that of cells cultured on 2-kPa substrates in the absence or presence of Y-27632, respectively. (**F**) Pai-1 mRNA expression was then characterized in cells cultured on 32-kPa substrates in the presence of 10 μg/mL TGF-β-neutralizing antibodies (TGF-β AB), 10 μM HA-1077, 50 μM blebbistatin, 100 nM cytochalasin D, or media only. Pai-1 expression was significantly lower in the presence of all contractility inhibitors analyzed compared with that of cells cultured on 32-kPa substrates in media alone ($P < 0.01$). Reactions were performed in triplicate; results shown were pooled from three independent experiments ($N = 9$). ** and *** denote $P < 0.01$ and $P < 0.001$, respectively.

Fn-coated glass with the addition of 10 μM ROCK inhibitor Y-27632 and found that cell contractility decreased to levels similar to those observed on soft Fn substrates and Ln-coated glass (data not shown). To initially characterize the role of cell contractility in the observed stiffness-mediated EMT events, RLE-6TN cells were cultured for five days on substrates of various stiffnesses in the presence of Y-27632, and EMT events were characterized. In the presence of the Y-27632, the cells retained an epithelial morphology regardless of the underlying substrate (Figure 9). The inhibition of ROCK likely has global effects on many aspects of cell signaling; we therefore sought to confirm more specifically that stiffness-mediated EMT in ATII cells is caused by increased cell contractility and subsequent increased activation of TGF-β.

We analyzed EMT in ATII cells cultured for five days on soft substrates (E = 2 kPa) in the presence of 5 ng/mL active TGF-β, 0.5 U/mL of the contractility agonist thrombin, or a combination of thrombin and TGF-β-neutralizing antibodies. In addition to thrombin's direct proteolytic activation of TGF-β at concentrations above 5 U/mL (Taipale et al. 1992; Wipff et al. 2007), thrombin has also been shown to lead to nonproteolytic integrin-mediated activation of TGF-β through binding to protease-activated receptor 1 (Jenkins et al. 2006). Cells were cultured on stiff substrates (E = 32 kPa) in the presence of TGF-β-neutralizing antibodies or integrin-αvβ6-neutralizing antibodies to prevent integrin-mediated mechano-activation of TGF-β. In the presence of active TGF-β or thrombin, cells cultured on soft substrates showed a predominantly mesenchymal phenotype (Figure 6 C–D, H–I, M–N, and R), whereas cells cultured in the presence of both thrombin and TGF-β-neutralizing antibodies showed a predominantly epithelial phenotype (Figure 6 E, J, O, and R). The converse was observed on stiff substrates in the presence of TGF-β- or integrin-αvβ6-neutralizing antibodies, with cells showing a predominantly epithelial morphology (Figure 6 F–G, K–L, P–Q, and R). Western blots for the epithelial and mesenchymal markers corresponding to each of these results can be seen in Appendix B. These data indicate that contractility-induced EMT involves TGF-β signaling. However, in addition to inducing contractility, thrombin signaling through additional pathways might account, in part, for some of the subtle observed differences in phenotype, as compared with those observed in response to exogenous TGF-β.

To characterize the role of TGF-β activation in the observed events, the MLEC assay was performed (Figure 6S). Cells cultured on soft gels in the presence of thrombin activated TGF-β significantly more than those in soft control conditions ($P < 0.001$). Further addition of TGF-β-neutralizing antibodies as a control abrogated the thrombin-induced enhanced TGF-β signal. In addition, cells cultured on stiff gels in the presence of either TGF-β- or integrin-αvβ6-neutralizing antibodies showed an abrogation of active TGF-β (data not shown). To further characterize the role of thrombin in integrin-mediated TGF-β activation and rule out possible proteolytic activation of TGF-β by thrombin, cells were cultured on soft substrates in the presence of both thrombin and integrin-αvβ6-neutralizing antibodies and were found to show a predominantly epithelial phenotype (Figure 10). To determine if stiffness affects TGF-β receptor activation, cells were cultured on soft or stiff substrates in the presence of exogenously added active TGF-β- and integrin-αvβ6-neutralizing antibodies and were found to show predominantly mesenchymal phenotypes on soft substrates and robust mesenchymal phenotypes on stiff substrates (Figure 10).

Pulse of Active TGF-β Is Sufficient to Induce EMT on Soft Substrates

To determine the relative time-course of events, a pulse–chase experiment with cells cultured on soft gels was performed. ATII cells were pulsed with 5 ng/mL active TGF-β or 0.5 U/mL thrombin for 48 hours and chased by replacing the medium with standard media for three days, recapitulating the total time of the earlier five-day experiments. EMT was then analyzed. Cells pulsed with TGF-β were found to undergo EMT (Figure 11 A, C, E, and G). Furthermore, blocking additional residual matrix-bound TGF-β signaling through the addition of a TGF-β-neutralizing antibody after the TGF-β pulse resulted in cells with a predominantly mesenchymal morphology (Figure 12); however, cells cultured in these conditions began to regain cytokeratin expression (Appendix B).

In contrast, cells pulsed with thrombin for two days showed an epithelial morphology on day five (Figure 11 B, D, F, and G). These data suggest that a minimum level of TGF-β signaling might be required to initiate the EMT program and that only a sustained contraction of epithelial cells is capable of achieving this threshold. Cell contractility was measured to determine if the addition of active TGF-β or thrombin resulted in an increase in cell contractility, either acutely or long term. Cells were cultured for 24 hours on soft substrates in the presence or absence of active TGF-β or thrombin, and cell contractility was found to increase significantly ($P < 0.05$) in the presence of either stimulant, as compared with cells cultured in standard media alone. Interestingly, upon removal of the cell culture additives, the cells initially incubated with thrombin showed a decrease in single-cell contractility over the course of three days, whereas the cells initially incubated with TGF-β maintained their increase in cell contractility over the time course and did not return to basal levels (Figure 11H).

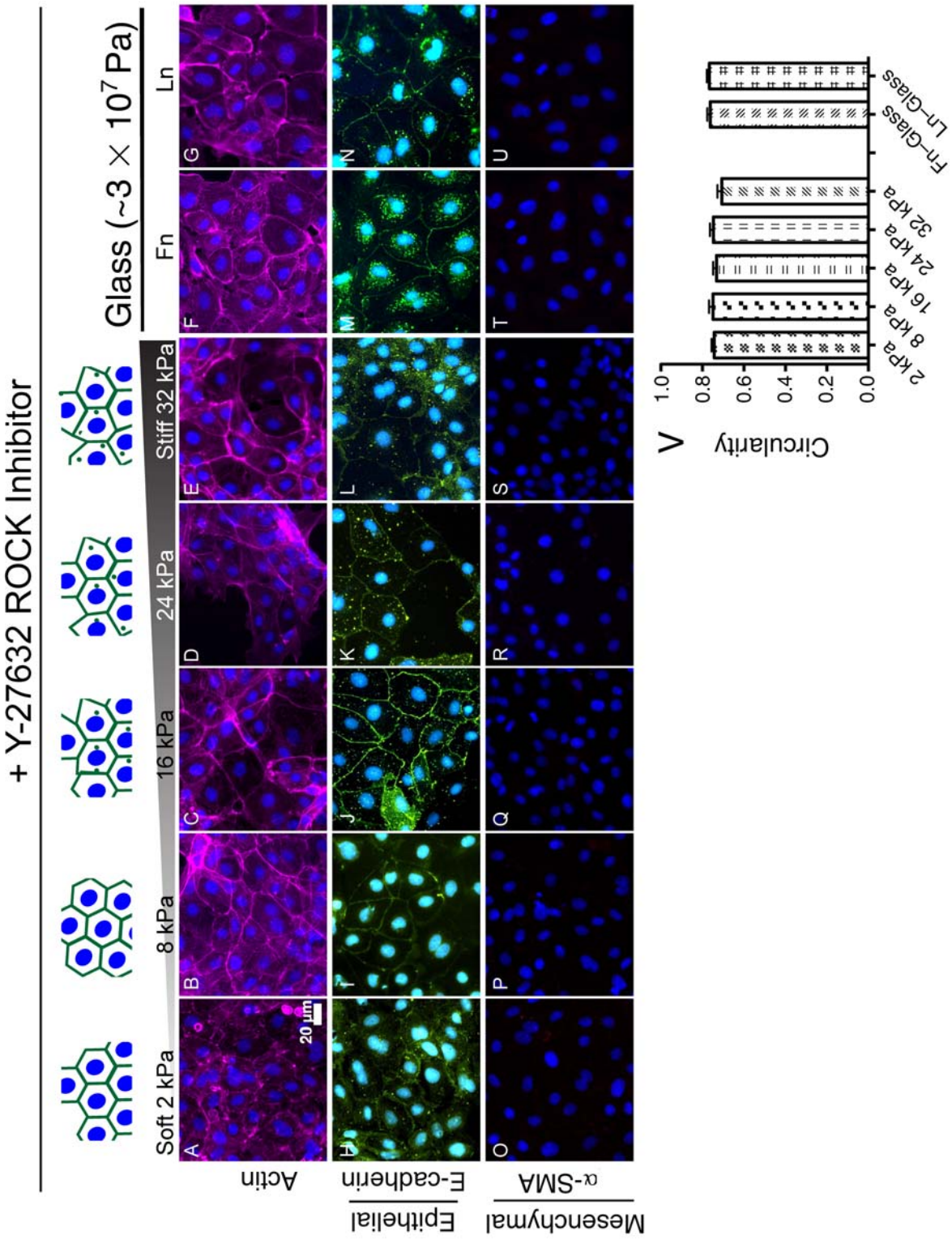

Figure 9. Stiffness-mediated EMT is dependent on cell contractility. RLE-6TN cells were cultured for five days on substrates of various degrees of stiffness in the presence of 10 μM Y-27632, and EMT responses were analyzed through (**A–G**) changes in actin cytoskeleton alignment and (**V**) cell circularity (data pooled from three experiments; at least 10 cells analyzed per experiment, for a minimum of $N = 30$ for each condition) and changes in epithelial and mesenchymal protein expression through immunofluorescence staining for (**H–N**) E-cadherin and (**O–U**) α-SMA. Experiments were performed in triplicate; representative images are shown.

Induction of EMT Events on Soft Substrates by TGF-β or Thrombin Pulses Is Dose-Dependent

To further elucidate the role of TGF-β and sustained contraction in the induction of EMT, EMT was characterized in response to various levels of TGF-β and thrombin after two or five days in culture. RLE-6TN cells were cultured on soft substrates in the presence of various levels of either active TGF-β (0.01, 0.1, or 5 ng/mL) or thrombin (0.5, 1, or 4 U/mL) for the initial 48 hours and then media with (continuous) or without (pulse) these same additives for three additional days (Figure 5). The levels of TGF-β chosen were based on the amount of TGF-β activated by RLE-6TN cells in the presence of 0.5 U/mL thrombin in previous experiments.

EMT events were then analyzed at two or five days as before. It was found that after two or five days in culture with continuous exposure to TGF-β or thrombin, cells showed a predominantly mesenchymal phenotype. Cells

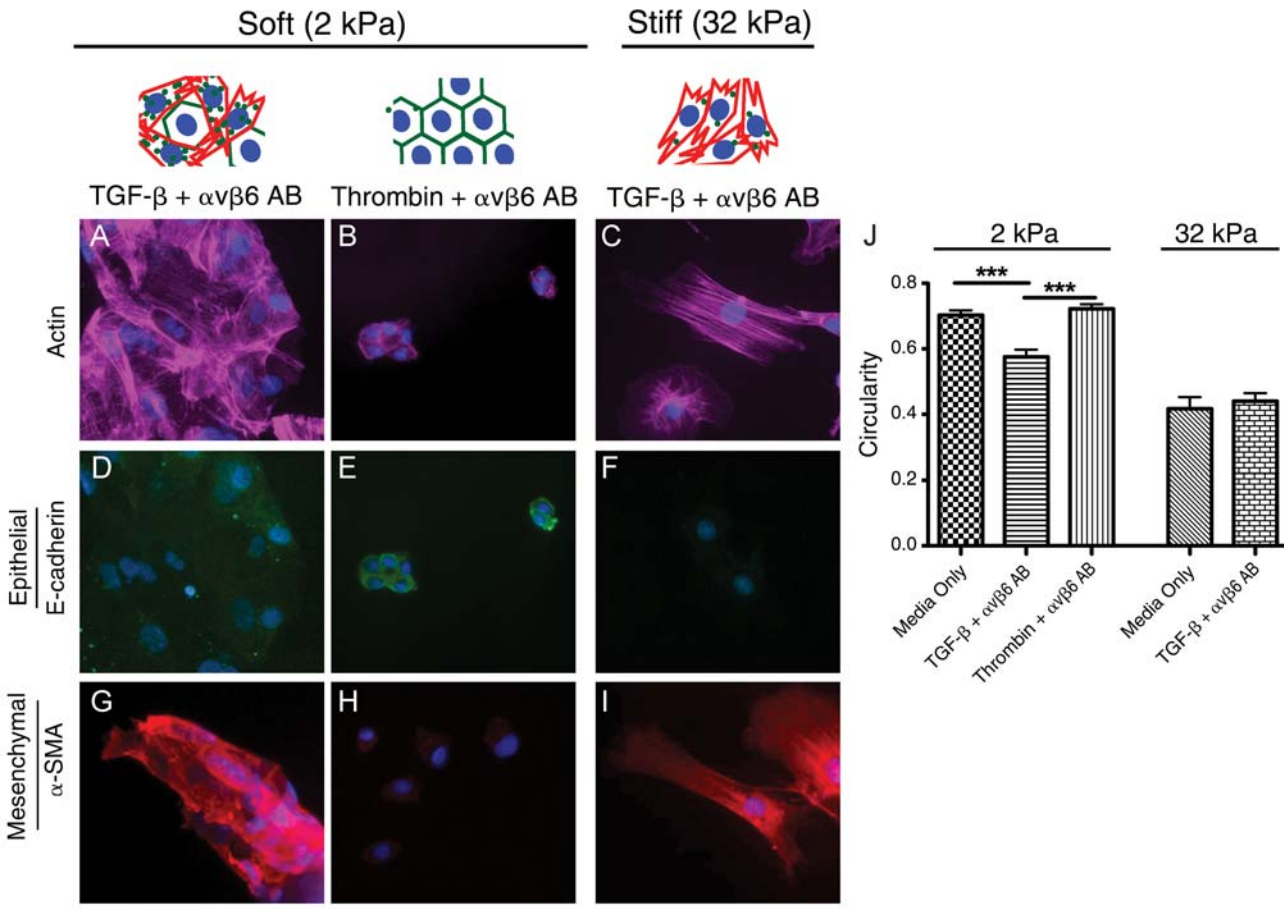

Figure 10. Integrin-αvβ6-neutralizing antibodies inhibit thrombin-induced EMT on soft substrates but do not affect TGF-β-mediated EMT on either soft or stiff substrates. RLE-6TN cells were cultured for five days on (**A**, **D**, **G**) soft (2-kPa) substrates or (**C**, **F**, **I**) stiff (32-kPa) substrates in the presence of both TGF-β and integrin-**α**vβ6-neutralizing antibodies (**α**vβ6 AB) or on (**B**, **E**, **H**) soft (2-kPa) substrates in the presence of both thrombin and integrin-**α**vβ6-neutralizing antibodies. EMT events were then analyzed through (**A**, **B**, **C**) changes in actin cytoskeleton alignment and (**J**) cell circularity (data pooled from three experiments; at least 10 cells analyzed per experiment, for a minimum of $N = 30$ for each condition) and changes in epithelial and mesenchymal protein expression through immunofluorescence staining for (**D**, **E**, **F**) E-cadherin and (**G**, **H**, **I**) **α**-SMA. Experiments were performed in triplicate; representative images are shown. In **J**, *** denotes $P < 0.001$.

pulsed with 4 U/mL thrombin, like cells pulsed with 5 ng/mL TGF-β (Figure 11, Appendix B), were found to maintain a mesenchymal phenotype at day five. However, cells pulsed with low levels of TGF-β (0.01 ng/mL), like cells pulsed with low levels of thrombin (0.5 U/mL, Figure 11, Appendix B), reverted to a predominantly epithelial phenotype (Figure 13). Cells pulsed with intermediate doses (1 U/mL thrombin or 0.1 ng/mL TGF-β) showed a mixed phenotype on day five. These data strongly suggest that, although low levels of TGF-β signaling can initiate an EMT program with continuous exposure, a threshold is required to maintain the program after removal of the TGF-β. Below this critical threshold, EMT can be reversed on soft substrates. It was also found that cells increasingly activated TGF-β in response to increasing concentrations of thrombin (Figure 13 T–U). As expected, addition of exogenous active TGF-β resulted in a dose-dependent increase in the observed levels of active TGF-β. Amounts of both active and total TGF-β were lower after five days, as compared with identical conditions after 48 hours, except with the addition of 5 ng/mL TGF-β, which produced similar values of approximately 10 ng/mL for both time points (Figure 7B).

Overall, we were able to demonstrate that there is a delicate balance between ECM stiffness, TGF-β, and EMT. Because we found that matrix stiffnesses that mimic fibrotic lung led to increased cell contractility, TGF-β activation, and spontaneous EMT, we sought to understand if

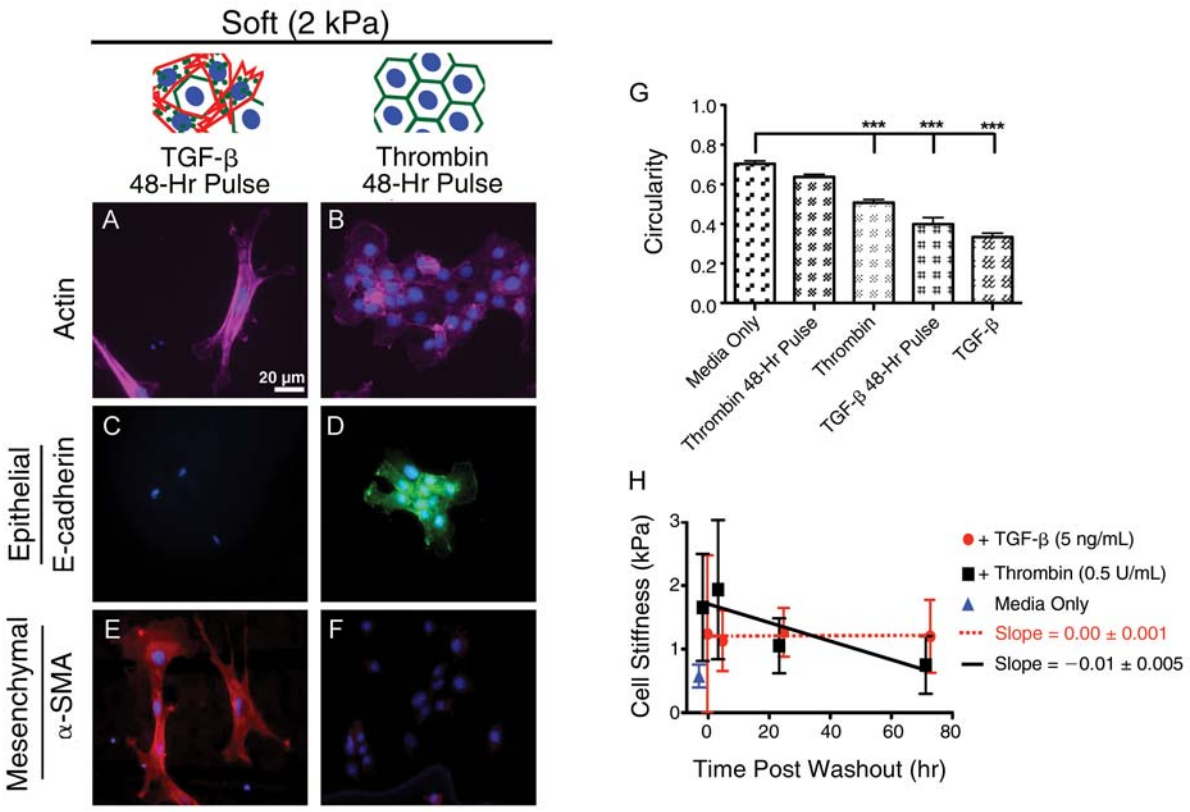

Figure 11. EMT events are induced on soft substrates with a TGF-β pulse but not a thrombin pulse. RLE-6TN cells were cultured for five days on soft (2-kPa) substrates in the presence of (**A**, **C**, **E**) 5 ng/mL active TGF-β or (**B**, **D**, **F**) 0.5 U/mL thrombin for the initial 48 hours and then standard media without additives for three additional days. EMT events were analyzed through (**A–B**) changes in actin cytoskeleton alignment and (**G**) cell circularity (data pooled from three experiments; at least 10 cells analyzed per experiment, for a minimum of $N = 30$ for each condition) and changes in epithelial and mesenchymal protein expression through immunofluorescence staining for (**C–D**) E-cadherin and (**E–F**) α-SMA. (**H**) Single-cell elasticity was measured using AFM force mapping to characterize cell stiffening on 2-kPa substrates in response to overnight stimulation with either active TGF-β or thrombin and 3, 24, and 72 hours after washout (N = a minimum of 10 cells with multiple measurements per cell; for single-cell analysis, single force points were taken from at least five perinuclear regions that were > 300 nm in height). Experiments were performed a minimum of three times ($N = 3$; multiple cell were analyzed per experiment); representative images are shown. *** denotes $P < 0.001$.

exposure to external stimuli associated with the progression of fibrotic pathologies exacerbates the effects seen with stiffness-mediated EMT.

AIM 2: $PM_{2.5}$ EXACERBATES STIFFNESS-INDUCED EMT EVENTS IN A CONCENTRATION-DEPENDENT MANNER

Exposure to $PM_{2.5}$ has been associated with a number of lung diseases, including asthma, bronchitis, COPD, and fibrosis (Abbey et al. 1998, 1999; Goss et al. 2004; Mazzoli-Rocha et al. 2010; Riva et al. 2011; Veljkovic et al. 2011). Previous studies have shown that exposure to small particles, in the submicron range, results in more toxic and fibrotic effects on alveolar cells than exposure to larger particles because of the smaller particles' higher surface-to-mass ratio, which creates a greater oxidant-generating potential (Bonner 2007). In addition, various components of the particles can activate cytokines and growth factors, including TGF-β (Anderson et al. 1997, Barry-Hamilton et al. 2010; Bonner 2007; Dagher et al. 2005). As shown in Aim 1, TGF-β is a potent inducer of EMT. To date, no studies have examined the effect of $PM_{2.5}$ in conjunction with substrate stiffness on alveolar epithelial cell EMT, one of the possible mechanisms that drive pulmonary fibrosis. We hypothesized that exposure of alveolar epithelial cells to $PM_{2.5}$ would exacerbate the induction of the stiffness-mediated EMT observed in Aim 1. This combined effect, if demonstrated, would provide validation that

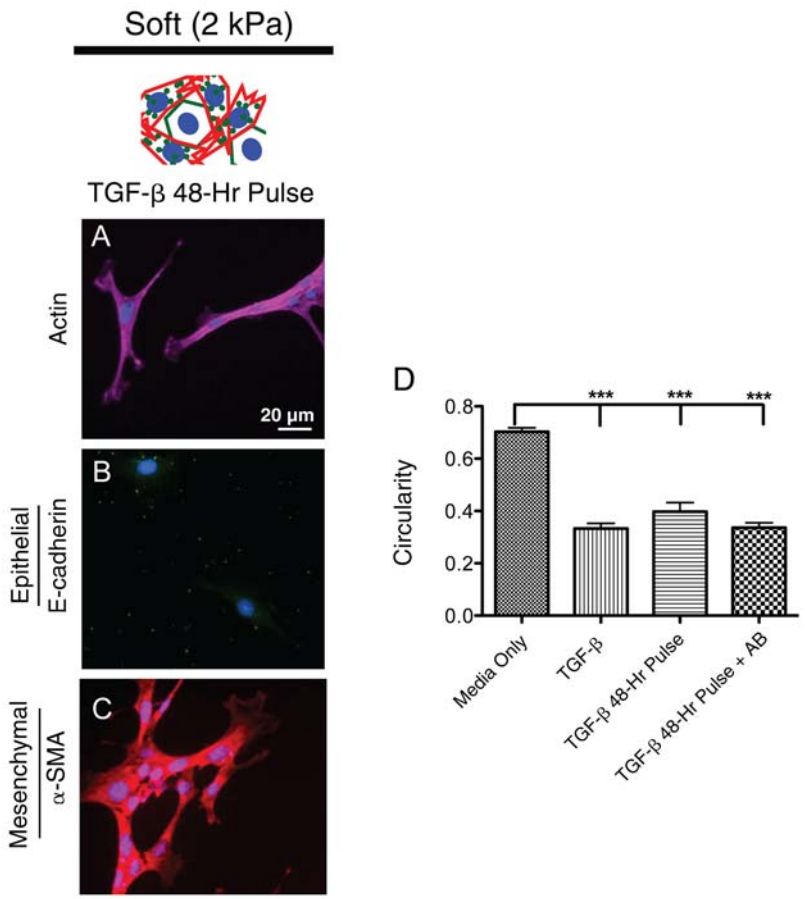

Figure 12. EMT events are induced on soft substrates with a TGF-β pulse when residual matrix-bound TGF-β is blocked after the pulse. RLE-6TN cells were cultured for five days on soft (2-kPa) substrates in the presence of 5 ng/mL active TGF-β for the initial 48 hours and then standard media without TGF-β for three additional days. To block any residual matrix-bound TGF-β after the pulse, a TGF-β-inhibiting antibody (AB) was added to the media for the last three days of culture. EMT events were then analyzed through (**A**, **D**) changes in actin cytoskeleton alignment and cell circularity and changes in epithelial and mesenchymal protein expression through immunofluorescence staining for (**B**) E-cadherin and (**C**) α-SMA. Experiments were performed a minimum of three times; representative images are shown for each independent experiment. *** denotes $P < 0.001$.

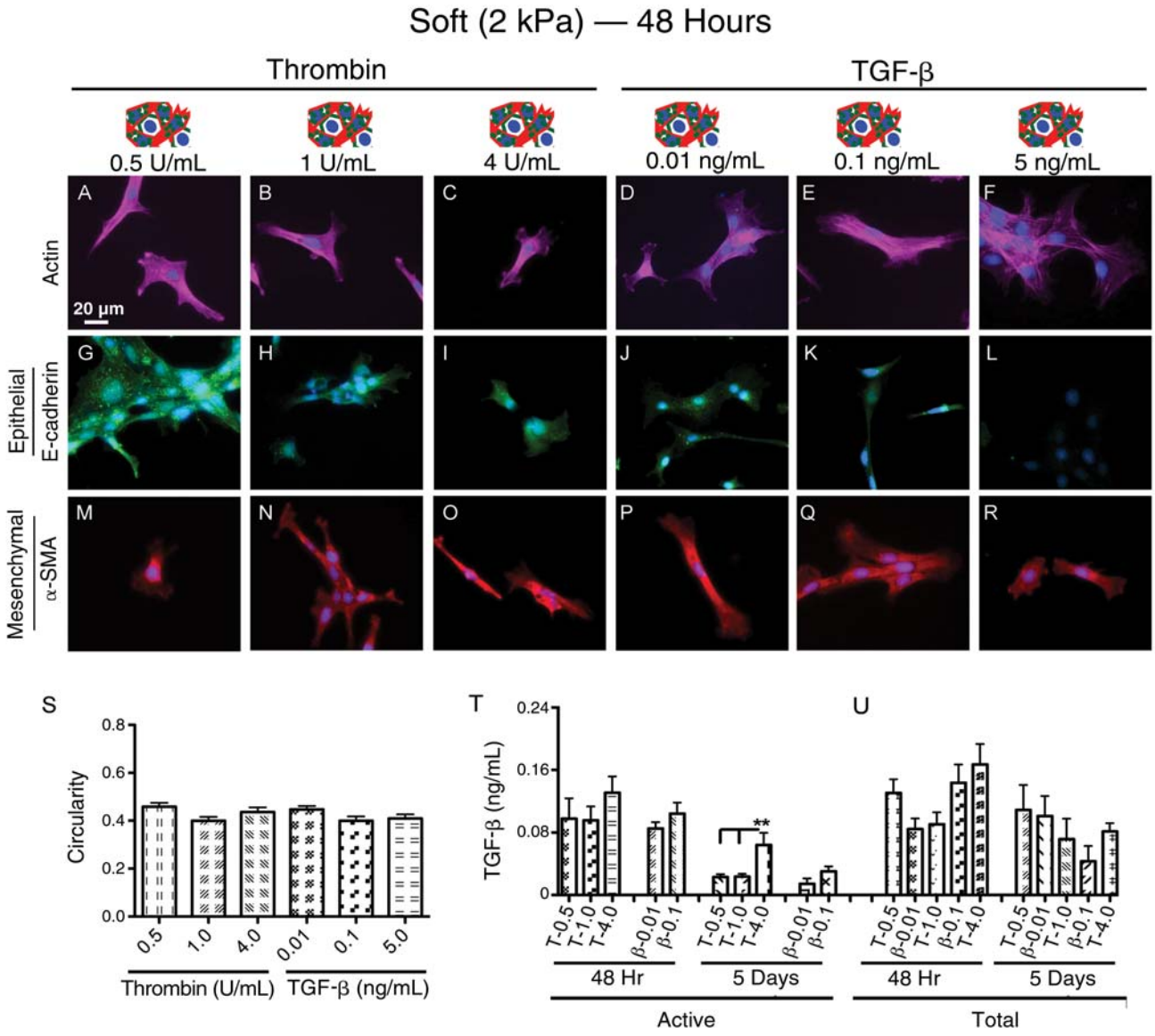

Figure 13. Induction of EMT events on soft substrates by a thrombin or TGF-β pulse is dose-dependent. RLE-6TN cells were cultured for two days on soft (2-kPa) substrates in the presence of various levels of active TGF-β (β) (0.01, 0.1, or 5 ng/mL) or thrombin (T) (0.5, 1, or 4 U/mL). EMT events were analyzed at two days through (**A–F**) changes in actin cytoskeleton alignment and (**S**) cell circularity (N = at least 30 per condition; data were pooled from three experiments, and 10 or more cells were analyzed per condition) and changes in epithelial and mesenchymal protein expression through immunofluorescence staining for (**G–L**) E-cadherin and (**M–R**) α-SMA as well as through (**Appendix B**) western blotting for E-cadherin, cytokeratin, α-SMA, P4H, and GAPDH. (**T–U**) Levels of active and total TGF-β were determined through the MLEC assay (T and β denote thrombin and TGF-β concentrations in U/mL and ng/mL, respectively) (N = 9; data were pooled from three experiments). RLE-6TN cells were also cultured for two days as described above and then for three additional days in media with (Continuous [C]) or without (Pulse [P]) the same additives. EMT events were analyzed at five days through (**W–DD**) changes in actin cytoskeleton alignment and (**V**) cell circularity (N = at least 30 per condition; data were pooled from three experiments, and 10 or more cell were analyzed per condition) and changes in epithelial and mesenchymal protein expression through immunofluorescence staining for (**EE–LL**) E-cadherin and (**MM–TT**) α-SMA as well as through (**Appendix B**) western blotting for E-cadherin, cytokeratin, α-SMA, P4H, and GAPDH. Experiments were performed in triplicate; representative images are shown. *, **, and ***denote $P < 0.05$, $P < 0.01$, and $P < 0.001$, respectively. *(Figure continues next page.)*

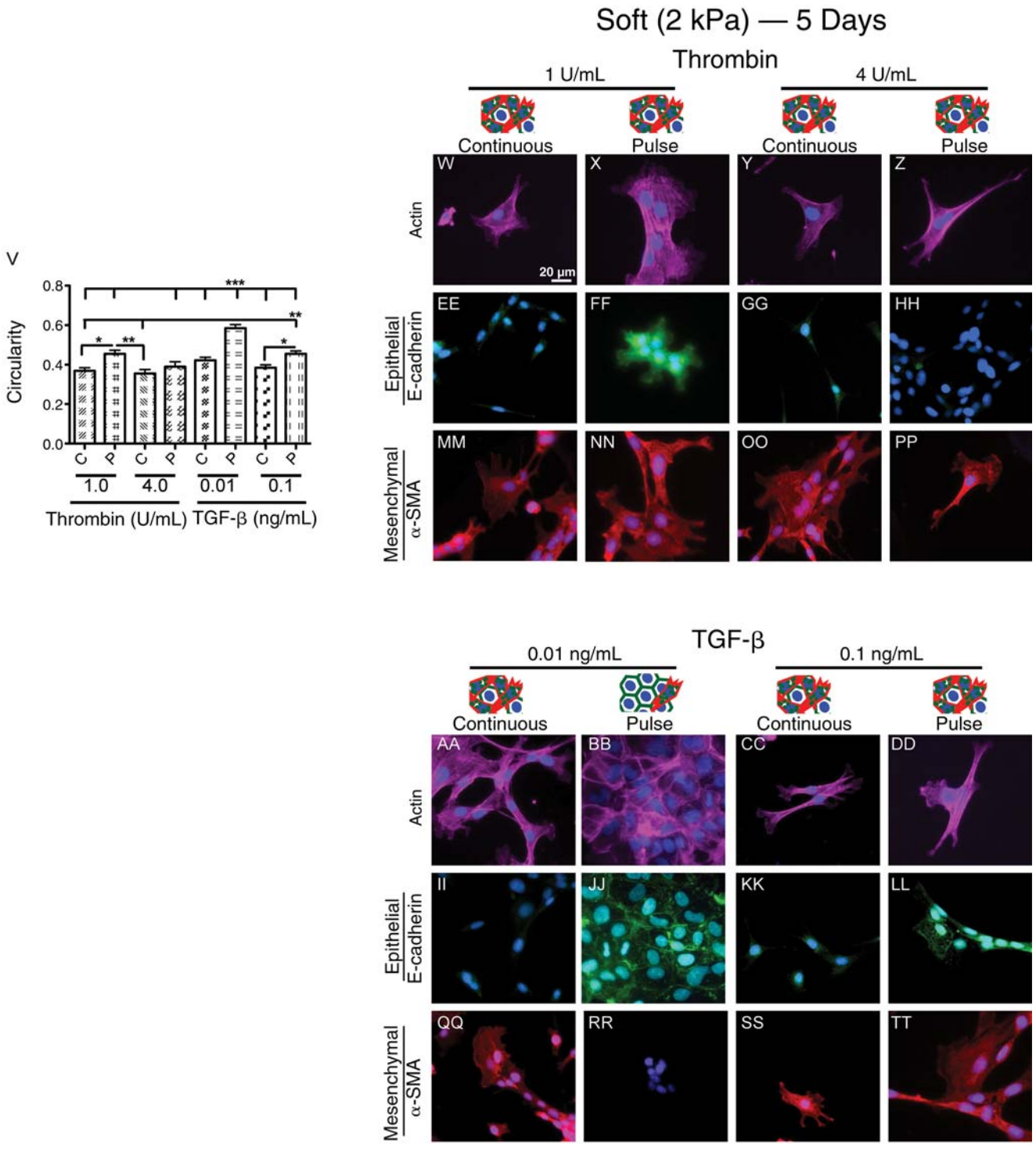

Figure 13 (*Continued*).

exposure to $PM_{2.5}$ can further drive a fibrotic state, leading to increased progression of lung disease. For Aim 2, then, we cultured alveolar epithelial cells on PA gels of increasing substrate stiffness with or without the addition of $PM_{2.5}$ and evaluated EMT events and TGF-β activation through immunohistochemistry, western blotting, AFM, and the MLEC assay.

Setup of Particle Composition Monitor

The $PM_{2.5}$ used in this analysis was collected between March 1 and June 30, 2004, at the ASACA site (as part of the longer-term ASACA study), using three-channel PCMs (Butler et al. 2003). The PCMs collected $PM_{2.5}$ samples for 24 hours. The samples were analyzed for metallic, ionic, and carbonaceous species in the $PM_{2.5}$ size range. The monitors were controlled by a data acquisition system that activated sampling, sequenced the filters, and controlled sample flow to a flow rate of 16.7 L/min through each channel. The filters were installed approximately one day before sampling and removed one day after exposure to ambient air. The PCMs were mounted approximately 2.5 m above the ground (Butler et al. 2003). Regular maintenance of the PCMs was performed over the collection period.

Ambient PM Characterization

The average ambient PM concentration measured at the South DeKalb monitoring site over the period during which the filter samples used for this analysis were collected was 14.2 $\mu g/m^3$. Concentrations of water-soluble sulfate, nitrate, and ammonium as well as elemental and organic carbon were determined from these samples. In addition, data on these species, as well as on elemental analyses, were available from a nearby (approximately 30 m) monitoring site (also in South DeKalb) run by the Georgia Environmental Protection Division (GaEPD). The same data are also reported as part of the U.S. EPA Air Quality System. The ASACA data (and the filters used) were available daily during the period; the GaEPD data were collected at the South DeKalb site every third day. Table 1 summarizes and compares our data on the composition of these components (sulfate, nitrate, ammonium, elemental carbon, and organic carbon) with the GaEPD data reported for the site. The ionic and carbonaceous composition of the $PM_{2.5}$ shows that the bulk of the $PM_{2.5}$ was sulfate and organic carbon (Table 1), of which a significant fraction was elemental carbon. It is important to note that both our collected data and the GaEPD data were highly similar and showed approximately a 1:1 relationship, as shown in Figure 14. A more complete presentation of the $PM_{2.5}$'s composition, including elemental concentrations measured at the GaEPD site and a comparison of the average ionic and carbonaceous PM concentrations measured in our study versus those measured in the samples collected every third day during the same period by the GaEPD (for source apportionment), is shown in Appendix C (available on the HEI Web site).

Source-Apportionment Modeling of $PM_{2.5}$

Measurements were used to conduct chemical-mass-balance source apportionment for the days that coincided with the samples used in our analysis, as previously described (Lee et al. 2007) and where GaEPD data were available (i.e., every third day). The reason for conducting source apportionment using the GaEPD data was the need to have concentrations for elemental species. The good agreement between the ASACA and GaEPD sampling data (and the close proximity of the two sets of monitors) suggests that very similar air masses were being sampled and that the source apportionment conducted using the concentrations measured at the GaEPD site was applicable to the filter samples collected as part of the ASACA monitoring. On average, the most prominent sources for the analyzed $PM_{2.5}$ were ammonium sulfate and bisulfate, which are largely formed from coal burning in the region and which together accounted, on an average day, for 45% of the apportioned mass, with biomass burning at 11%, gasoline-fueled vehicles at 10%, and diesel vehicles at 7%. Secondary sulfate and ammonium — formed from gas-phase reactions of SO_2, forming sulfuric acid, which then reacts with ammonia — dominate the primary (directly emitted) coal PM in the data shown in Table 2. Coal combustion is the largest contributor to SO_2 emissions in the region (Blanchard et al. 2013). Secondary organic carbon — formed from the oxidation of organic gases from biogenic emissions, biomass burning, mobile sources, and solvents — accounted, on a daily average basis, for 12% of the $PM_{2.5}$ mass. (As is often done with chemical-mass-balance results, secondary species are presented separately, without attribution to a specific source, because they are not included in the source profiles and, as seen in the case of the secondary organic carbon, can come from many sources.) The source distribution summarized in Table 2 was expected, because coal is a major fuel for electricity generation, the sampling site was near two freeways, March and April are the months when prescribed fires are most common in the Southeast, and organic gas emissions can be significant during this period, particularly from biogenic and mobile sources.

In summary, results from our particle analysis showed that the composition was primarily sulfate, related ammonium, and organic carbon with smaller amounts of elemental carbon and that the primary sources were those

Table 1. Comparison of Species Analyses for PM from the GaEDP and ASACA Sites at South DeKalb

	GaEDP Data (μg/m³)					ASACA Data (μg/m³)				
Date	NH_4	NO_3	SO_4	OC	EC	NH_4	NO_3	SO_4	OC	EC
March 2004										
1	0.43	0.85	1.72	3.72	0.45	0.58	0.52	1.92	3.78	0.33
4	1.06	0.85	3.38	6.79	1.75	1.20	0.58	3.77	10.03	1.59
7	0.34	0.22	1.41	3.38	1.09	0.40	0.15	1.37	4.06	1.16
10	1.85	1.57	4.41	3.63	0.74	1.85	1.42	4.62	3.91	0.64
13	0.77	1.04	1.71	5.59	0.59	0.87	1.09	1.91	5.44	0.33
16	0.98	0.52	3.02	4.99	0.85	1.06	0.43	3.16	5.25	0.64
19	1.04	0.59	3.06	6.53	2.25	0.91	0.56	2.94	8.31	2.21
22	1.28	0.98	2.99	2.19	0.28	1.40	0.97	3.50	1.59	0.24
25	1.23	0.75	3.37	7.62	1.19	1.12	0.61	3.68	8.91	0.75
28	0.63	0.73	2.24	6.76	1.38	0.87	0.59	2.65	7.24	1.10
31	1.00	0.81	2.51	1.87	0.40	1.09	0.75	2.76	1.94	0.54
April 2004										
3	1.13	0.73	3.38	3.22	0.52	1.32	0.67	3.74	2.77	0.32
6	0.46	0.29	1.37	5.07	1.47	0.38	0.30	1.52	4.55	1.56
12	3.10	2.13	7.86	4.54	0.58	3.43	2.03	7.93	4.80	0.27
15	0.78	0.55	2.22	3.76	0.91	0.71	0.53	2.32	3.71	1.00
18	1.43	0.42	4.50	7.14	1.33	1.48	0.57	5.00	8.81	1.08
21	0.82	0.67	2.74	4.32	0.80	0.78	0.50	2.69	4.30	0.52
24	1.33	0.69	4.38	6.72	1.86	1.54	0.78	4.38	8.15	1.60
27	0.98	0.58	3.23	3.88	1.05	1.06	0.48	3.14	3.30	0.88
30	2.03	0.75	6.53	3.41	0.25	2.57	0.51	7.07	2.84	0.06
May 2004										
3	1.21	0.36	3.86	2.15	0.34	1.32	0.32	3.84	1.79	0.48
9	2.00	0.59	5.90	7.96	0.82	3.25	0.81	8.93	7.65	0.67
12	1.89	0.69	6.58	3.62	0.27	1.88	0.59	5.55	3.54	0.17
15	0.72	0.69	2.71	3.60	0.35	1.06	0.53	3.43	4.77	0.44
18	0.98	0.72	3.28	4.26	1.08	2.30	0.52	7.06	4.16	1.13
21	2.12	0.52	7.80	6.42	2.21	2.44	0.62	7.92	6.42	1.14
24	1.55	0.51	6.73	4.28	1.21	1.82	0.59	6.10	4.95	1.36
30	1.10	0.59	5.31	4.09	0.47	0.57	0.24	2.38	0.92	0.28

leading to sulfate, biomass burning, and mobile sources. After analyzing the composition of our particles, we isolated total $PM_{2.5}$ from the Teflon filters and added it to cell culture media at 1:100, 1:1000, and 1:10,000 dilutions, which correspond to concentrations of 0.1, 1, and 10 μg/cm², respectively. These dilutions were used for all of the following experiments.

Addition of $PM_{2.5}$ from DeKalb County Further Drives EMT on Higher Substrate Stiffnesses

As described in the previous experiments, we used PA gels of various stiffnesses cross-linked with surface-immobilized Fn, cultured alveolar epithelial cells for five days with or without the addition of various concentrations of $PM_{2.5}$, and analyzed the cells for differing EMT responses. EMT was characterized through analysis of cell circularity and the expression of various epithelial and mesenchymal

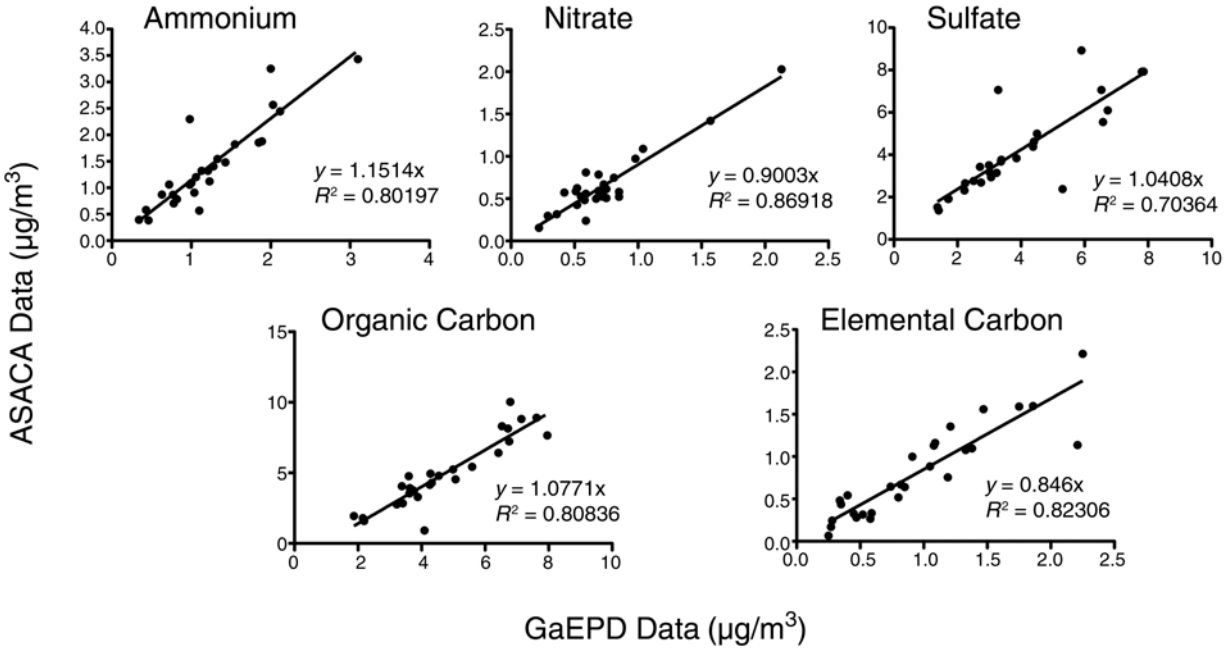

Figure 14. Measurements of major studied PM components are in agreement with previously reported measurements. Teflon filters from the ASACA monitoring site in South DeKalb were collected and analyzed for ammonium, nitrate, sulfate, organic carbon, and elemental carbon. The results were compared with data from the nearby (30 m) GaEPD monitoring site and showed a nearly 1:1 agreement.

markers by immunofluorescence staining and western blots. We had previously shown that alveolar epithelial cells undergo EMT on Fn-coated glass coverslips but retain an epithelial phenotype on Ln-coated glass coverslips; these conditions were used as controls. As expected, EMT was observed in the cells on the Fn-coated glass, as indicated by high levels of α-SMA expression and low levels of E-cadherin expression at cell–cell contacts. Conversely, the cells cultured on the Ln-coated glass showed an epithelial phenotype, as indicated by low levels of α-SMA expression and maintenance of E-cadherin expression at cell–cell contacts. Cells cultured without $PM_{2.5}$ that were stained for either epithelial or mesenchymal markers after five days showed a loss of epithelial markers and subsequent gain of mesenchymal markers as substrate stiffness was increased. This effect was enhanced with the addition of $PM_{2.5}$. As seen in Figure 15, when $PM_{2.5}$ was added at the 1:100 concentration, the cells showed an increase in the expression of α-SMA at lower substrate stiffnesses when compared with stiffness-matched controls (with no $PM_{2.5}$ added). In addition, there appeared to be a concentration threshold for $PM_{2.5}$ that was correlated with the observed increase in EMT.

EMT was also analyzed by cell circularity and cytoskeletal organization. Again, alveolar epithelial cells were cultured for five days on substrates of various stiffnesses with or without the addition of $PM_{2.5}$ at 1:100, 1:1000, or 1:10,000 dilutions and then stained to visualize the actin cytoskeleton. The cells cultured on the soft substrates and on the Ln-coated glass without the addition of $PM_{2.5}$ showed typical rounded epithelial morphology and diffuse cortical staining for actin. As substrate stiffness was increased, the cells showed an elongated morphology and thick, aligned actin filaments indicative of stress fibers. In addition, when $PM_{2.5}$ was added to the cultures, most notably at the 1:100 concentration, the cells showed increased EMT events, as shown by enhanced staining for actin filament stress fibers. Interestingly, cells cultured on 8-kPa gels showed a considerable increase in mesenchymal phenotype with the addition of $PM_{2.5}$ when compared with controls matched for substrate stiffness. This substrate stiffness is of particular interest because it most closely matches that of slightly fibrotic lung tissue. In addition, the increase appeared to be concentration-dependent, with a slightly more significant EMT response seen at the 1:100 concentration, as compared with the 1:1000 and 1:10,000. Finally, cell circularity was calculated

Table 2. Source Apportionment for $PM_{2.5}$ from the GaEPD Site at South DeKalb[a,b]

Date	GV (%)	DV (%)	Dust (%)	Burn (%)	Coal (%)	AMSULF (%)	AMBSULF (%)	AMNITR (%)	SOC (%)
March 2004									
1	13.22	0.00	3.01	19.41	0.75	0.00	28.76	15.52	19.33
4	9.73	12.65	1.26	17.23	0.68	9.58	22.59	8.50	17.80
7	14.14	19.92	12.31	13.62	1.73	0.84	25.48	4.47	7.48
10	8.81	4.45	2.45	7.57	1.50	36.49	13.68	17.73	7.31
13	8.06	4.36	2.83	11.17	1.76	12.11	12.04	15.44	32.23
16	10.45	6.09	2.76	16.18	0.39	19.10	20.76	6.97	17.30
19	16.53	21.24	3.47	8.53	0.58	16.75	12.87	5.75	14.28
22	11.24	0.00	3.87	10.08	1.45	45.05	10.53	17.77	0.00
25	10.13	7.41	6.26	10.50	0.58	20.04	11.36	6.97	26.75
28	7.61	11.73	3.18	9.05	1.01	0.00	25.10	8.98	33.34
31	9.94	3.40	2.47	5.59	0.56	38.77	19.88	18.73	0.66
April 2004									
3	15.10	0.00	2.92	11.65	2.07	25.90	26.60	11.69	4.08
6	18.82	20.42	6.87	11.43	1.88	10.86	9.55	4.52	15.65
12	3.47	0.00	2.24	5.97	0.50	43.37	17.47	16.22	10.75
15	17.12	9.74	4.50	11.49	1.48	20.40	17.26	9.64	8.36
18	18.16	0.33	4.44	13.19	0.17	24.27	17.66	3.93	17.84
21	12.03	0.82	16.59	19.07	1.51	7.93	26.28	8.92	6.85
24	14.29	12.47	4.37	14.70	0.49	15.00	22.10	5.99	10.58
27	13.84	10.87	9.41	9.86	0.73	16.08	25.94	7.81	5.47
30	1.21	0.00	5.95	11.90	0.45	33.68	32.67	7.70	6.45
May 2004									
3	11.75	2.08	1.57	5.21	0.23	40.93	31.52	6.71	0.00
9	5.81	2.94	5.42	8.62	0.41	31.92	14.92	4.63	25.32
12	1.49	0.00	6.90	10.54	0.40	26.31	39.87	7.05	7.45
15	5.89	0.00	7.69	17.90	0.65	0.08	44.41	12.31	11.06
18	6.32	10.63	3.74	8.78	0.34	12.59	32.86	10.40	14.34
21	7.39	16.61	2.52	4.69	0.72	20.71	32.76	3.59	11.02
24	6.15	9.45	1.97	5.44	0.71	8.19	54.60	4.98	8.51
30	3.02	0.00	2.96	16.72	0.20	0.00	59.77	7.26	10.08
June 2004									
2	8.62	11.23	2.50	4.69	0.14	3.85	63.35	2.45	3.18
Average	10.01	6.86	4.70	11.06	0.83	18.65	26.64	9.06	12.19

[a] The percentages of source-apportioned mass are shown by day. These differ somewhat from the average of the mass contributed over the measurements divided by the average total PM mass for the period.

[b] GV denotes gasoline-fueled vehicles; DV, diesel vehicles; Burn, biomass burning; AMSULF, ammonium sulfate; AMBSULF, ammonium bisulfate; AMNITR, ammonium nitrate; and SOC, secondary organic carbon.

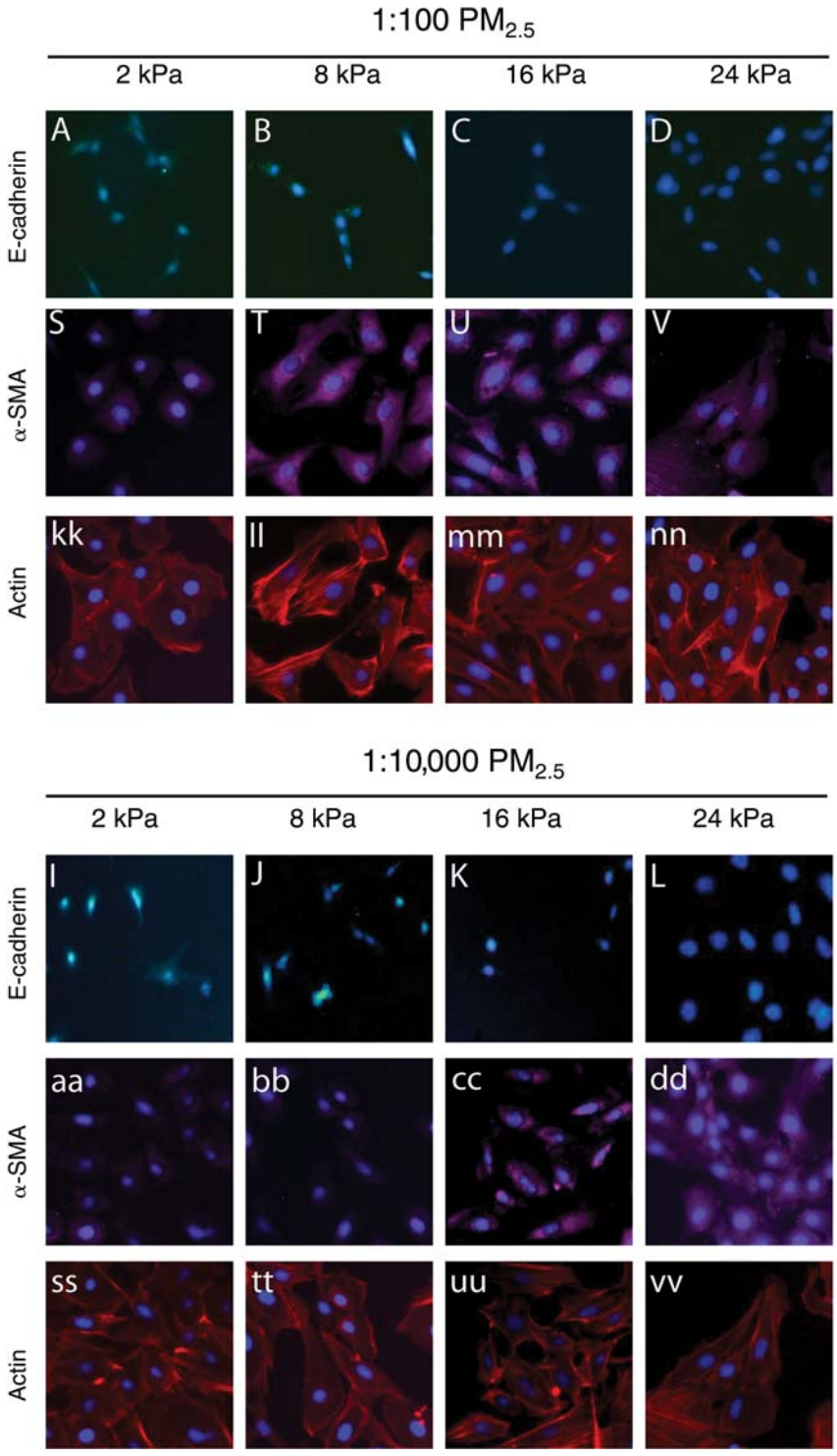

Figure 15. Analysis of EMT in RLE-6TN cells cultured with added $PM_{2.5}$ on Fn substrates of increasing stiffness. RLE-6TN cells were cultured for five days on Fn PA gels or Fn- or Ln-coated glass with the addition of 1:100, 1:1000, or 1:10,000 concentrations of $PM_{2.5}$. EMT responses were analyzed through changes in epithelial and mesenchymal protein expression through immunofluorescence staining for (**A–R**) E-cadherin and (**S–jj**) α-SMA as well as (**kk–bbb**) changes in the actin cytoskeleton. Experiments were performed in triplicate; representative images are shown. *(Figure continues next page.)*

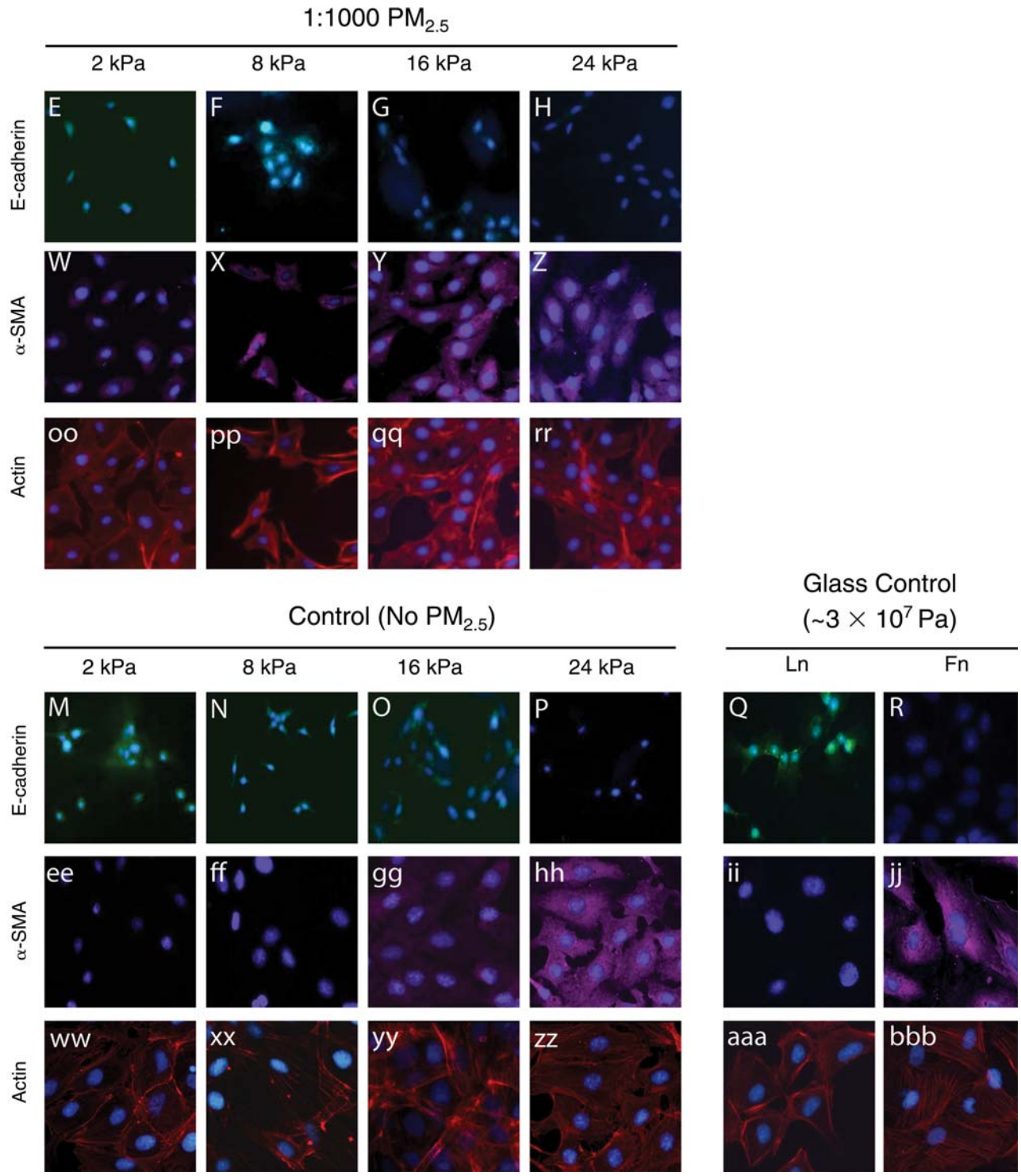

Figure 15 ***(Continued).***

to quantify differences in the observed cell shapes. Values closer to 1 indicate a more rounded, epithelial-like cell (Figure 16). Statistical significance is shown for each experimental group, as compared with its same-substrate-stiffness group with no $PM_{2.5}$ added. The results supported the observed immunohistochemistry results, showing that the addition of $PM_{2.5}$, most notably at the 1:100 concentration, resulted in decreased circularity values (indicative of more elongated cells and hence of EMT events).

The differentiation from an epithelial to a mesenchymal phenotype was further quantified by western blot analysis for E-cadherin and cytokeratin (epithelial) and α-SMA and prolyl 4-hydroxylase (P4H) (mesenchymal) protein expression. The western blots were quantified as fold change, as compared with expression on 2-kPa gels, normalizing for protein loading with GAPDH. Higher expression of E-cadherin and cytokeratin was seen on the lower substrate stiffnesses, as compared with the higher substrate stiffnesses with or without the addition of $PM_{2.5}$. Although expression of E-cadherin was seen on all substrate stiffnesses, the localization was lost from cell–cell contacts, a finding that agreed with previous literature, which found that E-cadherin was still expressed intracellularly. When cells were cultured with the addition of $PM_{2.5}$, we observed an increase in the expression of P4H at lower substrate stiffnesses, as compared with the same samples with no $PM_{2.5}$ added. In addition, we observed decreased expression of both of the measured epithelial markers, E-cadherin and cytokeratin, with the addition of $PM_{2.5}$ at the 1:100 concentration on matched substrate stiffnesses. For example, the expression of E-cadherin and cytokeratin decreased markedly at 8 kPa with the addition of a 1:100 concentration of $PM_{2.5}$, whereas the expression of P4H increased significantly, as compared with the control (no added $PM_{2.5}$). This phenomenon was observed for all concentrations of added $PM_{2.5}$ but was most significant at the higher 1:100 concentration, suggesting that there is a dose-dependent effect on EMT (Figure 17). Statistical significance is shown for each experimental group, as compared with its same-substrate-stiffness group with no $PM_{2.5}$ added.

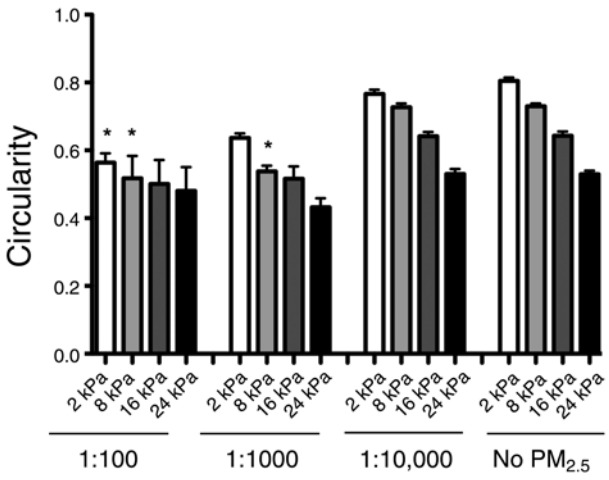

Figure 16. Cell circularity decreases when cells are cultured with added $PM_{2.5}$. RLE-6TN cells were cultured for five days on PA gels of increasing degrees of stiffness or Fn- or Ln-coated glass, and $PM_{2.5}$ was added at various concentrations. Cells were stained with Texas Red phalloidin to visualize the actin cytoskeleton, and circularity was analyzed. Values closer to 1 indicate a more rounded, epithelial-like cell ($N = 3$). Significance is shown for comparisons with controls of the same substrate stiffness and no added $PM_{2.5}$. * denotes $P < 0.05$.

Alveolar Epithelial Cells Show Increased Cortical Stiffness with the Addition of $PM_{2.5}$

We showed previously that during EMT epithelial cell stiffness increases with increasing substrate stiffnesses. Using AFM, we therefore investigated whether the EMT observed with the addition of $PM_{2.5}$ resulted in increased cell contractility. Because of the significant increases in the expression of the mesenchymal marker P4H at 8 kPa with the addition of $PM_{2.5}$, as compared with the control, we cultured alveolar epithelial cells for five days on 8-kPa gels with the various added concentrations of $PM_{2.5}$ or no added $PM_{2.5}$. Statistical significance is shown in comparison with the control. We observed a concentration-dependent increase in cell contractility with the addition of the increasing concentrations of $PM_{2.5}$, as compared with the 8-kPa control. When the cells were cultured with the addition of either 1:100 or 1:1000 concentrations of $PM_{2.5}$, cell contractility increased (with average elastic moduli of 2.8 and 2.4 kPa, respectively), as compared with that of cells cultured with the 1:10,000 concentration or no addition of $PM_{2.5}$ (with average elastic moduli of 1.5 and 1.4 kPa, respectively). These results indicate that the addition of $PM_{2.5}$ increases cell contractility and likely contributes to the observed increases in EMT events (Figure 18). Statistical significance is shown compared with the control (with no $PM_{2.5}$ added).

Alveolar Epithelial Cells Show Increased TGF-β Activation with the Addition of $PM_{2.5}$

In Aim 1, we showed that increased matrix stiffness leads to contractile forces, ultimately enabling the activation of TGF-β, a primary EMT inducer. Because we saw increases in cell contractility with the addition of $PM_{2.5}$, we investigated whether the addition of $PM_{2.5}$ also resulted in differences in TGF-β activation, which could be an explanation for the increases in EMT events. To determine if the addition of various concentrations of $PM_{2.5}$ to alveolar cells on various substrate stiffnesses induced TGF-β activation, the MLEC assay was performed (Figure 19). The same experimental groups and controls were used as for the

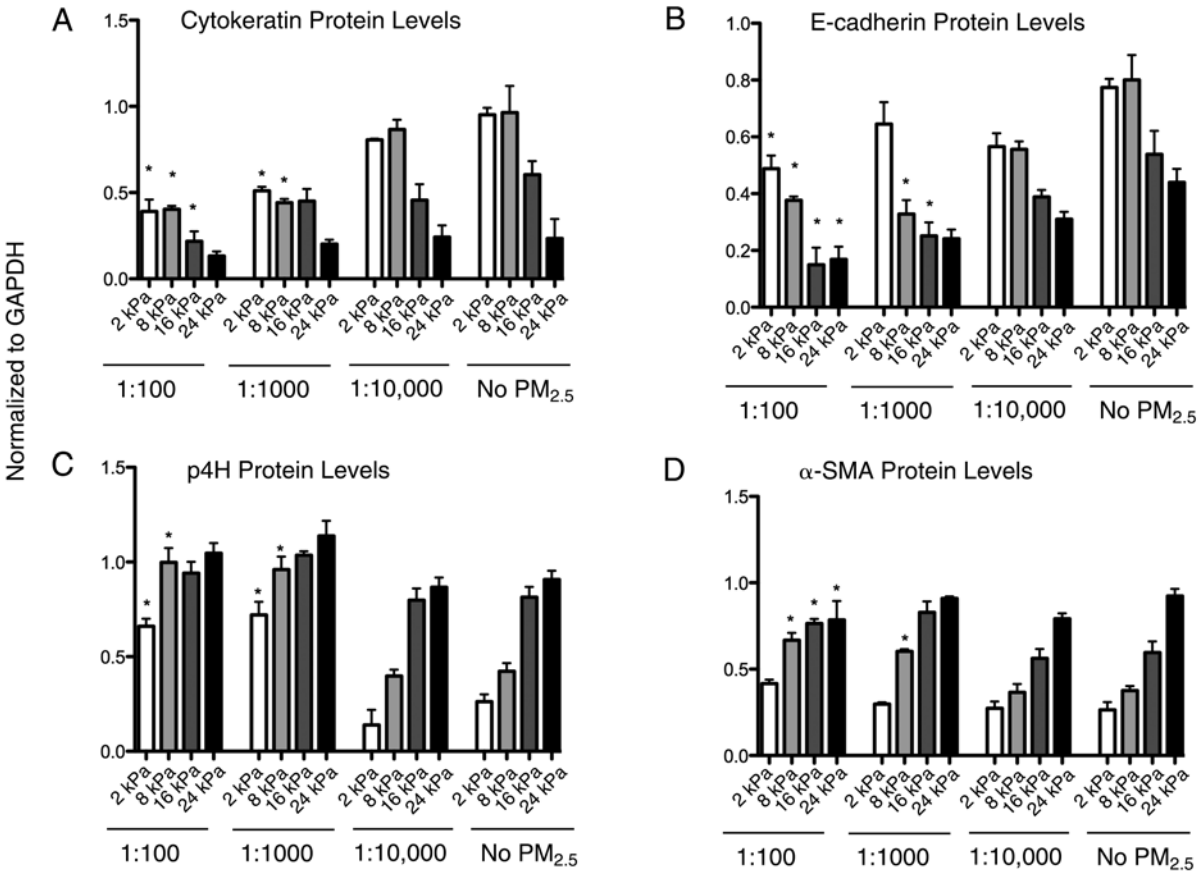

Figure 17. Addition of $PM_{2.5}$ induces EMT. RLE-6TN cells were cultured for five days on substrates of increasing degrees of stiffness with or without the addition of $PM_{2.5}$. Cells were lysed and analyzed by western blot for changes in protein expression of (**A–B**) cytokeratin and E-cadherin and (**C–D**) p4H and α-SMA ($N = 3$). Significance is shown for comparisons with controls of the same substrate stiffness and no added $PM_{2.5}$. Representative blots are shown in Appendix B. * denotes $P < 0.05$.

immunohistochemistry and western blot experiments. In the controls (i.e., with no $PM_{2.5}$ added), alveolar epithelial cells were found to activate TGF-β increasingly in response to increases in substrate stiffness. As expected, the control groups cultured on Fn-coated glass showed high levels of TGF-β activation, whereas those cultured on Ln-coated glass showed significantly less TGF-β activation. When $PM_{2.5}$ was added to the cultures for five days, the cells were found to activate significantly greater amounts of TGF-β in a dose-dependent manner, as compared with the cells at the same substrate stiffnesses and no $PM_{2.5}$ added. Of particular interest was the comparison of TGF-β activation across the $PM_{2.5}$ concentrations at 8 kPa, a physiologically relevant stiffness for human lung fibrosis. With the addition of $PM_{2.5}$ at this substrate stiffness, an increase was observed in TGF-β activation similar to that observed on higher substrate stiffnesses and Fn-coated glass without the $PM_{2.5}$ (Figure 19). Statistical significance is shown for each experimental group, as compared with its same-substrate-stiffness group with no $PM_{2.5}$ added. $PM_{2.5}$ addition to a solution of inactive TGF-β was found insufficient to activate the TGF-β strongly, suggesting that the observed increases in TGF-β activation are mediated by the cells (data not shown).

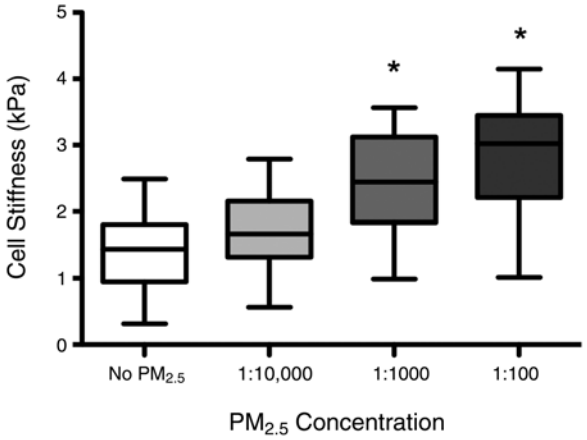

Figure 18. Cell stiffness increases with increasing $PM_{2.5}$ doses. RLE-6TN cells were cultured for five days on substrates with or without the addition of $PM_{2.5}$. Single-cell elasticity was measured using AFM nanoindentation to characterize cell stiffening in response to substrate stiffness and $PM_{2.5}$. Averages of cell stiffness for each gel mixture are shown ($N = 10$). Significance is reported for differences between each PM concentration and the control (i.e., no $PM_{2.5}$ added) ($P < 0.01$). Significance is shown for each group compared with its same-substrate-stiffness group with no $PM_{2.5}$ added. Boxes denote the 25th to 75th percentile of values, with central horizontal line as the median; whiskers extend vertically to the most extreme measurements within 1.5 times the interquartile range of the 25th and 75th percentile values, respectively. * denotes $P < 0.05$.

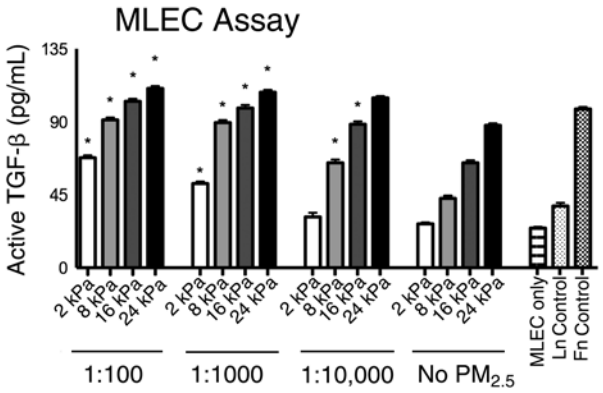

Figure 19. Stiffness-mediated EMT with $PM_{2.5}$ is mediated by TGF-β activation. RLE-6TN cells were cultured for five days on substrates of increasing degrees of stiffness with or without the addition of $PM_{2.5}$, and levels of TGF-β activation were determined using the MLEC assay. * denotes $P < 0.05$.

DISCUSSION, CONCLUSIONS, AND IMPLICATIONS

The work in Aim 1 provided evidence that the micromechanical environment with which epithelial cells interact is a strong driving force for EMT. The stiffer the substrate is, the stronger the pressure on the epithelial cell to undergo EMT. This unique finding raises questions about what is currently known about EMT. Specifically, the vast majority of in vitro EMT research to date has been performed on substrates with nonphysiologic (i.e., gigapascal) stiffness (Chang et al. 2011; Kim et al. 2006; Thiery and Sleeman 2006; Thiery et al. 2009; Willis and Borok 2007; Willis et al. 2006; Yang et al. 2010).

Although the stiffness of the cellular microenvironment clearly plays a significant role in defining the resident cell phenotype (Engler et al. 2006; Liu et al. 2010; Paszek et al. 2005; Wipff and Hinz 2008; Wipff et al. 2007), the origins of increased tissue stiffness are still poorly understood. It is likely that stiffness arises from the residential cell population and the overproduction or activation of cross-linking enzymes. Fibroblasts that have differentiated down a contractile, myofibroblastic pathway are known to show significant contractile force (Wipff and Hinz 2008; Wipff et al. 2007). Such cell-derived forces are capable of stressing the surrounding ECM, leading to increased microenvironmental stiffness. Additionally, recent evidence suggests that even normal fibroblast subpopulations might show significant differences in their capacity to exert force on their matrix (Barker et al. 2004; Zhou et al. 2010). Several investigations have shown that lysyl oxidase in the tumor microenvironment is sufficient to cross-link and stiffen the tumor stroma (Levental et al. 2009), and transglutaminases have long been known to catalyze ECM cross-linking and have recently been shown to result in tissue stiffening (Santhanam et al. 2010). As mentioned previously, the prevailing thought is that EMT precedes tissue stiffening, yet several reports indicate that tissue stiffening occurs prior to the onset of fibrosis.

The data reported for Aim 1, in the first part of the study, indicated that tissue–substrate stiffness is necessary but not sufficient to induce spontaneous EMT. Stiffness in the context of EMT depends on the ECM ligand. Increased stiffness acts synergistically with Fn to promote EMT through contraction-mediated TGF-β activation, whereas Ln substrates inhibit EMT. These data corroborate previous

findings on tissue culture on glass and TCP with respect to the role of ECM proteins in EMT (Kim et al. 2006) and support recent evidence that integrin-specificity drives mechanotransduction and compliance matching.

Furthermore, the application of force to the focal adhesion complex leads to recruitment and activation of signaling proteins such as focal adhesion kinase (FAK), sarcoma kinase (Src), and Src homology 2 domain containing–transforming protein 1 (Shc), whose major downstream targets are Rho guanosine triphosphatases. Importantly, activation of the Rho signaling cascade leads to cytoskeletal rearrangement and increased cell contractility. These cytoskeletal and contractile perturbations are now directly linked to activation of TGF-β by way of integrin-mediated release of the active growth factor from latency-associated protein (Hinz 2009; Kim et al. 2006; Wipff and Hinz 2008; Wipff et al. 2007). The consequence of this "secondary effect" of tissue stiffness is the transformation of cell types — from fibroblasts to myofibroblasts (Wipff and Hinz 2008; Wipff et al. 2007), EMT, etc. Overall, our work has demonstrated that tissue compliance is a critical factor in the determination of EMT and that matrix stiffness acts as a mediator of cell contractility and subsequent TGF-β activation. These findings, along with others', suggest that therapeutic approaches to fibrosis that focus only on the cell are critically flawed. A pathologic extracellular microenvironment (the ECM and its mechanical properties) sends profibrotic signals that promote the progression of the disease despite any acute eradication of the resident cells. How one modifies the biochemical and biophysical microenvironment might be a greater determinant in the success of future therapeutics.

The data reported for Aim 2, in the second part of the study, showed that on cultures with matched substrate stiffnesses, the addition of $PM_{2.5}$ was associated with the exacerbation of stiffness-induced EMT. We first showed by immunohistochemistry, cell phenotype analyses, and western blotting for EMT protein markers that, at higher concentrations of $PM_{2.5}$ (1:100), mesenchymal markers were expressed in cultures with lower substrate stiffnesses that had lacked mesenchymal marker protein expression without added $PM_{2.5}$. We found, furthermore, that $PM_{2.5}$ was also involved in increasing epithelial cell contractility. Although no experiments were done to measure cell contractility directly, our findings for Aim 1 led us to infer that increased cell stiffness likely leads to increased cell contraction. As shown in Aim 1, this increased cell contraction might be a prominent mechanism for the activation of TGF-β and the observed spontaneous EMT.

Although there were several limitations to this preliminary study, our results are a first step toward elucidating how environmental stimuli might exacerbate existing pulmonary pathologies by leading to increased fibrotic phenotypes. Future studies are needed to directly determine the specific role of particle composition and size on the observed EMT effects. In the current study, our particle-extraction methods might have resulted in slight biasing effects of particle size and surface area. In order to determine if the EMT effects seen were based solely on particle composition, a control study focusing on a nonreactive particle such as elemental carbon should be included to show whether the observed effects were caused by treatment with our particular $PM_{2.5}$ rather than by treatment with any nanoparticle.

In addition, based on our observations in Aim 1 and the fact that addition of $PM_{2.5}$ increases cell stiffness, one possible mechanism by which the addition of $PM_{2.5}$ results in increased EMT is by further increasing cell contractility, leading ultimately to the observed increases in TGF-β. Future control studies will be needed to test whether the $PM_{2.5}$ is acting through cell contraction–mediated TGF-β signaling pathways. Specifically, ATII cells will need to be cultured in a manner similar to that described in the current study with the addition of $PM_{2.5}$ in the presence of cell-contraction inhibitors. In addition, there are several different mechanisms that might lead to ATII cell contraction, including but not limited to Rho–ROCK activity, myosin light-chain kinase phosphorylation, actin polymerization, and myocardin-related transcription factor-A signaling. Future studies exploring each of these pathways will elucidate more clearly how $PM_{2.5}$ affects ATII EMT.

Although we predict that $PM_{2.5}$ leads to increased cell contraction, resulting in mechanical activation of TGF-β, several other biochemical activation mechanisms are possible. The alveolar epithelium forms a continuous, highly regulated physical barrier that serves as a protector against inhaled environmental agents, including $PM_{2.5}$. During EMT, the tight cell junctions and E-cadherin expression commonly seen in the epithelium are lost. This loss of structure has been implicated in allowing enhanced signaling between the epithelium and underlying immune cells (Nawijn et al. 2011). Previous studies have implicated enhanced immune-cell activation and inflammation in the release of reactive oxygen species that leads to the activation of TGF-β (Bonner 2007; Mazzoli-Rocha et al. 2010; Veljkovic et al. 2011; Zou et al. 2013). Furthermore TGF-β itself is able to induce the production of reactive oxygen species as part of its signal transduction pathway. As shown in the current study, TGF-β is a potent inducer of EMT. These facts taken together suggest that the higher levels of EMT seen on exposure to $PM_{2.5}$ might be the result of a positive feedback loop in which enhanced

exposure to the $PM_{2.5}$ through loss of cell–cell junctions exposes the cell to being more susceptible to the effects of surrounding immune cells and inflammatory signals, which can further activate TGF-β and drive additional EMT progression.

Overall, our work — showing increased cell contractility, TGF-β activation, and EMT events in response to $PM_{2.5}$ exposure — highlights the importance of studying not only the micromechanical environment in lung disease, but also the exposure to environmental injury adjuvants in already diseased lung models. Our findings indicate that increased substrate stiffness is able to lead to increased cell contraction, TGF-β activation, and subsequent EMT, representing one of the initial stages of pulmonary fibrosis. Furthermore, exposure to environmental stimuli, such as $PM_{2.5}$, is associated with increases in EMT events. These preliminary results suggest that $PM_{2.5}$ might play a role in additionally driving a pre-existing fibrotic phenotype in pulmonary cells. Because of the possible implications of our study, future work should focus on further elucidation of the pathways that both tissue stiffness and $PM_{2.5}$ engage to initiate the EMT program and of how these pathways intersect. The principal unanswered question that remains is how $PM_{2.5}$ engages the cell cytoskeletal signaling mechanisms. The logical culprits are reactive oxygen and nitrogen species; however, based on current literature, it remains unclear what the critical signaling protein targets of reactive oxygen species are that induce cell cytoskeletal contraction.

REFERENCES

Abbey DE, Burchette RJ, Knutsen SF, McDonnell WF, Lebowitz MD, Enright PL. 1998. Long-term particulate and other air pollutants and lung function in nonsmokers. Am J Respir Crit Care Med 158:289–298.

Abbey DE, Nishino N, McDonnell WF, Burchette RJ, Knutsen SF, Beeson WL, et al. 1999. Long-term inhalable particles and other air pollutants related to mortality in nonsmokers. Am J Respir Crit Care Med 159:373–382.

Abe M, Harpel JG, Metz CN, Nunes I, Loskutoff DJ, Rifkin DB. 1994. An assay for transforming growth factor-b using cells transfected with a plasminogen activator inhibitor-1 promoter-luciferase construct. Anal Biochem 216:276–284.

Anderson HR, Spix C, Medina S, Schouten JP, Castellsague J, Rossi G, et al. 1997. Air pollution and daily admissions for chronic obstructive pulmonary disease in 6 European cities: results from the APHEA project. Eur Respir J 10:1064–1071.

Anderson JM, Rodriguez A, Chang DT. 2008. Foreign body reaction to biomaterials. Semin Immunol 20:86–100.

Annes JP, Chen Y, Munger JS, Rifkin DB. 2004. Integrin alphaVbeta6-mediated activation of latent TGF-beta requires the latent TGF-beta binding protein-1. J Cell Biol 165(5):723–34.

Aoyagi-Ikeda K, Maeno T, Matsui H, Ueno M, Hara K, Aoki Y, et al. 2011. Notch induces myofibroblast differentiation of alveolar epithelial cells via TGF-ss/Smad3 pathway. Am J Respir Cell Mol Biol 45:136–144.

Arnoux V, Nassour M, L'Helgoualc'h A, Hipskind RA, Savagner P. 2008. Erk5 controls Slug expression and keratinocyte activation during wound healing. Mol Biol Cell 19:4738–4749.

Barker TH, Grenett HE, MacEwen MW, Tilden SG, Fuller GM, Settleman J, et al. 2004. Thy-1 regulates fibroblast focal adhesions, cytoskeletal organization and migration through modulation of p190 RhoGAP and Rho GTPase activity. Exp Cell Res 295:488–496.

Barry-Hamilton V, Spangler R, Marshall D, McCauley S, Rodriguez HM, Oyasu M, et al. 2010. Allosteric inhibition of lysyl oxidase-like-2 impedes the development of a pathologic microenvironment. Nat Med 16:1009–1017.

Batlle E, Sancho E, Franci C, Dominguez D, Monfar M, Baulida J, et al. 2000. The transcription factor snail is a repressor of E-cadherin gene expression in epithelial tumour cells. Nat Cell Biol 2:84–89.

Becker S, Soukup JM, Gilmour MI, Devlin RB. 1996. Stimulation of human and rat alveolar macrophages by urban air particulates: effects on oxidant radical generation and cytokine production. Toxicol Appl Pharmacol 141:637–648.

Blanchard CL, Tanenbaum S, Hidy GM. 2013. Source attribution of air pollutant concentrations and trends in the Southeastern Aerosol Research and Characterization (SEARCH) network. Environ Sci Technol 47:13536–13545.

Bonner JC. 2007. Lung fibrotic responses to particle exposure. Toxicol Pathol 35:148–153.

Boutet A, De Frutos CA, Maxwell PH, Mayol MJ, Romero J, Nieto MA. 2006. Snail activation disrupts tissue homeostasis and induces fibrosis in the adult kidney. EMBO J 25:5603–5613.

Butler AJ, Andrew MS, Russell AG. 2003. Daily sampling of $PM_{2.5}$ in Atlanta: results of the first year of the assessment of spatial aerosol composition in Atlanta study. J Geophys Res-Atmos 108.

Camara J, Jarai G. 2010. Epithelial-mesenchymal transition in primary human bronchial epithelial cells is Smad-dependent and enhanced by fibronectin and TNF-alpha. Fibrogenesis Tissue Repair 3:2.

Chang CJ, Chao CH, Xia W, Yang JY, Xiong Y, Li CW, et al. 2011. p53 regulates epithelial-mesenchymal transition and stem cell properties through modulating miRNAs. Nat Cell Biol 13:317–323.

Choquet D, Felsenfeld DP, Sheetz MP. 1997. Extracellular matrix rigidity causes strengthening of integrin-cytoskeleton linkages. Cell 88:39–48.

Coward WR, Saini G, Jenkins G. 2010. The pathogenesis of idiopathic pulmonary fibrosis. Ther Adv Respir Dis 4:367–388.

Dagher Z, Garcon G, Gosset P, Ledoux F, Surpateanu G, Courcot D, et al. 2005. Pro-inflammatory effects of Dunkerque city air pollution particulate matter 2.5 in human epithelial lung cells (L132) in culture. J Appl Toxicol 25:166–175.

Degryse AL, Tanjore H, Xu XC, Polosukhin VV, Jones BR, Boomershine CS, et al. 2011. TGFβ signaling in lung epithelium regulates bleomycin-induced alveolar injury and fibroblast recruitment. Am J Physiol Lung Cell Mol Physiol. 300:L887–L897.

Derynck R, Zhang YE. 2003. Smad-dependent and Smad-independent pathways in TGF-beta family signalling. Nature 425:577–584.

Diaz-Sanchez D, Jyrala M, Ng D, Nel A, Saxon A. 2000. In vivo nasal challenge with diesel exhaust particles enhances expression of the CC chemokines rantes, MIP-1alpha, and MCP-3 in humans. Clin Immunol 97:140–145.

Dreher KL, Jaskot RH, Lehmann JR, Richards JH, McGee JK, Ghio AJ, et al. 1997. Soluble transition metals mediate residual oil fly ash induced acute lung injury. J Toxicol Environ Health 50:285–305.

Duband JL, Thiery JP. 1982. Appearance and distribution of fibronectin during chick embryo gastrulation and neurulation. Dev Biol 94:337–350.

Engler AJ, Griffin MA, Sen S, Bonnemann CG, Sweeney HL, Discher DE. 2004. Myotubes differentiate optimally on substrates with tissue-like stiffness: pathological implications for soft or stiff microenvironments. J Cell Biol 166:877–887.

Engler AJ, Sen S, Sweeney HL, Discher DE. 2006. Matrix elasticity directs stem cell lineage specification. Cell 126:677–689.

Fehrenbach H. 2001. Alveolar epithelial type II cell: defender of the alveolus revisited. Respir Res 2:33–46.

Felton VM, Borok Z, Willis BC. 2009. N-acetylcysteine inhibits alveolar epithelial-mesenchymal transition. Am J Physiol Lung Cell Mol Physiol 297:L805–812.

Georges PC, Hui JJ, Gombos Z, McCormick ME, Wang AY, Uemura M, et al. 2007. Increased stiffness of the rat liver precedes matrix deposition: implications for fibrosis. Am J Physiol Gastrointest Liver Physiol 293:G1147–1154.

Georges PC, Janmey PA. 2005. Cell type-specific response to growth on soft materials. J Appl Physiol 98:1547–1553.

Gharaee-Kermani M, Hu B, Phan SH, Gyetko MR. 2009. Recent advances in molecular targets and treatment of idiopathic pulmonary fibrosis: focus on TGFbeta signaling and the myofibroblast. Curr Med Chem 16:1400–1417.

Goss CH, Newsom SA, Schildcrout JS, Sheppard L, Kaufman JD. 2004. Effect of ambient air pollution on pulmonary exacerbations and lung function in cystic fibrosis. Am J Respir Crit Care Med 169:816–821.

Guaita S, Puig I, Franci C, Garrido M, Dominguez D, Batlle E, et al. 2002. Snail induction of epithelial to mesenchymal transition in tumor cells is accompanied by MUC1 repression and ZEB1 expression. J Biol Chem 277:39209–39216.

Hay ED. 1995. An overview of epithelio-mesenchymal transformation. Acta Anat (Basel) 154:8–20.

Hinz B. 2009. Tissue stiffness, latent TGF-beta1 activation, and mechanical signal transduction: implications for the pathogenesis and treatment of fibrosis. Curr Rheumatol Rep 11:120–126.

Holgate ST, Davies DE, Lackie PM, Wilson SJ, Puddicombe SM, Lordan JL. 2000. Epithelial-mesenchymal interactions in the pathogenesis of asthma. J Allergy Clin Immunol 105:193–204.

Iwano M, Plieth D, Danoff TM, Xue C, Okada H, Neilson EG. 2002. Evidence that fibroblasts derive from epithelium during tissue fibrosis. J Clin Invest 110:341–350.

Jain L, Chen XJ, Ramosevac S, Brown LA, Eaton DC. 2001. Expression of highly selective sodium channels in alveolar

type II cells is determined by culture conditions. Am J Physiol Lung Cell Mol Physiol 280:L646–658.

Jain R, Shaul PW, Borok Z, Willis BC. 2007. Endothelin-1 induces alveolar epithelial-mesenchymal transition through endothelin type A receptor-mediated production of TGF-beta1. Am J Respir Cell Mol Biol 37:38–47.

Jenkins RG, Su X, Su G, Scotton CJ, Camerer E, Laurent GJ, et al. 2006. Ligation of protease-activated receptor 1 enhances alpha(v)beta6 integrin-dependent TGF-beta activation and promotes acute lung injury. J Clin Invest 116:1606–1614.

Kasai H, Allen JT, Mason RM, Kamimura T, Zhang Z. 2005. TGF-beta1 induces human alveolar epithelial to mesenchymal cell transition (EMT). Respir Res 6:56.

Kim KK, Kugler MC, Wolters PJ, Robillard L, Galvez MG, Brumwell AN, et al. 2006. Alveolar epithelial cell mesenchymal transition develops in vivo during pulmonary fibrosis and is regulated by the extracellular matrix. Proc Natl Acad Sci U S A 103:13180–13185.

Kim Y, Kugler MC, Wei Y, Kim KK, Li X, Brumwell AN, et al. 2009. Integrin alpha3beta1-dependent beta-catenin phosphorylation links epithelial Smad signaling to cell contacts. J Cell Biol 184:309–322.

Kuwano K, Kunitake R, Kawasaki M, Nomoto Y, Hagimoto N, Nakanishi Y, et al. 1996. P21Waf1/Cip1/Sdi1 and p53 expression in association with DNA strand breaks in idiopathic pulmonary fibrosis. Am J Respir Crit Care Med 154:477–483.

Lee S, Russell AG, Baumann K. 2007. Source apportionment of fine particulate matter in the southeastern United States. J Air Waste Manag Assoc 57:1123–1135.

Levental KR, Yu H, Kass L, Lakins JN, Egeblad M, Erler JT, et al. 2009. Matrix crosslinking forces tumor progression by enhancing integrin signaling. Cell 139:891–906.

Liu F, Mih JD, Shea BS, Kho AT, Sharif AS, Tager AM, et al. 2010. Feedback amplification of fibrosis through matrix stiffening and COX-2 suppression. J Cell Biol 190:693–706.

Maher TM, Wells AU, Laurent GJ. 2007. Idiopathic pulmonary fibrosis: multiple causes and multiple mechanisms? Eur Respir J 30:835–839.

Mason RJ. 2006. Biology of alveolar type II cells. Respirology 11 Suppl:S12–15.

Mazzoli-Rocha F, Fernandes S, Einicker-Lamas M, Zin WA. 2010. Roles of oxidative stress in signaling and inflammation induced by particulate matter. Cell Biol Toxicol 26:481–498.

Meltzer EB, Noble PW. 2008. Idiopathic pulmonary fibrosis. Orphanet J Rare Dis 3:8.

Nawijn MC, Hackett TL, Postma DS, van Oosterhout AJ, Heijink IH. 2011. E-cadherin: gatekeeper of airway mucosa and allergic sensitization. Trends Immunol 32:248–255.

Oberdörster G, Oberdörster E, Oberdörster J. 2005. Nanotoxicology: an emerging discipline evolving from studies of ultrafine particles. Environ Health Perspect 113:823–839.

Paszek MJ, Zahir N, Johnson KR, Lakins JN, Rozenberg GI, Gefen A, et al. 2005. Tensional homeostasis and the malignant phenotype. Cancer Cell 8:241–254.

Pelham RJ Jr, Wang Y. 1997. Cell locomotion and focal adhesions are regulated by substrate flexibility. Proc Natl Acad Sci USA 94:13661–13665.

Pelham RJ Jr, Wang YL. 1998. Cell locomotion and focal adhesions are regulated by the mechanical properties of the substrate. Biol Bull 194:348–349; discussion 349–350.

Rahimi RA, Leof EB. 2007. TGF-beta signaling: a tale of two responses. J Cell Biochem 102:593–608.

Riva DR, Magalhaes CB, Lopes AA, Lancas T, Mauad T, Malm O, et al. 2011. Low dose of fine particulate matter ($PM_{2.5}$) can induce acute oxidative stress, inflammation and pulmonary impairment in healthy mice. Inhal Toxicol 23:257–267.

Santhanam L, Tuday EC, Webb AK, Dowzicky P, Kim JH, Oh YJ, et al. 2010. Decreased S-nitrosylation of tissue transglutaminase contributes to age-related increases in vascular stiffness. Circ Res 107:117–125.

Selman M, Pardo A. 2006. Role of epithelial cells in idiopathic pulmonary fibrosis: from innocent targets to serial killers. Proc Am Thorac Soc 3:364–372.

Shi Y, Massague J. 2003. Mechanisms of TGF-beta signaling from cell membrane to the nucleus. Cell 113:685–700.

Spruit MA, Janssen DJ, Franssen FM, Wouters EF. 2009. Rehabilitation and palliative care in lung fibrosis. Respirology 14:781–787.

Taipale J, Koli K, Keski-Oja J. 1992. Release of transforming growth factor-beta 1 from the pericellular matrix of cultured fibroblasts and fibrosarcoma cells by plasmin and thrombin. J Biol Chem 267:25378–25384.

Thannickal, VJ, Horowitz JC. 2006. Evolving concepts of apoptosis in idiopathic pulmonary fibrosis. Proc Am Thorac Soc 3:350–356.

Thevenot PT, Saravia J, Jin N, Giaimo JD, Chustz RE, Mahne S, et al. 2013. Radical-containing ultrafine particulate matter initiates epithelial-to-mesenchymal transitions in airway epithelial cells. Am J Respir Cell Mol Biol 48:188–197.

Thiery JP, Acloque H, Huang RY, Nieto MA. 2009. Epithelial-mesenchymal transitions in development and disease. Cell 139:871–890.

Thiery JP, Sleeman JP. 2006. Complex networks orchestrate epithelial-mesenchymal transitions. Nat Rev Mol Cell Biol 7:131–142.

Tse JR, Engler AJ. 2010. Preparation of hydrogel substrates with tunable mechanical properties. Curr Protoc Cell Biol Chapter 10:Unit 10 16.

Uhal BD, Joshi I, Hughes WF, Ramos C, Pardo A, Selman M. 1998. Alveolar epithelial cell death adjacent to underlying myofibroblasts in advanced fibrotic human lung. Am J Physiol 275:L1192–1199.

Veljkovic E, Jiricny J, Menigatti M, Rehrauer H, Han W. 2011. Chronic exposure to cigarette smoke condensate in vitro induces epithelial to mesenchymal transition-like changes in human bronchial epithelial cells, BEAS-2B. Toxicol In Vitro 25:446–453.

Vicovac L, Aplin JD. 1996. Epithelial-mesenchymal transition during trophoblast differentiation. Acta Anat (Basel) 156:202–216.

Vogel V, Sheetz M. 2006. Local force and geometry sensing regulate cell functions. Nat Rev Mol Cell Biol 7:265–275.

Willis BC, Borok Z. 2007. TGF-beta-induced EMT: mechanisms and implications for fibrotic lung disease. Am J Physiol Lung Cell Mol Physiol 293:L525–534.

Willis BC, duBois RM, Borok Z. 2006. Epithelial origin of myofibroblasts during fibrosis in the lung. Proc Am Thorac Soc 3:377–382.

Willis BC, Liebler JM, Luby-Phelps K, Nicholson AG, Crandall ED, du Bois RM, et al. 2005. Induction of epithelial-mesenchymal transition in alveolar epithelial cells by transforming growth factor-beta1: potential role in idiopathic pulmonary fibrosis. Am J Pathol 166:1321–1332.

Wipff PJ, Hinz B. 2008. Integrins and the activation of latent transforming growth factor beta1: an intimate relationship. Eur J Cell Biol 87:601–615.

Wipff PJ, Rifkin DB, Meister JJ, Hinz B. 2007. Myofibroblast contraction activates latent TGF-beta1 from the extracellular matrix. J Cell Biol 179:1311–1323.

Wozniak MA, Desai R, Solski PA, Der CJ, Keely PJ. 2003. ROCK-generated contractility regulates breast epithelial cell differentiation in response to the physical properties of a three-dimensional collagen matrix. J Cell Biol 163:583–595.

Wynn TA. 2008. Cellular and molecular mechanisms of fibrosis. J Pathol 214:199–210.

Xu GP, Li QQ, Cao XX, Chen Q, Zhao ZH, Diao ZQ, et al. 2007. [Effect of Smad7 on transforming growth factor-beta1-induced alveolar epithelial to mesenchymal transition]. Zhonghua Yi Xue Za Zhi 87:1918–1923.

Xu J, Lamouille S, Derynck R. 2009. TGF-beta-induced epithelial to mesenchymal transition. Cell Res 19:156–172.

Yang MH, Hsu DS, Wang HW, Wang HJ, Lan HY, Yang WH, et al. 2010. Bmi1 is essential in Twist1-induced epithelial-mesenchymal transition. Nat Cell Biol 12:982–992.

Zhou G, Dada LA, Wu M, Kelly A, Trejo H, Zhou Q, et al. 2009. Hypoxia-induced alveolar epithelial-mesenchymal transition requires mitochondrial ROS and hypoxia-inducible factor 1. Am J Physiol Lung Cell Mol Physiol 297:L1120–1130.

Zhou Y, Hagood JS, Lu B, Merryman WD, Murphy-Ullrich JE. 2010. Thy-1-integrin alphav beta5 interactions inhibit lung fibroblast contraction-induced latent transforming growth factor-beta1 activation and myofibroblast differentiation. J Biol Chem 285:22382–22393.

Zou W, Zou Y, Zhao Z, Li B, Ran P. 2013. Nicotine induced epithelial-mesenchymal transition via Wnt/beta-catenin signaling in human airway epithelial cells. Am J Physiol Lung Cell Mol Physiol 304:L199–209.

APPENDICES AVAILABLE ON THE WEB

Appendices A, B, and C contain supplemental material not included in the printed report. They are available on the HEI Web site *http://pubs.healtheffects.org*.

Appendix A. The Role of Mechanics in Particle Uptake

Appendix B. Representative Western Blots for Epithelial and Mesenchymal Protein Levels

Appendix C. Species and Elemental Analyses of $PM_{2.5}$ from ASACA and GaEPD Monitoring Sites in South DeKalb

ABOUT THE AUTHORS

Thomas H. Barker, Ph.D., is an associate professor in the Wallace H. Coulter Department of Biomedical Engineering at the Georgia Institute of Technology and Emory University School of Medicine in Atlanta, Georgia, and holds an adjunct appointment in the Department of Medicine, Division of Pulmonary, Allergy and Critical Care Medicine. He earned his B.S. in chemistry and physics from Oglethorpe University in Atlanta, Georgia, and his M.S. and Ph.D. in biomedical engineering at the University of Alabama at Birmingham, Alabama, in 2001 and 2003, respectively, conducting research on vascular clotting proteins as biomaterials for tissue repair and regulation of cell–matrix interactions. After graduation, he held postdoctoral fellowships in ECM biology and biomaterials at the Hope Heart Institute at the University of Washington in Bellevue, Washington, and at l'École Polytechnique Fédérale de Lausanne in Lausanne, Switzerland. In 2006, he joined the faculty of Georgia Tech. His research activities center on ECM biology and engineering, integrating engineering applications and basic cell and molecular biology approaches to the understanding and control of cell phenotypes through the design of engineered ECMs. He was the principle investigator on this HEI research study.

Marilyn M. Dysart, Ph.D., is a graduate research fellow in the Wallace H. Coulter Department of Biomedical Engineering at the Georgia Institute of Technology and Emory University School of Medicine in Atlanta, Georgia. She earned her B.S. in biomedical engineering in 2008 from the University of Virginia in Charlottesville, Virginia, where her undergraduate research focused on engineering stem cells for angiogenic control. She joined the graduate program at Georgia Tech and Emory in 2009 and earned her Ph.D. in 2014. Her research focuses on understanding the roles of integrin binding and substrate stiffness in the EMT process and the utilization of this information to build biomaterials for tissue regeneration. She performed the studies investigating the role of $PM_{2.5}$ and substrate stiffness in modulating alveolar EMT for this HEI research study.

Ashley C. Brown, Ph.D., is a postdoctoral fellow in the Georgia Institute of Technology School of Chemistry and Biochemistry and the Wallace H. Coulter Department of Biomedical Engineering at Georgia Tech and Emory University School of Medicine in Atlanta, Georgia. She earned her B.S. in biosystems engineering in 2006 from Clemson University in Clemson, South Carolina, and her Ph.D. in biomedical engineering from Georgia Tech in 2011. Her Ph.D. studies were completed in the laboratory of Thomas Barker and focused on understanding the roles of integrin-specific binding to ECM ligands and substrate stiffness in the EMT process. She performed the studies investigating the role of substrate stiffness and TGF-β signaling in modulating alveolar EMT for this HEI research study.

Alison M. Douglas, B.S.E., is a biomedical engineering graduate research assistant seeking her Ph.D. in the laboratory of Thomas Barker at the Wallace H. Coulter Department of Biomedical Engineering at the Georgia Institute of Technology and Emory University School of Medicine in Atlanta, Georgia. She earned her B.S.E. in biomedical engineering in 2010 from Tulane University in New Orleans, Louisiana, where her undergraduate research in the laboratory of Dr. David A. Rice focused on biomedical-device development. As a graduate student, she became interested in understanding how ECM stiffness affects cellular phenotype and performed the particle endocytosis experiments for this HEI research study.

Vincent F. Fiore, Ph.D., is a postdoctoral fellow in the Wallace H. Coulter Department of Biomedical Engineering at the Georgia Institute of Technology and Emory University School of Medicine in Atlanta, Georgia. He earned his B.S.E. in bioengineering from Pennsylvania State University in State College, Pennsylvania. After graduation, he held an industrial internship at the biotech start-up NanoHorizons in State College, where his work focused on the development of polymeric–silver composite nanoparticles for antimicrobial applications in the textile industry. He joined the graduate program at Georgia Tech and Emory in 2008, and his research focuses on the role of mechanical forces in controlling signaling pathways from cell–matrix adhesions. He performed mechanical testing of ex vivo tissue samples and cells for this HEI research study.

Armistead G. Russell, Ph.D., is the Howard T. Tellepsen chair and professor of environmental engineering at the Georgia Institute of Technology. He earned his B.S. in mechanical engineering from Washington State University in Pullman, Washington, and his M.S. and Ph.D. degrees in mechanical engineering at the California Institute of Technology in Pasadena, California, in 1980 and 1985, respectively; he conducted his research at the Caltech Environmental Quality Laboratory. After graduation, he became a professor at Carnegie Mellon University in Pittsburgh, Pennsylvania, and joined Georgia Tech in 1996, where his research is aimed at better understanding the dynamics of air pollutants and the resulting health effects. He and his students provided air quality samples and conducted the associated source apportionment for this HEI research study.

OTHER PUBLICATIONS RESULTING FROM THIS RESEARCH

Brown AC, Fiore VF, Sulchek TA, Barker TH. 2013. Physical and chemical microenvironmental cues orthogonally control the degree and duration of fibrosis-associated epithelial-to-mesenchymal transitions. J Pathol 229:25–35.

ABBREVIATIONS AND OTHER TERMS

α-SMA	alpha smooth muscle actin
AFM	atomic force microscopy
ANOVA	analysis of variance
ASACA	Assessment of Spatial Aerosol Composition in Atlanta
ATI	alveolar type I epithelial cell
ATII	alveolar type II epithelial cell
COPD	chronic obstructive pulmonary disease
DMEM/F12	Dulbecco's Modified Eagle's Medium with Ham's F-12 Nutrient Mixture
E	elastic modulus (also known as the Young modulus)
ECM	extracellular matrix
FAK	focal adhesion kinase
EMT	epithelial-to-mesenchymal transition
FBS	fetal bovine serum
Fn	fibronectin
GaEPD	Georgia Environmental Protection Division
GAPDH	glyceraldehyde 3-phosphate dehydrogenase
GTPase	guanosine triphosphate hydrolase
IACUC	Institutional Animal Care and Use Committee
kPa	kilopascal
Ln	laminin
MLEC	mink lung epithelial cell
NIH	National Institutes of Health
P4H	prolyl 4-hydroxylase
PA	polyacrylamide
PCM	particle composition monitor
PM	particulate matter
$PM_{2.5}$	PM with an aerodynamic diameter ≤ 2.5 μm
qPCR	quantitative polymerase chain reaction
RLE-6TN	rat lung epithelial-T-antigen negative
ROCK	Rho-associated kinase
Shc	Src homology 2 domain containing–transforming protein 1
Src	sarcoma (kinase)
TCP	tissue culture plastic
TGF-β	transforming growth factor beta
TNF-α	tumor necrosis factor alpha
WINS	Well Impactor Ninety-Six

Research Report 182, *Synergistic Effects of Particulate Matter and Substrate Stiffness on Epithelial-to-Mesenchymal Transition*, T. H. Barker et al.

INTRODUCTION

Exposure to particulate matter (PM*) from combustion sources has been associated with lung inflammation and injury, which trigger repair responses to restore normal tissue function. Dysregulation of these responses can result, over time, in fibrotic changes that include an increase in myofibroblasts, which promote abnormal deposition of collagen in the subepithelial layer of alveoli, with consequent stiffness of the extracellular matrix (ECM) and impairment of gas exchange. Fibrosis in the lung can be progressive and fatal, as in idiopathic fibrosis, and is also a feature of chronic pulmonary diseases such as asthma, and it is thus important to understand profibrotic processes.

In March 2008, Dr. Thomas H. Barker of the Georgia Institute of Technology and Emory University in Atlanta submitted an application entitled "Extracellular Matrix Stiffness Associated with Pulmonary Fibrosis Sensitizes Alveolar Epithelial Cells" in response to Request for Applications 07-1, the "Walter A. Rosenblith New Investigator Award." This award was established to provide support for an outstanding new investigator at the assistant professor level to conduct work in the area of air pollution and health and is unrestricted with respect to the topic of research.

In his application to HEI, Barker proposed to study the effects of PM on fibrosis using both biophysical and biochemical approaches. He hypothesized that increases in the stiffness of the ECM would enhance alveolar type II (ATII) epithelial cell endocytosis of particles and would involve activation of Rho guanosine triphosphate hydrolase (GT-Pase), a key regulator of cell contractility (Provenzano and Keely 2011). The study would utilize both a mouse model of fibrosis and cultured epithelial cells. The HEI Health Research Committee thought that Barker was a strong candidate for the award and that his proposal was innovative and so recommended the study for funding. During the course of the study, the scope of the research evolved and the aims of the study were modified, with the elimination of the mouse work, with approval from the Committee. The work presented in the Investigators' Report focuses on the role of matrix stiffness on epithelial-to-mesenchymal transition (EMT) and on how ambient PM affects this transition. The study of PM uptake by epithelial cells is provided in Appendix A of the Investigators' Report (available on the HEI Web site).

This Critique is intended to aid the sponsors of HEI and the public by highlighting both the strengths and limitations of the study and by placing the Investigators' Report into a broader scientific perspective.

BACKGROUND

Fibrosis can result from dysregulation of healing processes after lung injury. The hallmark of fibrosis is the accumulation and proliferation of fibroblasts and their differentiation to myofibroblasts in interstitial spaces. Fibroblasts can be derived from various cell sources. One theory proposes that they are derived from alveolar epithelial cells undergoing EMT (Chambers 2008).

During EMT, epithelial cells lose their polarity and shape and undergo either apoptosis or transition to mesenchymal cells with an elongated spindle-shaped morphology. These mesenchymal cells can migrate to the interstitium and further evolve into fibroblasts and myofibroblasts (Willis and Borok 2007). During EMT, epithelial cells stop synthesizing E-cadherin, a cell adhesion molecule, and produce mesenchymal markers such as the cytoskeletal protein alpha smooth muscle actin (α-SMA), which confers internal contractile properties on fibroblasts. These steps and the mediators involved are illustrated in Critique Figure 1.

EMT is also associated with activation of the profibrotic transforming growth factor beta (TGF-β), a key regulator of fibroblast proliferation and ECM production, and with consequent accumulation of collagen (Fernandez and

Dr. Thomas H. Barker's 3-year study, "Extracellular Matrix Stiffness Associated with Pulmonary Fibrosis Sensitizes Alveolar Epithelial Cells," began in October 2009. Total expenditures were $250,000. The draft Investigators' Report from Barker and colleagues was received for review in February 2013. A revised report, received in October 2013, was accepted for publication in February 2014. During the review process, the HEI Health Review Committee and the investigators had the opportunity to exchange comments and to clarify issues in both the Investigators' Report and the Review Committee's Critique. (As a coinvestigator on the report by Barker et al., Review Committee member Dr. Armistead G. Russell was not involved in the report's evaluation.)

* A list of abbreviations and other terms appears at the end of the Investigators' Report.

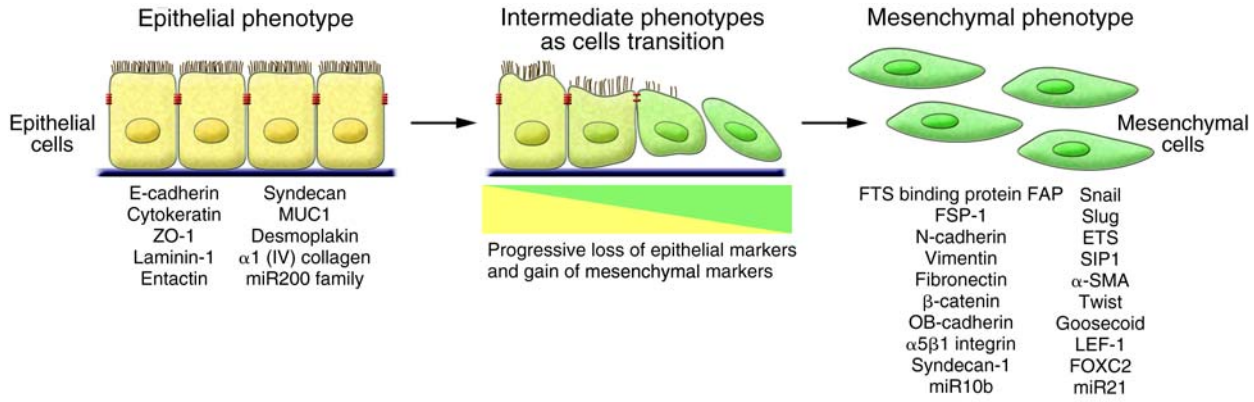

Critique Figure 1. Schematic representation of EMT. EMT involves a functional transition of polarized epithelial cells into mobile mesenchymal cells that secrete components of the extracellular matrix. The epithelial and mesenchymal cell markers commonly used by EMT researchers are listed in the figure. Abbreviations: ZO-1 denotes zonula occludens protein-1; MUC1, mucin-1, cell-surface associated; a1 (IV) collagen, collagen alpha-1(IV) chain; miR, microRNA; FTS binding protein FAP, serum thymic factor–binding fibroblast activation protein; FSP-1, fibroblast-specific protein-1; N-cadherin, neural cadherin; β-catenin, catenin (cadherin-associated protein), beta 1, 88kDa; OB-cadherin, osteoblast cadherin; ETS, E26 transformation–specific transcription-factor family; SIP1, survival of motor neuron protein–interacting protein 1; LEF-1, lymphoid enhancer–binding factor 1; and FOXC2, forkhead box protein C2. (Reprinted from Kalluri and Weinberg 2009 with permission from the American Society for Clinical Investigation.)

Eickelberg 2012). TGF-β is produced by a wide variety of cell types, including epithelial cells and fibroblasts (Fernandez and Eickelberg 2012). The majority of TGF-β is present in the ECM in a latent form and becomes activated during EMT through various pathways (Willis and Borok 2007). The ECM consists of proteins (primarily collagen fibers) and sugars and serves two primary roles: to provide structural support to the surrounding tissue and to provide biomechanical cues that modulate the behavior of cells and tissue (Cox and Erler 2011).

The accumulation of excessive levels of ECM components (primarily collagen and fibronectin) leads to altered biochemical and mechanical matrix properties, such as loss of elasticity. It has been shown that changes in ECM stiffness can affect the behavior of the surrounding cells. In their review of ECM, Provenzano and Keely (2011) defined matrix stiffness as "internal resistance to deformation produced by force." They explained that cells sense this stiffness and respond by generating internal forces that pull against the ECM (i.e., the cells become more contractile). A key mediator of these processes is Rho GTPase (Chambers 2008).

In summary, EMT is a process by which the lung responds to injury. Under normal healing conditions, apoptosis (programmed cell death) of fibroblasts terminates the progression of EMT to fibrosis. However, persistence of TGF-β and collagen deposition promotes the development of fibrosis (Chambers 2008). Exposure to PM has been associated with airway inflammation and asthma exacerbation and might therefore play a role in the development of fibrosis. However, the clinical effects of ambient air pollution on pulmonary fibrosis have not been studied.

In the current study, Barker and colleagues developed and evaluated an in vitro cellular model that mimics EMT and studied the effects of exposure to PM on this process.

AIMS

The central hypotheses of the study were that alveolar epithelial cells grown on fibronectin substrates of increasing degrees of stiffness would become increasingly contractile and undergo EMT and that the addition of fine particulate matter (PM ≤ 2.5 μm in aerodynamic diameter [$PM_{2.5}$]) would enhance these effects.

These hypotheses were tested in cells grown in vitro using a combination of mechanical and biologic approaches by addressing the following specific aims:

- Determine the effects of substrate stiffnesses that ranged from values seen in healthy tissue to those seen in fibrotic tissue on lung-epithelial-cell contractility, induction of EMT, and activation of TGF-β.
- Determine whether exposure to $PM_{2.5}$ exacerbates the effects of substrate stiffness on EMT and cell contractility.

STUDY DESIGN AND METHODS

Before addressing these aims, Barker and colleagues used a well-characterized model of fibrosis — intratracheal administration of bleomycin into mice (reviewed in Mouratis and Aidinis 2011) — to determine relevant values of matrix stiffness (also referred to as substrate stiffness) to use in their in vitro experiments. They then explored the role of substrate stiffness in particle uptake by cultured epithelial cells, one of the original aims stated in the application (presented in Appendix A).

The in vitro experimental model consisted of rat ATII epithelial cells cultured on increasingly stiff substrates with or without the addition of various concentrations of ambient $PM_{2.5}$ to the culture media (in multi-well plates). Barker and colleagues used two types of ATII cells: primary cells isolated from the lungs of male Sprague Dawley rats and RLE-6TN, a spontaneously immortalized cell line derived from a Fischer 344 rat.

The substrate consisted of polyacrylamide–bisacrylamide gels cross-linked to fibronectin, with varying concentrations of bisacrylamide to achieve increasing degrees of stiffness (reported as the elastic modulus, in Pascal units), ranging from 2 to 32 kPa. The elastic modulus was measured by atomic force microscopy. Glass coverslips coated with fibrin (a protein shown to stiffen alveolar epithelial cells) and laminin (a protein in the ECM that modulates cell functions) were used as positive and negative controls, respectively. The cells were grown on these substrates for five days before EMT analysis. Apart from the initial experiments to evaluate the EMT model (Figure 4 of the Investigators' Report), all subsequent experiments used the RLE-6TN cell line.

Particle uptake was measured by exposing RLE-6TN cells grown on substrates of increasing stiffness for 16 hours to 2-μm fluorescent polystyrene particles for four hours. At the end of the exposure period the cells were analyzed by flow cytometry for the presence of particles inside the cells.

EMT was analyzed through changes in cell shape, cell contractility, expression of the cellular markers E-cadherin and α-SMA, and TGF-β activation. Specifically, the investigators characterized changes in cell shape (also referred to as circularity) by staining the cells with fluorescent dyes specific for actin (the key protein that makes up the cellular cytoskeleton) and for the cell nucleus and measuring the area and perimeter of individual stained cells; circularity is calculated from the ratio between the two measures. Cell contractility was measured as stiffness (using atomic force microscopy). Y-27632, an inhibitor of Rho GTPase, was added to the culture medium to evaluate the role of cell contractility in EMT.

Barker and colleagues used fluorescent antibodies specific to E-cadherin and α-SMA and examined the results by both fluorescent microscopy and western blots. The latter technique consists of separating proteins tagged with their specific antibody by gel electrophoresis. The levels of these proteins were quantified using image-processing software.

TGF-β activation was measured by the luminescence product of genetically engineered mink lung epithelial cells, which respond only to activated TGF-β. The cells were added on top of the ATII epithelial cells at the end of the experiment and co-cultured for 16 hours before the luminescence assay. For the total serum TGF-β assay, the ATII epithelial cells were heated at 85°C before adding the mink lung epithelial cells.

Ambient $PM_{2.5}$ for Aim 2 was collected on Teflon filters placed near two highways and a school in Atlanta in spring and summer 2004. The particles were extracted from the filters by sonication and resuspended in culture media after filtration to remove any large particles. Compositional data for sulfate, nitrate, ammonium, elemental carbon, and organic carbon were obtained from filters collected in parallel. Metal composition was measured in PM from filters collected during the same period at a nearby monitoring site operated by the Georgia Environmental Protection Division that was sampled every three days. Source apportionment was conducted using the chemical balance model.

STATISTICAL ANALYSIS

For Aim 1, each analysis data set consisted of measurements from multiple wells with substrates of increasing stiffness overlaid with epithelial cells. Each substrate stiffness was replicated in three wells, and the entire experimental procedure was repeated three or more times (on different days), for a total of nine or more observations for each substrate stiffness. Each measurement was treated as an independent observation regardless of whether measurements were obtained on the same or different days. The independent variable was substrate stiffness. The data were analyzed using one-way analysis of variance (ANOVA) after determining that there were no interactions between days and substrate in a two-way ANOVA.

For Aim 2, each analysis data set consisted of measurements obtained by adding various concentrations of PM or culture media with no PM (the control) to wells of increasing substrate stiffness. Each PM concentration was tested in triplicate at each substrate stiffness. As in Aim 1, the entire procedure was repeated on three or more different days using new batches of particulate-containing media, and there were thus nine or more replicates for each substrate stiffness at a given PM concentration. The independent variables were substrate stiffness and PM concentration. The

data were analyzed using two-way ANOVA after determining that there were no interactions with day of the experiment when using three-way ANOVA.

SUMMARY OF KEY RESULTS

AIM 1: ROLE OF SUBSTRATE STIFFNESS IN EMT

Cultured ATII epithelial cells transitioned to mesenchymal cells on substrates of increased stiffness, as documented by loss of cell circularity, decreased expression of E-cadherin, and increased expression of α-SMA. Increased substrate stiffness was associated with increased cell contractility and increased activated TGF-β, while total TGF-β was unchanged. The addition of the Rho GTPase inhibitor prevented EMT.

The role of TGF-β was further demonstrated in an experiment in which ATII cells were grown on a soft substrate in media containing various concentrations of active TGF-β for two or five days. Exposure to TGF-β for five days was associated with decreased cell circularity, changes in surface markers, and increased cell stiffness. However, the development of EMT after exposure to TGF-β for only the first two days was dependent on the TGF-β concentration; cells exposed to a low concentration of TGF-β did not develop the mesenchymal phenotype.

AIM 2: ROLE OF $PM_{2.5}$ IN SUBSTRATE-STIFFNESS-MEDIATED EMT

Addition of ambient $PM_{2.5}$ at the highest concentration (10 μg/cm^2 at a 1:100 dilution of the PM sample) reduced the circularity of cells grown on substrates of 8-kPa stiffness and higher. No effects of $PM_{2.5}$ were observed in cells cultured on laminin. The E-cadherin surface marker decreased and α-SMA increased at the 1:100 dilution, as compared with the response in non-exposed control cells at the same substrate stiffness. Cell stiffness was also increased by $PM_{2.5}$ on substrates of the same stiffness, as compared with non-exposed cells. Alveolar epithelial cells also showed increased TGF-β activation with increasing substrate stiffness when exposed to $PM_{2.5}$, as compared with non-exposed cells.

PARTICLE UPTAKE

The results showed that the polystyrene particles were internalized by the ATII cells but that the process was not affected by increased substrate stiffness. Cells pretreated with an inhibitor of Rho GTPase had increased particle endocytosis, disproving the original hypothesis that increased Rho activity would be associated with increased particle uptake.

HEALTH REVIEW COMMITTEE EVALUATION

In its independent review of the study, the Committee thought that the study was carefully performed, with interesting mechanistic observations. The in vitro model of cell cultures grown on substrates of various degrees of stiffness was novel and potentially useful in understanding the role of matrix stiffness in EMT.

The methods used were thought to be appropriate and to reflect the state of the art. The combination of biologic and mechanical techniques for assessing interactions between airway epithelial cells and the underlying matrix and for characterizing EMT was a strength of the work. The analysis of particle composition was a useful addition to the study. A limitation was that most of the experiments were conducted using immortalized cells, which have different properties from primary cells.

The Committee expressed concerns about the statistical analyses used. It noted that the investigators did not use standard methods for the analysis of randomized block designs, such as the design used in this study, where the entire experiment was repeated on three different days and treatments were randomly assigned within each day. Thus the one-way ANOVA used for Aim 1 did not properly adjust for the variation caused by the experiments' being conducted on different days (a blocking factor). The investigators explained that they had tried a two-way ANOVA, but because they found no interactions between day and the variable of interest (substrate stiffness), they conducted only the one-way ANOVA. However, the Committee concluded that each replication of the experiment on a different day should properly be viewed as a blocking factor; these blocks could be an important source of variation, and omitting them from the analysis could lead to incorrect estimation of the variance of the data even if the factors did not interact with the variable of interest. The Committee's comments are even more relevant for the analyses in Aim 2, in which two-way ANOVA was used to assess the effects of substrate stiffness and PM concentration without accounting for day as a blocking factor. As in the analyses for Aim 1, this approach also excluded replication of the experiment on different days as an important source of variation, but in this case the day-to-day variation was potentially more important because it was associated with the use of PM from different filters (with different compositions). The Committee thought that this blocking factor should be included in all the statistical analyses and that,

without additional information, it is impossible to be sure what effect it might have had on the results. The preferred analyses would have used two- and three-way ANOVA models appropriate for completely randomized designs.

Despite these concerns, the Committee agreed with the investigators' overall conclusion that, in their cell culture system, the results supported their hypothesis that greater stiffness of the extracellular substrate drives EMT, as measured by decreased expression of E-cadherin and increased expression of α-SMA and cell contractility. In addition, using an inhibitor of cell contractility and treating cells grown on a soft substrate with TGF-β, the investigators showed that cell contractility and activation of TGF-β play a key role in EMT. The results also supported the investigators' hypothesis that exposure to PM would enhance the effect of substrate stiffness on EMT and TGF-β activation, as compared with those of non-exposed cells.

The possibility of PM effects on EMT was also supported in a recent study of bronchial EMT in infant mice exposed by inhalation to 0.2-μm amorphous silica particles coated with an organic compound that generates free radicals (Thevenot et al. 2013). Cells stained with both E-cadherin and α-SMA were observed in the subepithelial layers, suggesting that epithelial cells had acquired the mesenchymal phenotype. However, in that study TGF-β did not appear to be involved.

Overall, the study by Barker and colleagues highlights the potential importance of cell–matrix interaction when evaluating the effects of environmental triggers and provides a basis for future work. However, the question of how PM taken up by the cells might affect EMT remains open, in part because there was no increase in PM uptake with increased substrate stiffness. Barker and colleagues speculate that the higher levels of EMT seen with exposure to $PM_{2.5}$ might be a result of a positive feedback loop in which loss of cell–cell junctions (associated with decreased levels of E-cadherin) makes the cell more susceptible to the effects of surrounding immune cells and inflammatory signals that can further activate TGF-β and drive additional EMT progression. Alternatively, PM might increase cell contractility, which in turn might lead to mechanical activation of TGF-β. The Committee thought that considerable work will be needed to confirm these initial observations, understand the mechanisms, and determine whether they are relevant to in vivo processes and the development of fibrosis.

ACKNOWLEDGMENTS

The Health Review Committee thanks the ad hoc reviewers for their help in evaluating the scientific merit of the Investigators' Report. The Committee is also grateful to Annemoon van Erp and Geoffrey Sunshine for their oversight of the study, to Maria Costantini for her assistance in preparing its Critique, to George Simonson for science editing of the Report and its Critique, to Ruth Shaw for its composition, and to Hope Green, Fred Howe, Bernard Jacobson, and Carol Moyer for their roles in preparing this Research Report for publication.

REFERENCES

Chambers RC. 2008. Abnormal wound healing responses in pulmonary fibrosis: focus on coagulation signalling. Eur Respir Rev 109:130–137.

Cox TR, Erler JT. 2011. Remodeling and homeostasis of the extracellular matrix: implications for fibrotic diseases and cancer. Dis Model Mech 4:165–178.

Fernandez IE, Eickelberg O. 2012. The impact of TGF-β on lung fibrosis: from targeting to biomarkers. Proc Am Thorac Soc 9:111–116.

Kalluri R, Weinberg RA. 2009. The basics of epithelial-mesenchymal transition. J Clin Invest 119:1420–1428.

Mouratis MA, Aidinis V. 2011. Modeling pulmonary fibrosis with bleomycin. Curr Opin Pulm Med 17:355–361.

Provenzano PP, Keely PJ. 2011. Mechanical signaling through the cytoskeleton regulates cell proliferation by coordinated focal adhesion and Rho GTPase signaling. J Cell Sci 124:1195–1205.

Thevenot PT, Saravia J, Jin N, Giaimo JD, Chustz RE, Mahne S, et al. 2013. Radical-containing ultrafine particulate matter initiates epithelial-to-mesenchymal transitions in airway epithelial cells. Am J Respir Cell Mol Biol 48:188–197.

Willis BC, Borok Z. 2007. TGF-β-induced EMT: mechanisms and implications for fibrotic lung disease. Am J Physiol Lung Cell Mol Physiol 293:L525–534.

RELATED HEI PUBLICATIONS

Number	Title	Principal Investigator	Date
Research Reports			
178	National Particle Component Toxicity (NPACT) Initiative Report on Cardiovascular Effects		2013
	Section 2. NPACT animal toxicologic study of cardiovascular effects of mixed vehicle emissions combined with non-vehicular particulate matter	M.J. Campen	
174	Cardiorespiratory Biomarker Responses in Healthy Young Adults to Drastic Air Quality Changes Surrounding the 2008 Beijing Olympics	J. Zhang	2013
166	Advanced Collaborative Emissions Study (ACES) Subchronic Exposure Results: Biologic Responses in Rats and Mice and Assessment of Genotoxicity		2012
	Part 1. Biologic responses in rats and mice to subchronic inhalation of diesel exhaust from U.S. 2007-compliant engines: report on 1-, 3-, and 12-month exposures in the ACES bioassay	J.D. McDonald	
	Part 2. Assessment of genotoxicity after exposure to diesel exhaust from U.S. 2007-compliant diesel engines: report on 1- and 3-month exposures in the ACES bioassay	J.C. Bemis	
	Part 3. Assessment of genotoxicity and oxidative stress after exposure to diesel exhaust from U.S. 2007-compliant diesel engines: report on 1- and 3-month exposures in the ACES bioassay	L.M. Hallberg	
	Part 4. Effects of subchronic diesel engine emissions exposure on plasma markers in rodents: report on 1- and 3-month exposures in the ACES bioassay	D.J. Conklin and M. Kong	
165	Allergic Inflammation in the Human Lower Respiratory Tract Affected by Exposure to Diesel Exhaust	M.A. Riedl	2012
145	Effects of Concentrated Ambient Particles and Diesel Engine Exhaust on Allergic Airway Disease in Brown Norway Rats	J.R. Harkema	2009
138	Health Effects of Real-World Exposure to Diesel Exhaust in Persons with Asthma	J. Zhang	2009
134	Black-Pigmented Material in Airway Macrophages from Healthy Children: Association with Lung Function and Modeled PM_{10}	J. Grigg	2008
129	Particle Size and Composition Related to Adverse Health Effects in Aged, Sensitive Rats	F.F. Hahn	2003
126	Effects of Exposure to Ultrafine Carbon Particles in Healthy Subjects and Subjects with Asthma	M.W. Frampton	2004

Printed copies of these reports can be obtained from HEI; pdf's are available for free downloading at http://pubs.healtheffects.org

RELATED HEI PUBLICATIONS

Number	Title	Principal Investigator	Date
Research Reports (*Continued*)			
118	Controlled Exposures of Healthy and Asthmatic Volunteers to Concentrated Ambient Particles in Metropolitan Los Angeles	H. Gong Jr.	2003
112	Health Effects of Acute Exposure to Air Pollution	S.T. Holgate	2003
	Part I. Healthy and Asthmatic Subjects Exposed to Diesel Exhaust		
	Part II. Healthy Subjects Exposed to Concentrated Ambient Particles		
110	Particle Characteristics Responsible for Effects on Human Lung Epithelial Cells	A.E. Aust	2002
68	Pulmonary Toxicity of Inhaled Diesel Exhaust and Carbon Black in Chronically Exposed Rats		
	Part I. Neoplastic and Nonneoplastic Lung Lesions	J.L. Mauderly	1994
	Part II. DNA Damage	K. Randerath	1995
	Part III. Examination of Possible Target Genes	S.A. Belinsky	1995
30	Influence of Experimental Pulmonary Emphysema on Toxicological Effects from Inhaled Nitrogen Dioxide and Diesel Exhaust	J.L. Mauderly	1989
HEI Perspectives			
2	Understanding the Health Effects of Components of the Particulate Matter Mix: Progress and Next Steps		2002

Printed copies of these reports can be obtained from HEI; pdf's are available for free downloading at http://pubs.healtheffects.org

HEI BOARD, COMMITTEES, and STAFF

Board of Directors

Richard F. Celeste, Chair *President Emeritus, Colorado College*

Sherwood Boehlert *Of Counsel, Accord Group; Former Chair, U.S. House of Representatives Science Committee*

Enriqueta Bond *President Emerita, Burroughs Wellcome Fund*

Purnell W. Choppin *President Emeritus, Howard Hughes Medical Institute*

Michael T. Clegg *Professor of Biological Sciences, University of California–Irvine*

Jared L. Cohon *President Emeritus and Professor, Civil and Environmental Engineering and Engineering and Public Policy, Carnegie Mellon University*

Stephen Corman *President, Corman Enterprises*

Linda Rosenstock *Dean Emerita and Professor of Health Policy and Management, Environmental Health Sciences and Medicine, University of California–Los Angeles*

Henry Schacht *Managing Director, Warburg Pincus; Former Chairman and Chief Executive Officer, Lucent Technologies*

Warren M. Washington *Senior Scientist, National Center for Atmospheric Research; Former Chair, National Science Board*

Archibald Cox, Founding Chair *1980–2001*

Donald Kennedy, Vice Chair Emeritus *Editor-in-Chief Emeritus,* Science*; President Emeritus and Bing Professor of Biological Sciences, Stanford University*

Health Research Committee

David L. Eaton, Chair *Dean and Vice Provost of the Graduate School, University of Washington–Seattle*

David Christiani *Elkan Blout Professor of Environmental Genetics, Harvard School of Public Health*

Francesca Dominici *Professor of Biostatistics and Senior Associate Dean for Research, Harvard School of Public Health*

David E. Foster *Phil and Jean Myers Professor Emeritus, Department of Mechanical Engineering, Engine Research Center, University of Wisconsin–Madison*

Uwe Heinrich *Professor, Hannover Medical School; Executive Director, Fraunhofer Institute for Toxicology and Experimental Medicine, Hanover, Germany*

Barbara Hoffmann *Professor of Environmental Epidemiology and Head of Environmental Epidemiology of Aging, IUF-Leibniz Research Institute for Environmental Medicine, and Professor, Medical Faculty, Heinrich Heine University of Düsseldorf, Germany*

Allen L. Robinson *Raymond J. Lane Distinguished Professor and Head, Department of Mechanical Engineering, and Professor, Department of Engineering and Public Policy, Carnegie Mellon University*

Richard L. Smith *Director, Statistical and Applied Mathematical Sciences Institute, University of North Carolina–Chapel Hill*

HEI BOARD, COMMITTEES, and STAFF

Health Review Committee

James A. Merchant, Chair *Professor and Founding Dean, College of Public Health, University of Iowa*

Michael Brauer *Professor, School of Environmental Health, University of British Columbia, Canada*

Bert Brunekreef *Professor of Environmental Epidemiology, Institute of Risk Assessment Sciences, University of Utrecht, the Netherlands*

Mark W. Frampton *Professor of Medicine and Environmental Medicine, University of Rochester Medical Center*

Stephanie London *Senior Investigator, Epidemiology Branch, National Institute of Environmental Health Sciences*

Roger D. Peng *Associate Professor, Department of Biostatistics, Johns Hopkins Bloomberg School of Public Health*

Armistead Russell *Howard T. Tellepsen Chair of Civil and Environmental Engineering, School of Civil and Environmental Engineering, Georgia Institute of Technology*

Lianne Sheppard *Professor of Biostatistics, School of Public Health, University of Washington–Seattle*

Officers and Staff

Daniel S. Greenbaum *President*

Robert M. O'Keefe *Vice President*

Rashid Shaikh *Director of Science*

Barbara Gale *Director of Publications*

Jacqueline C. Rutledge *Director of Finance and Administration*

April Rieger *Corporate Secretary*

Zachary Abbott *Research Assistant*

Kate Adams *Senior Scientist*

Hanna Boogaard *Staff Scientist*

Adam Cervenka *Research Assistant*

Aaron J. Cohen *Principal Scientist*

Maria G. Costantini *Principal Scientist*

Philip J. DeMarco *Compliance Manager*

Hope Green *Editorial Assistant*

L. Virgi Hepner *Senior Science Editor*

Anny Luu *Executive Assistant*

Nicholas Moustakas *Policy Associate*

Hilary Selby Polk *Senior Science Editor*

Evan Rosenberg *Staff Accountant*

Margarita Shablya *Science Administrative Assistant*

Robert A. Shavers *Operations Manager*

Geoffrey H. Sunshine *Senior Scientist*

Annemoon M.M. van Erp *Managing Scientist*

Donna J. Vorhees *Senior Scientist*

Katherine Walker *Senior Scientist*

HEALTH
EFFECTS
INSTITUTE

101 Federal Street, Suite 500
Boston, MA 02110, USA
+1-617-488-2300
www.healtheffects.org

RESEARCH
REPORT

Number 182
November 2014